Characterization of novel potassium transport proteins from Chlorella viruses

TECHNISCHE UNIVERSITÄT DARMSTADT

Vom Fachbereich Biologie der Technischen Universität Darmstadt

zur Erlangung des akademischen Grades

eines Doctorum rerum naturalium

genehmigte Dissertation von

Dipl.-Biol. Timo Greiner

aus Erbach

Berichterstatter: Prof. Dr. Gerhard Thiel
Mitberichterstatter: Prof. Dr. Adam Bertl

Eingereicht am: 05.05.2011
Mündliche Prüfung am: 15.07.2011

Darmstadt 2011

D17

„Der Strom der Wahrheit fließt durch die Kanäle von Irrtümern.“

Rabindranath Tagore,
indischer Dichter und Philosoph (1861 – 1941)

1. Contents

2. Chapter 1 – General Introduction

2.1. Potassium transport systems

The alkali metal potassium plays, in its ionic form, a major role in all forms of life, where it fulfils a variety of functions, e.g. activation of enzymes, charge stabilization of anions or maintenance of electrical potentials across membranes (Evans and Sorger 1966). To control the concentration of K^+ at its sites of action a large variety of potassium ion transporting systems are evolved, e.g. potassium channels, potassium transporters and pumps (Mäser *et al*. 2001; Rodriguez-Navarro 2000). Potassium transporting systems can be found in all three domains of life, i.e. *Eukarya*, *Bacteria* and *Archaea* (Mäser *et al*. 2001, Rodriguez-Navarro 2000; Corratgé-Faillie *et al.* 2010), and also in the world of viruses (Plugge *et al.* 2000).

2.2. Ion channels

Ion channels are integral membrane proteins that facilitate an energetically favourable pathway for specific ions across a biological membrane (Hille 2001). The hydrophobic membranes of cells are high energetical barriers for charged ions, such as K^+, Na^+ or Cl^-, i.e. ions with importance for cell chemistry. The energy necessary for an ion to cross the membrane is in the range of 50 kcal*mol^{-1} (Parsegian 1969). Due to ion channels this energy barrier is decreased down by more than an order of magnitude to 2 – 3 kcal*mol^{-1}. The concept is shown in **Fig. 1** as simplified cartoon (Berneche and Roux 2001; Fyles 2006).

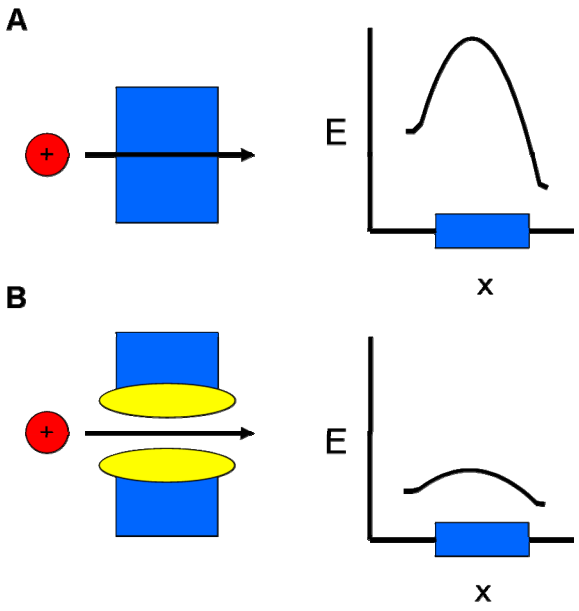

Fig. 1: **(A)** a cation crossing a membrane by direct diffusion and the energy E required to move across the membrane along the x-axis as simplified cartoon. **(B)** a cation passing through an ion channel with decreased energy requirements (according to Fyles 2006).

Basically, ion channels exhibit three characteristic properties: a) rapid conduction of ions, b) high ion selectivity and c) regulation of activity by gating (see **Fig. 2**; MacKinnon 2004). The conductance of ions through a channel is close to the diffusion-limit in water, meaning that up to 10^8 ions per second can cross the channel (Hille 1970). Ion channels are highly selective for specific ions, e.g. some potassium channels are up to 1000 times more selective for K^+ than for Na^+ (Hille 2001). The regulation of channel activity is achieved by the so-called gating. Gating means the stochastic switching between two states of a channel: the conducting open state and the non-conducting closed state (Neher and Sakmann 1976). The gating mechanisms are not fully understood for all channels. Currently two major hypotheses are discussed for potassium channels: a) a gating by the so-called bundle-crossing. The outer transmembrane domains of each pore subunit make at the cytosolic entry into the channel a crossover and therebye forms a gate (Perozo *et al.* 1999), and b) a double-function of the selectivity filter, which facilitates selectivity and gating (Zheng and Sigworth 1997; Lu *et al.* 2001). It has also been shown that both types of gating can be found in the same channel, e.g. KcsA (Perozo et al. 1999; Blunck et al. 2006; Cuello et al. 2010).

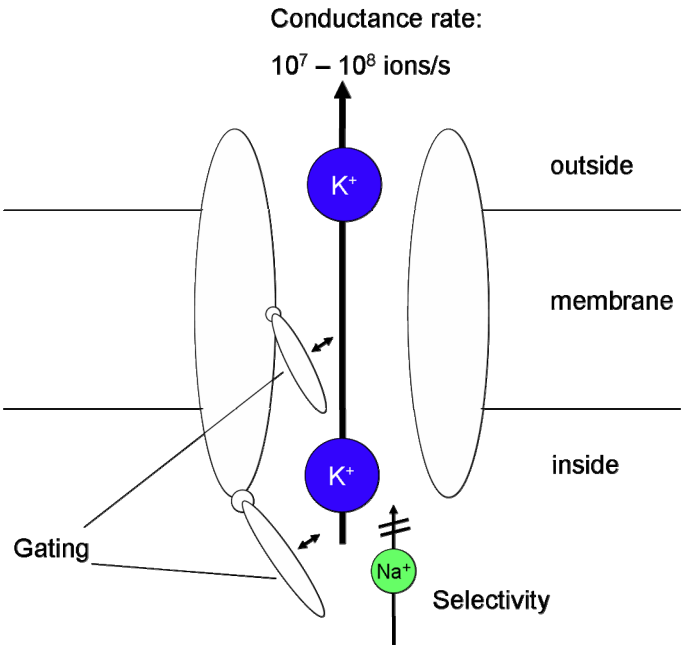

Fig. 2: Basic principles of an ion channel
Sketch of a potassium channel that illustrates the principles of an ion channel, i.e. a high conductance rate of up to 10^8 ions/s, selectivity for a specific ion, in this case for K^+ and not for Na^+, and gating, here illustrated as door that switches between an open and a closed state either in the filter or at the cytosolic entry into the channel (or both) (after MacKinnon 2004).

In general, ion channels are classified according to the ion which they transport best, i.e. potassium channels, sodium channels, chloride channels, etc. Another functional classification refers to their gating properties, e.g. voltage-gated channels, ligand-gated channels or mechanosensitive channels (Hille 2001).

2.3. Potassium channels

Potassium channels are ion channels which selectively facilitate the conductance of potassium ions (K^+) (Hille 2001). They are present in all biological entities and fulfil a large variety of functions. For instance they play major roles in the control of the heart beat, the activity of the nervous system and in osmoregulation, just to mention a few (Hille 2001). Potassium channels also exist in the world of viruses (Plugge *et al.* 2000; Thiel *et al*. 2010b). It will be shown in this thesis, that viral K^+ channels exhibit remarkable properties.

Potassium channels are highly diverse in their amino acid sequence, yet they all show a common topology (Doyle *et al.* 1998; Jiang *et al.* 2002; Jiang *et al.* 2003; Kuo *et al.* 2003; Long *et al.* 2005). The core unit of all potassium channels consists of at least two transmembrane domains (TMs) with a highly conserved region within them: the selectivity filter with the amino acid sequence TxxTxGF/YG (Miller 1992; Jan and Jan 1992). The functional unit of a K^+ channel is generally built by four of these subunits. An example for this small, so-called 2 TM type potassium channel, is the group of Kir channels (K^+ inward rectifier) (Nishida *et al.* 2007), the bacterial channel KcsA (see below, Doyle *et al.* 1998) or the viral potassium channel Kcv (Plugge *et al.* 2000). Bigger potassium channels, e.g. the 6TM type potassium channels, consist of the same 2TM-type pore plus 4 additional TMs. In the case of the so called voltage-dependent (Kv) channels the four additional TMs function as voltage sensor module (Long *et al.* 2005). The K^+ channel KAT1 from *Arabidopsis thaliana* is an example for such a Kv channel in plants (Schachtman *et al.* 1992). In addition to this most common tetrameric building principle there are also so-called tandem type potassium channels. They have two pore regions in tandem per subunit. The functional channel is, in this case, built up by a dimer (Goldstein *et al.* 1996).

Revealing the structure of membrane proteins is a particular challenge enterprise since it generally relies on the crystallization of these proteins. Thanks to the pioneering work of MacKinnon and co-workers, the bacterial potassium channel KcsA from *Streptomyces lividans* could be crystallized and its structure resolved by x-ray crystallography with a resolution of 2 – 4 Å (**Fig. 3 A** and **B**; Doyle *et al.* 1998; MacKinnon 2004). This has led to the understanding of basic structure-function correlates for K^+ conductance through the channels. Potassium ions in water are, just as other ions, surrounded by a hydration shell. The interior of the pore, especially the filter region with the aforementioned signature sequence, mimics the hydration shell of potassium ions with electrostatic interactions of the amino acid´s oxygen atoms (**Fig. 3 C** and **D**). Thus, the dehydration of K^+ when entering the pore requires no energy.

Based on the structure data it is assumed that the selectivity of the channel is determined by the size of the pore in correlation with the transported ion. **Fig. 4** illustrates this: K^+ fits into the pore. The ion radius has the right size and favours the interactions between ion and the proteins carboxyl groups in the pore. Na^+ on the other hand has a smaller ion radius. The interaction with the carboxyl groups is less favourable and, thus, Na^+ cannot pass the pore (MacKinnon 2004).

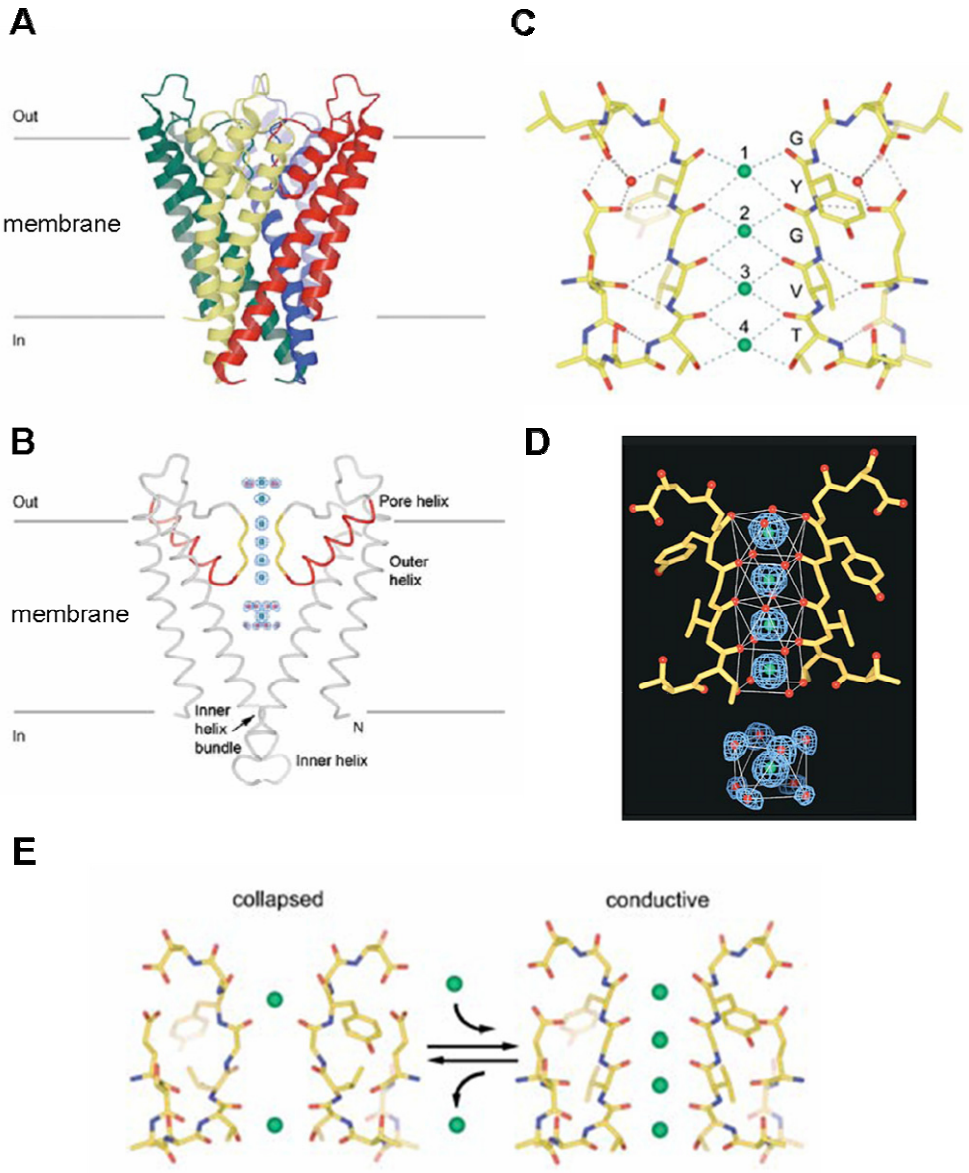

Fig. 3: Structure of a potassium channel

(A) Structure of KcsA inserted in a membrane illustrated as ribbon representation. The subunits are shown in different colors. **(B)** shows two of the subunits to highlight the structural features, i.e. the filter region (yellow), the pore helix (red) and outer and inner helix. K^+ ions within the pore are shown as blue circles, water molecules (= the hydration shell) are shown as red circles. **(C)** shows details of the selectivity filter and the coordination of K^+ ions (green) by the carboxylic groups (red) of the filter's amino acids. **(D)** shows how the filter mimics the hydration shell of a K^+ ion (green). **(E)** illustrates how four K^+ ions within the filter stabilize the channel, which leads to the conducting state (right side). With less K^+ ions, the filter collapses. This results in a non-conducting state (left side). Pictures were adapted and modified from MacKinnon 2004.

Stability and function of the potassium channel relies on an adequate amount of K^+ ion in the filter. **Fig. 3 E** illustrates this: with a low amount of K^+ the filter collapses in the middle. The channel is in a non-conducting state. With higher amounts of K^+ the protein is stabilized and, thus, can be in a conducting state (MacKinnon 2004). Experiments with other channel proteins confirms this: SDS-Page analysis with invitro-synthesized Kcv from chlorella virus PBCV-1 revealed the high stability of the tetrameric channel only in the presence of K^+ in the buffer (Shim *et al.* 2007; Pagliuca *et al.* 2007; Chatelain *et al.* 2009).

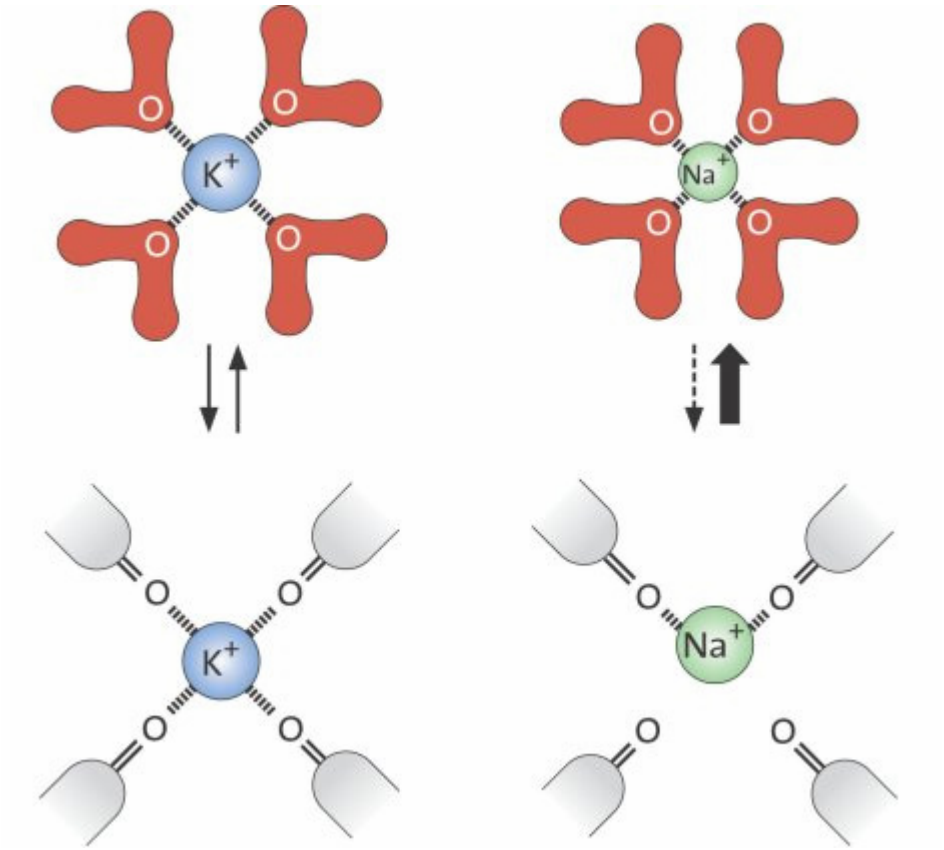

Fig. 4: Selectivity of a potassium channel

Shown are the ions K^+ and Na^+ with their respective hydration shells. The size of the shell is determined by the ions charge and radius (upper pictures). The filter of a potassium channel has the same radius as the hydration shell of K^+. Thus, switching from hydrated state to protein coordinated state is in equilibrium. Na^+ on the other hand has a smaller ion radius than K^+. It is not fully coordinated in by the carboxylic groups of the filter, thus the entering in the filter is energetically not favoured (picture is adapted from http://nobelprize.org/nobel_prizes/chemistry/laureates/2003/chempub4bhigh.jpg).

2.4. Viral ion channels and viral potassium channels

Several viruses have shown to encode for small, ~100 amino acid long, ion channel proteins, e.g. Vpu from HIV-1, M2 from Influenza virus A, NB from Influenza virus B, 6K from Alpha virus and p7 from

HCV (Fischer and Sansom 2002). Some of them, like M2 from Influenza virus are essential for replication, whereas others like the Vpu from HIV-1 seems to have a more accessory character (Strebel 2007). Selectivity among the viral channels can vary from highly selective ion channels as in the case of the proton channel M2, to less selective channels. An example for the latter is Vpu, which only discriminates between monovalent and divalent cations (Schubert *et al*. 1996). Viral ion channels are putative targets for drugs that act as channel blockers. An example for this is the adamantane derivate amantadine, which specifically blocks the M2 channel and was used as flu medicine (Wang *et al.* 1993). Thus, viral ion channels are most interesting study objects in pharmacology. Due to their minimal size they are also most useful as study objects for basic structure-function analyses (Thiel *et al.* 2010b); this will be the subject of this study.

The first viral potassium channel was found in the chlorella virus PBCV-1 (*Paramecium bursaria Chlorella* virus-1), a dsDNA virus (family *Phycodnaviridae*) that infects the *Chlorella* endosymbiont of the "green" *Paramecium bursaria* (Van Etten *et al*. 1983). The channel was designated Kcv for $\underline{K}^+$ channel chlorella virus (**Fig. 5**; Plugge *et al.* 2000). The protein monomer has a size of 94 amino acids and exhibits many structural hallmarks of potassium channels, i.e. two membrane spanning domains, a pore region and a selectivity filter with the highly conserved signature sequence TxxTxGFGD. Further, PBCV-1 Kcv (Kcv_{PBCV-1}) has a turret domain upstream of the pore domain and a 12 amino acid long cytoplasmic N-terminal region and is lacking a cytoplasmic c-terminus (Gazzarrini *et al.* 2003). With these structural properties Kcv_{PBCV-1} resembles the core of potassium channels of higher organisms (Thiel *et al.* 2010b). When expressed in *Xenopus laevis* oocytes, PBCV-1 Kcv generates a distinct conductance with some voltage-dependent features (Abenavoli *et al*. 2009). Kcv_{PBCV-1} is sensitive to channel blockers like Ba^{2+} and amantadine, but shows only a weak sensitivity to tetraethyl ammonium (TEA) (Gazzarrini *et al.* 2003). The channel was also successfully expressed in mammalian HEK293 cells (human embryonic kidney 293 cells), chinese hamster ovary cells (CHO cells) and yeast (Gazzarrini *et al.* 2003; Hertel *et al.* 2010; Chatelain *et al.* 2009). Finally channel activity could also be recorded after reconstitution of purified Kcv protein in planar lipid bilayers (Shim *et al.* 2007; Pagliuca *et al*. 2007). The single channel features measured in the bilayer were similar to those recorded in *Xenopus laevis* oocytes, leaving no doubt that the viral protein is indeed a channel.

The family of chlorella viruses is large and shows an enormous variety. Four families are known so far, each specifically infecting an endosymbiotic *Chlorella* species (Van Etten *et al.* 2010). Three of these chlorella virus families were extensively studied and more than 50 full genomic sequences were obtained (Fitzgerald *et al.* 2007a-c; Van Etten *et al.* unpublished data). Nearly all virus isolates contained a Kcv homolog. To date, only one virus, Pbi virus Fr483, was found to lack a Kcv homolog.

Instead of a channel Pbi virus Fr483 encodes for a potassium transporter (Fitzgerald *et al*. 2007a) that will be discussed in chapter 4.

Chlorella viruses have proven to be a quasi unlimited source for new potassium channel genes with a large diversity in sequence and in structure (Thiel *et al*. 2010b). For example, the Kcv of ATCV-1 (*Acanthocystis turfacea Chlorella* virus-1), prototype of the most recently found chlorella virus group (SAG viruses) (Bubeck and Pfitzner 2005) contains a fully functional potassium channel protein with a size of only 82 amino acids per monomer (Gazzarrini *et al.* 2009). Most interestingly, the functional characteristics of this channel differ a lot from that of Kcv_{PBCV-1}. A bulk of studies has already shown that this structural variability in combination with the small size of the Kcv proteins can help to understand important structure-function principles in these channels. These insights can be extrapolated to complex potassium channels in general, because the Kcv channels represent in many respects the pore module of all K^+ channels. In this context, previous work has already shown the importance of salt-bridge formation for gating (Hertel *et al.* 2010), the anchoring effect of lysine or arginine residues in the TM (Gebhardt *et al*. 2011a) and the stabilization by pi-stacking between the two TMs (Gebhardt *et al.* 2011b).

The finding of K^+ channel genes in viruses has also provided some information on the role of these proteins in the viral life cycle (Thiel *et al.* 2010a). In general, Kcv is expressed as late gene (Yanai-Balser *et al.* 2010) and there is strong evidence that it is part of the virion and plays a fundamental role in the early phase of infection (Thiel *et al.* 2010a). It has been shown that a Kcv channel is required for the infection of *Chlorella* NC64A by the chloroviruses (Thiel *et al.* 2010a; Greiner *et al.* 2009). The assumption is that the virus particle carries the channel in its internal membrane. After attachment to the host cell wall and after digestion of a hole into the wall, the viral internal membrane presumably fuses physically with the host plasma membrane. Due to the activity of Kcv a rapid depolarization of the host plasma membrane is initialized, which further results with secondary events in a rapid loss of K^+ from the host (Neupärtl *et al.* 2008; Agarkova *et al.* 2008). The consequence is that the high internal turgor pressure in the host ($\sim$ 1 Mpa; Thiel *et al.* 2010a) is drastically reduced. This makes the injection of viral DNA into the host cell possible. Also, due to the reduced internal pressure, another virus cannot facilitate the fusion of its membrane with the host membrane and is, thus, not able to infect the cell. Therefore, the competing virus is mutually excluded (Greiner *et al.* 2009).

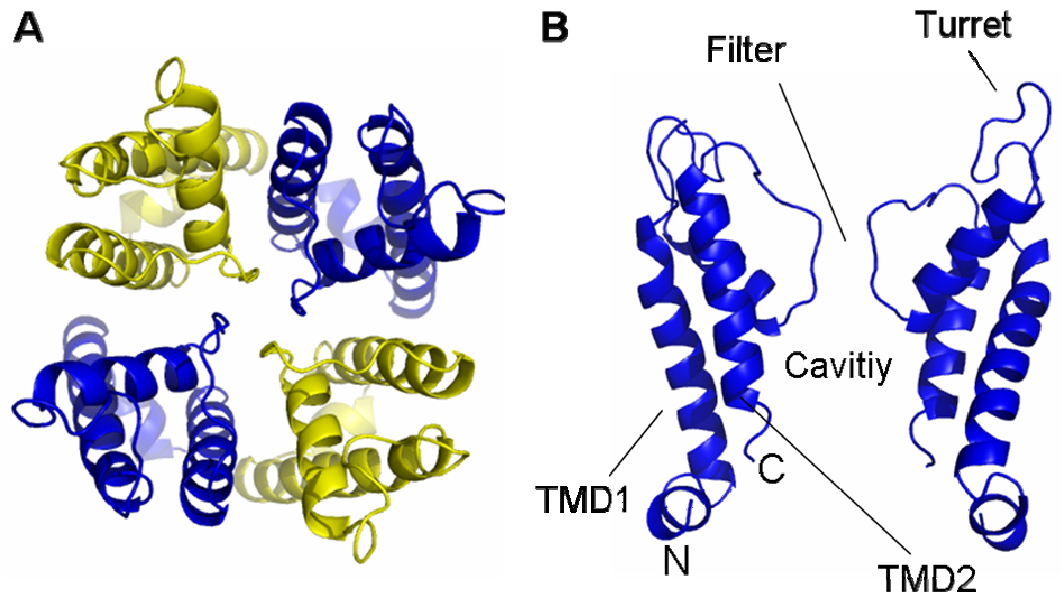

Fig. 5: The viral potassium channel Kcv from PBCV-1

Shown is a cartoon of the Kcv_{PBCV-1} tetramer from above **(A)**. The four subunits are colored in blue and yellow. **(B)** shows two subunits, which oppose each other with the structural features of Kcv, i.e. the pore, the filter, the cavity, the outer transmembrane domain (TMD1) and the inner transmembrane domain (TMD2). N and C mark N- and C-terminus of the protein (according to Tayefeh *et al.* 2009).

2.5. Potassium transporters

Potassium transporters differ from potassium channels with respect to their transport mechanisms and to the fact, that they can transport K^+ in form of a symport or antiport with other ions against a concentration gradient. The energy for this uphill transport of K^+ is derived frequently from a coupling to a downhill transport of H^+. Thus, plant potassium transporters for example can take up K^+ from an environment with μmolar K^+ content. Potassium transporters therefore belong to the high-affinity potassium uptake systems, whereas potassium channels belong to the low affinity potassium uptake systems (Epstein *et al.* 1963; Kim *et al.* 1998; Rodríguez-Navarro and Rubio 2006).

Two major types of potassium transporter, which are discussed in the literature, comprise the HAK/KUP/KT-like potassium transporters and the Ktr/TRK/HKT-like potassium transporters. Because of the general interest in K^+ transporters and the fact, that the examined transporter in this thesis belongs to the HAK/KUP/KT-like potassium transporters, I focus here only on these.

A major difference between potassium channels and potassium transporters is the lower transport rate of the latter, which is in the range of 10^2 to 10^4 ions per second (Hick and Hick 2009). Hence the

transporters are conducting potassium up to four orders of magnitude slower than channels; channels have, for reference, a transport rate of 10^7 to 10^8 ions per second (Hille 2001).

There are only limited data on the structure of HAK/KUP/KT-like potassium transporters since there is, as yet, no crystal structure available. Hydrophobicity plots of the amino acid sequences of HAK/KUP/KT-like potassium transporters suggest that they consist of 10 to 14 transmembrane domains with a large hydrophylic loop between the second and the third transmembrane. The second transmembrane domain contains a sequence (VFGD/IYGD), which is conserved among all HAK/KUP/KT-like potassium transporters and is discussed as putative filter sequence (Rigas *et al.* 2001). It is not yet clear of how many subunits the functional transporter is composed (Rigas *et al.* 2001).

Recently, a crystal structure was published for VbTrkH from *Vibrio parahaemolyticus* (Cao *et al.* 2011), another kind of potassium tranporter proteins from the Ktr/TRK/HKT family. The members of this family form homodimers, which contain four pore forming domains including four different selectivity filter sequences – TTTGAT, AIGGFS, TTAGFT and NNLGPG in the case of VbTrkH (Cao *et al.* 2011). They are, therefore, different from HAK/KUP/KT-like potassium transporters, but striking is the presence of glycine residues in the filter regions of Ktr/TRK/HKT-like potassium transporters, HAK/KUP/KT-like potassium transporters and also potassium channels.

HAK/KUP/KT-like potassium transporters do not discriminate between K^+ and Rb^+, a fact, which made it possible to use Rb^+ in flux experiments (Rodriguez-Navarro and Ramos 1984). Since the turnover rate of transporters is mostly too low for classical electrophysiological recording of the transporter activity the use of flux experiments has proved to be a powerful tool for the characterization of the transport properties these proteins (Kim *et al.* 1998; Rigas *et al.* 2001). The general picture is that HAK/KUP/KT-like potassium transporters preferentially transport potassium. But like K^+ channels they also transport Cs^+ (Zhu and Smolders 2000), but they do not transport NH_4^+ and they are even inhibited by this cation (Rodriguez-Navarro and Rubio 2006). Na^+ is also transported by them albeit with a low affinity (Rodriguez-Navarro and Rubio 2006). HAK/KUP/KT-like potassium transporters facilitate the transport of the ion by a symport with H^+ (Szcserba *et al*. 2009).

Unlike K^+ channels HAK/KUP/KT K^+ transporters are not encoded by all organisms. They can be found in plants (e.g. the Tiny Root hair-1 K^+ transporter (TRH1) in Arabidopsis thaliana (Rigas *et al.* 2001)), in fungi (e.g. the High Affinity K^+ transporter 1 (HAK1) in yeast (Banuelos *et al* 1995)) and in bacteria (e.g. the K^+ Uptake Protein 1 (KUP1) (Schleyer and Bakker 1993)). To date, no animal encoded HAK/KUP/KT K^+ transporter is known.

2.6. Viruses and the evolution of viral genes

Viruses are small biological entities that infect different kinds of cells. They consist of one kind of nucleic acid, which resembles the genome, a protein capsid and in several cases a lipid membrane, which is either within the capsid or surrounding it (Flint *et al*. 2009). In the case of the chlorella viruses the membrane is internal (Van Etten *et al.* 2010). Viruses vary in size, from small viruses with genomes of ~ 10 000 bp, e.g. HIV-1 or Influenza A virus, up to giants like Mimivirus that have a genome larger than 1 Mbp (Raoult et al. 2004). Viruses probably have multiple origins and can not be traced back to a common ancestor, thus they are polyphyletic (Moreira and Lopéz-García 2009).

Viruses depend on a host cell for their replication since they lack an own metabolism; they have a parasitic life style. They are highly diverse with regards to their host specificity and they vary greatly in their replication mechanisms. The classical view is that due to their dependence on a host cell, viruses do not evolve, but "get" evolved (Moreira and Lopéz-García 2009).

Yet, the common thinking about the origin of viral genes is, that they were acquired from the host. Thus, viruses are considered to be "pick-pockets". More recent findings however show that the evolution of viruses is more complex and that some virus species might be at the base of the tree of life (Villareal and DeFillipis 2000; Raoult *et al.* 2004) with some proteins being likely of viral origin. Especially this point renews the discussion on the role of viruses for life and the definition of "life" itself. With the viral potassium channels and transporters, we found interesting candidates, not only for structure-function analyses, but also for addressing questions in evolution within a host-virus system (see chapter 5).

2.7. Aim of the work

Aim of the first part of the present work is the detailed characterization of two related potassium channel proteins. The channels were derived from a unique environment with high natural potassium content. This study will characterize the basic properties of the two channels, such as selectivity and permeability. It also will present a detailed analysis of an unusual steep voltage-dependent block with cesium ions observed in one of the channels.

The second part deals with a viral potassium transporter. Only few chlorella viruses code for a putative potassium transporter, which to date, has not been examined. A first characterization of this protein will be done here. Pbi virus Fr483 so far known is the only chlorella virus lacking a potassium channel.

Here I test the hypothesis that a functional K^+ transporter can substitute for the role of the channel in the infection cycle.

The final part of the thesis is concerned wit the evolution of potassium channels. Together with the group of Prof. Hamacher (TU Darmstadt) we compiled a phylogenetic tree of the viral K^+ channels and the K^+ channels of a host. This is of great interest, because it helps to tackle the question whether the viral channels were picked up from their host or whether they are from another origin. The data stress the view that the Kcv channels were not picked up from the host; they may even be at the origin of the evolution of K^+ channels.

2.8. References

Abenavoli, A., DiFrancesco, M. L., Schroeder, I., Epimashko, S., Gazzarrini, S., Hansen, U. P., Thiel, G., Moroni, A. (2009): Fast and slow gating are inherent properties of the K^+ channel pore module. *J. Gen. Physiol.*, **134**, 219. doi:10.1085/jgp.200910266

Agarkova, I., Dunigan, D. D., Gurnon, J., Greiner, T, Barres, J., Thiel, G., Van Etten, J. L. (2008): Chlorovirus-Mediated Membrane Depolarization of *Chlorella* alters Secondary Active Transport of Solutes. *Journal of Virology*, **82**, 12181. doi:10.1128/JVI.01687-08

Banuelos, M. A., Klein, R. D., Alexander-Bowman, S. J., Rodríguez-Navarro, A. (1995): A potassium transporter of the yeast *Schwanniomyces occidentalis* homologous to the Kup system of *Escherichia coli* has a high concentrative capacity. *EMBO Journal*, **14**, 3021.

Berneche, S. and Roux, B. (2001): Energetics of ion conduction through the K^+ channel. *Nature*, **414**, 73. doi:10.1038/35102067

Blunck, R., Cordero-Morales, J. F., Cuello, L. G., Perozo, E., Bezanilla, F. (2006): Detection of the Opening of the Bundle Crossing in KcsA with Fluorescence Lifetime Spectrocopy Reveals the Existence of Two Gates for Ion Conduction. *JGP*, **128**, 569. doi:10.1085/jgp.200609638

Bubeck, J. A., Pfitzner, A. J. P (2005): Isolation and characterization of a new type of chlorovirus that infects an endosymbiotic Chlorella strain of the heliozoon Acanthocystis turfacea. *Journal of General Virology*, **86**, 2871. doi:10.1099/vir.0.81068

Cao, Y., Jin, X., Huang, H., Derebe, M. H., Levin, E. J., Kabaleeswaran, V., Pan, Y., Punta, M., Love, J., Weng, J., Quick, M., Ye, S., Kloss, B., Bruni, R., Martinez-Hackert, E., Hendrickson, W. A., Rost, B., Javitch, J. A., Rajashankar, K. R., Jiang, Y. and Zhou, M. (2011): Crystal structure of a potassium ion transporter, TrkH. *Nature*, **471**, 336. doi:10.1038/nature09731

Chatelain, F. C., Gazzarrini, S., Fujiwara, Y., Arrigoni, C., Domigan, C., Ferrara, G., Pantoja, C., Thiel, G., Moroni, A., Minor, D. L. (2009): Selection of Inhibitor-Resistant Viral Potassium Channels Identifies a Selectivity Filter Site that Affects Barium and Amantadine Block. *PLoS ONE*, **4**, e7496. doi:10.1371/journal.pone.0007496

Corratgé-Faillie, C., Jabnoune, M., Zimmermann, S., Véry, A.-A., Fizames, C., Sentenac, H. (2010): Potassium and sodium transport in non-animal cells: the Trk/Ktr/HKT transporter family. *Cellular and Molecular Life Sciences*, **67**, 2511. doi:10.1007/s00018-010-0317-7

Cuello, L. G., Jogini, V., Cortes, D. M., Pan, A. C., Gagnon, D. G., Dalmas, O., Cordero-Morales, J. F., Chakrapani, S., Roux, B., Perozo, E. (2010): Structural basis for the coupling between activation and inactivation gates in K^+ channels. *Nature*, **466**, 272. doi:10.1038/nature09136.

Doyle, D. A., Cabral, J. M., Pfuetzner, R. A., Kuo, A., Gulbis, J. M., Cohen, S. L., Chait, B. T., MacKinnon, R. (1998): The Structure of the Potassium Channel: Molecular Basis of K^+ Conduction and Selectivity. *Science*, **280**, 69. doi:10.1126/science.280.5360.69

Epstein, E., Rains, D. W., Elzam, O. E. (1963): Resolution of dual mechanisms of potassium absorption by barley roots. *PNAS*, **49**, 684.

Evans, H. J. and Sorger, G. J. (1966): Role of mineral elements with emphasis on the univalent cations. *Annual Review of Plant Physiology*, **17**, 47.

Fischer, W. B. and Sansom, M. S. P. (2002): Viral ion channels: structure and function. *Biochimica et Biophysica Acta*, **1561**, 27. doi:10.1016/S0304-4157(01)00009-0

Fitzgerald, L.A., Graves, M. V., Li, X., Feldblyum, T., Hartigan, J., and Van Etten, J. L. (2007a): Sequence and annotation of the 314-kb MT325 and the 321-kb FR483 viruses. *Virology*, **358,** 459. doi:10.1016/j.virol.2006.08.034

Fitzgerald, L.A., Graves, M.V., Li, X., Feldblyum, T., Nierman, T. and Van Etten, J. L. (2007b): Sequence and annotation of the 369-kb NY-2A and 345-kb AR158 viruses that infect Chlorella NC64A. *Virology*, **358,** 472. doi:10.1016/j.virol.2006.08.033

Fitzgerald, L.A., Graves, M. V., Li, X., Hartigan, J., Pfitzner, A. J., Hoffart, E., and Van Etten, J. L. (2007c): Sequence and annotation of the 288-kb ATCV-1 virus that infects an endosymbiontic chlorella strain of the heliozoon Acanthocystis turfacea. *Virology*, **362**, 350. doi:10.1016/j.virol.2006.12.028

Flint, S. J., Enquist, L. W., Racaniello, V. R., Skalka, A. M. (2009): Principles of Virology. Third Edition John Wiley & sons, ISBN 1555814433.

Fyles, T. M. (2006): Synthetic ion channels in bilayer membranes. *Chemical Society Reviews*, **36**, 335. doi:10.1039/b603256g

Gazzarrini, S., Severino, M., Lombardi, M., Morandi, M., DiFrancesco, D., Van Etten, J. L., Thiel, G., Moroni, A. (2003): The viral potassium channel Kcv: structural and functional features. *FEBS Lett.*, **552**, 12.

Gazzarrini, S., Kang, M., Abenavoli, A., Romani, G., Olivari, C., Gaslini, D., Ferrara, G., Van Etten, J. L., Kreim, M., Kast, S. M., Thiel, G., Moroni, A. (2009): Chlorella virus ATCV-1 encodes a functional potassium channel of 82 amino acids. *Biochem. J.*, **420**, 295. doi:10.1042/BJ20090095

Gebhardt, M., Hoffgaard, F., Hamacher, K., Kast, S. M., Moroni, A., Thiel, G. (2011a): Membrane Anchoring and Interaction between Transmembrane Domains are Crucial for K^+ Channel Function. *JBC*, **286**, 11299. doi:10.1074/jbc.M110.211672

Gebhardt, M., Tayefeh, S., Baumeister, D., Hertel, B., Greiner, T., Van Etten, J. L., Moroni, A., Kast, S. M., Thiel, G. (2011b): The relevance of Lys snorkeling in the outer transmembrane domain of small viral K^+ channels. Submitted.

Goldstein, S. A. N., Price, L. A., Rosenthal, D. N., Pausch, M. H. (1996): ORK1, a potassium-selective leak channel with two pore domains cloned from *Drosophila melnaogaster* by expression in *Saccharomyces cerevisiae*. *PNAS*, **93**, 13256.

Greiner, T., Frohns, F., Kang, M., Van Etten, J. L., Käsmann, A., Moroni, A., Hertel, B. and Thiel, G. (2009): Chlorella viruses prevent multiple infections by membrane depolarization of the host. *J. Gen Virol.*, **90**, 2033-2039. doi:10.1099/vir.0.010629-0

Hertel, B., Tayefeh, S., Kloss, T., Hewing, J., Gebhardt, M., Baumeister, D., Moroni, A., Thiel, G., Kast, S. M. (2010): Salt bridges in the miniature viral channel Kcv are important for function. *Eur Biophys J*, **39**, 1057. doi:10.1007/s00249-009-0451-z

Hick, C. and Hick, A. (2009): Intensivkurs Physiologie. Third Edition. Elsevier GmbH, Urban & Fischer Verlag, München. ISBN 978-3-437-41893-8

Hille, B. (1970): Ionic channels in nerve membranes. *Progress in Biophysics and Molecular Biology*, **21**, 1.

Hille, B. (2001): Ion Channels of Excitable Membranes. Third Edition. Sinauer Associates, Inc., Sunderland, Massachusetts, USA.

Jan, L. Y. and Jan, Y. N. (1992): Structural elements involved in specific K^+ channel functions. *Annu. Rev. Physiol.*, **54**, 537.

Jiang, Y., Lee, A., Chen, J., Cadene, M., Chait, B. T. and MacKinnon, R. (2002): Crystal structure and mechanism of a calcium-gated potassium channel. *Nature*, **417**, 515.

Jiang, Y., Lee, A., Chen, J., Ruta, V., Cadene, M., Chait, B. and MacKinnon, R. (2003): X-ray structure of a voltage-dependent K^+ channel. *Nature*, **423**, 33.

Kim, E., Myoung Kwak, J., Uozumi, N., Schroeder, J. (1998): *At*KUP1: An Arabidopsis Gene Encoding High-Affinity Potassium Transport Activity. *The Plant Cell*, **10**, 51. doi:10.1105/tpc.10.1.51

Kuo, A., Gulbis, J. M., Antcliff, J. F., Rahman, T., Lowe, E. D., Zimmer, J., Cuthbertson, J., Ashcroft, F. M., Ezaki, T., Doyle, D. A. (2003): Crystal structure of the potassium channel KirBac1.1 in the closed state. *Science*, **300**, 1922.

Long, S. B., Campbell, E. B. and MacKinnon, R. (2005): Crystal structure of a mammalian voltage-dependent Shaker family K^+ channel. *Science*, **309**, 897.

Lu, H., Marti, T., Booth, P. J. (2001): Proline Residues in Transmembrane-Helices Affect the Folding of Bacteriorhodopsin. *J. Mol. Biol.*, **308**, 437.

MacKinnon, R. (2004): Potassium Channels and the Atomic Basis of Selective Ion Conduction. *Bioscience Reports*, **24**, 75.

Mäser, P., Thomine, S., Schroeder, J. I., Ward, J. M., Hirschi, K., Sze, H., Talke, I. N., Amtmann, A., Maathuis, F. J. M., Sanders, D., Harper, J. F., Tchieu, J., Gribskov, M., Persans, M. W., Salt, D. E., Kim, S. A., Guerinot, M. L. (2001): Phylogenetic Relationships within Cation Transporter Families of Arabidopsis. *Plant Physiology*, **126**, 1646.

Miller, C. (1992): Ion channel structure and function. *Science*, **258**, 240.

Moreira, D. and Lopéz-García, P. (2009): Ten reasons to exclude viruses from the tree of life. *Nature Review Microbiology*, **7**, 306.

Neher, E. and Sakmann, B. (1976): Single-channel currents recorded from membrane of denervated frog muscle fibre. *Nature*, **260**, 799.

Neupärtl, M., Meyer, C., Woll, I., Frohns, F., Kang, M., Van Etten, J. L., Kramer, D., Hertel, B., Moroni, A. and Thiel, G. (2008): Chlorella viruses evoke a rapid release of K^+ from host cells during the early phase of infection. *Virology*, **372**, 340. doi:10.1016/j.virol.2007.10.024

Nishida, M., Cadene, M., Chait, B. T. and MacKinnon, R. (2007): Crystal structure of a Kir3.1-prokaryotic channel chimera. *The EMBO Journal*, **26**, 4005. doi:10.1038/sj.emboj.7601828

Pagliuca, C., Goetze, T. A., Wagner, R., Thiel, G., Moroni, A. and Parcej, D. (2007): Molecular Properties of Kcv, a Virus Encoded K^+ Channel. *Biochemistry*, **46**, 1079. doi:10.1021/bi061530w

Parsegian, A. (1969): Energy of an ion crossing a low dielectric membrane: solution to four relevant electrostatic problems. *Nature*, **221**, 844.

Perozo, E., Cortez, D. M., Cuello, L. G. (1999): Structural Rearrangements Underlying K^+-Channel Activation Gating. *Science*, **285**, 73. doi:10.1126/science.285.5424.73

Plugge, B., Gazzarrini, S., Nelson, M., Cerana, R., Van Etten, J. L., Derst, C., DiFrancesco, D., Moroni, A., Thiel, G. (2000): A Potassium Channel Protein Encoded By Chlorella Virus PBCV-1. *Science*, **287**, 1641. doi:10.1126/science.287.5458.1641

Raoult, D., Audic, S., Robert, C., Abergel, C., Renesto, P., Ogata, H., La Scola, B., Suzan, M., Claverie, J.-M. (2004): The 1.2-Megabase Genome Sequence of Mimivirus. *Science*, **306**, 1344. doi:10.1126/science.1101485

Rigas, S., Debrosses, G., Haralampidis, K., Vicente-Agullo, F., Feldmann, K. A., Grabov, A., Dolan, L., Hatzopoulos, P. (2001): *TRH1* encodes a Potassium Transporter Required for Tip Growth in Arabidopsis Root Hairs. *Plant Cell*, **13**, 139.

Rodriguez-Navarro, A. and Ramos, J. (1984): Dual system for potassium transport in Saccharomyces cerevisiae. *J Bacteriol*, **159**, 940.

Rodríguez-Navarro, A. (2000): Potassium transport in fungi and plants. *Biochimica et Biophysica Acta*, **1469**, 1. doi:10.1016/S0304-4157(99)00013-1

Rodríguez-Navarro, A. and Rubio, F. (2006): High-affinity potassium and sodium transport systems in plants. *Journal of Experimental Botany*, **57**, 1149. doi:10.1093/jbx/erj068

Schachtman, D. P., Schroeder, J. I., Lucas, W. J., Anderson, J. A. and Gaber, R. F. (1992): Expression of an inward-rectifying potassium channel by the Arabidopsis KAT1 cDNA. *Science*, **258**, 1654. doi:10.1126/science.8966547

Schleyer, M. and Bakker, E. P. (1993): Nucleotide sequence and 3'-end deletion studies indicate that the K(+)-uptake protein from kup from *Escherichia coli* is composed of a hydrophobic core linked to a large and partially essential hydrophilic C terminus. *J Bacteriol*, **175**, 6925.

Schubert, U., Ferrer-Montiel, A. V., Oblatt-Montal, M., Henklein, P., Strebel, K., Montal, M. (1996): Identification of an ion channel activity of the Vpu transmembrane domain and its involvement in the regulation of virus release of HIV-1 infected cells. *FEBS Letters*, **398**, 12. doi:10.1016/S0014-5793(96)01146-5

Shim, J. W., Yang, M., Gu, L. (2007): In vitro synthesis, tetramerization and and single channel characterization of virus-encoded potassium channel Kcv. *FEBS Letters*, **581**, 1027. doi:10.1016/j.febslet.2007.02.005

Strebel, K. (2007): HIV accessory genes Vif and Vpu. *Advances in Pharmacology*, **55**, 199. doi:10.1016/S1054-3589(07)55006-4

Szczerba, M. W., Britto, D. T., Kronzucker, H. J. (2009): K^+ transport in plants: Physiology and molecular biology. *Journal of Plant Physiology*, **166**, 447. doi:10.1016/j.jplph.2008.12.009

Tayefeh, S., Kloss, T., Kreim, M., Gebhardt, M., Baumeister, D., Hertel, B, Richter, C., Schwalbe, H., Moroni, A., Thiel, G. and Kast, S. M. (2009): Model development for the viral Kcv potassium channel. *Biophys. J.*, **96**, 485. doi:10.1016/j.bpj.2008.09.050

Thiel, G., Moroni, A., Dunigan, D., Van Etten, J. (2010a): Initial Events Associated with Virus PBCV-1 Infection of *Chlorella* NC64A. *Progress in Botany*, **71**, 169. doi:10.1007/978-3-642-02167-1_7

Thiel, G., Baumeister, D., Schroeder, I., Kast. S. M., Van Etten, J. L., Moroni, A. (2010b): Minimal art: Or why small viral K^+ channels are good tools for understanding structure function relations. *Biochimica et Biophysica Acta*, **1808**, 580. doi:10.1016/j.bbamem.2010.04.008

Van Etten, J. L., Burbank, D. E., Kuczmarski, D., Meints, R. H. (1983): Virus infection of culturable chlorella-like algae and development of a plaque assay. *Science*, **219**, 994.

Van Etten, J. L., Lane, L. C., Dunigan, D. D. (2010): DNA viruses: The Really Big Ones (giruses). *Annual Review of Microbiology*, **64**, 83. doi:10.1146/annurev.micro.112408.134338

Villarreal, L.P., DeFilippis, V. R. (2000): A hypothesis for DNA viruses as the origin of eukaryotic replication proteins. *J. Virol.*, **74**, 7079.

Wang, C., Takeuchi, K., Pinto, L. H., Lamb, R. A. (1993): Ion Channel Activity of Influenza A Virus M_2 Protein: Characterization of the Amantadine Block. *Journal of Virology*, **67**, 5585.

Yanai-Balser, G. M., Dunan, G. D., Eudy, J. D., Wang, D., Li, X., Agarkova, I. V., Dunigan, D. D., Van Etten, J. L. (2010): Microarray Analysis of *Paramecium bursaria* Chlorella Virus 1 Transcription. *Journal of Virology*, **84**, 532. doi:10.1128/JVI.01698-09

Zheng, J. and Sigworth, F. J. (1997): Selectivity Changes during Activation of Mutant Shaker Potassium Channels. *J. Gen. Physiol.*, **110**, 101.

Zhu, Y.-G. and Smolders, E. (2000): Plant uptake of radiocaesium: a review of mechanism, regulation and application. *Journal of Experimental Botany*, **51**, 1635.

3. Chapter 2 – Unusual steep voltage dependency for cesium block in miniature viral potassium channels

3.1. Abstract

Here we examine two new interesting Kcv types, Smith Kcv (Kcv_{Smith}) and Next-to-Smith Kcv ($Kcv_{Next\text{-}to\text{-}Smith}$). Both channels were found in viruses, which were isolated in alkaline lakes in central Nebraska/USA. The two channels exhibit a similar primary amino acid sequence differing in 11 out of 82 amino acids. Both channels are fully functional with selectivity for K^+; they also conduct Rb^+ and NH_4^+, but no Na^+ and Li^+. The selectivity sequence for cations of the two channels differs, even though they have an identical filter region. Mutational studies revealed that an exchange of a single amino acid in the outer transmembrane domain already inverted in $Kcv_{Next\text{-}to\text{-}Smith}$ the preference for K^+ and Rb^+ towards that of Kcv_{Smith}, implying a relevance of the outer transmembrane domain for selectivity. The two channels are sensitive to Ba^{2+} and Cs^+, but not to TEA or amantadine. Both channels are fully blocked by Ba^{2+} and the responsible binding site for Ba^{2+} in the filter region could be identified by site-directed mutagenesis. Most notable is the difference in the mode of Cs^+ block. While Kcv_{Smith} is blocked in a moderate voltage-dependent manner, $Kcv_{Next\text{-}to\text{-}Smith}$ exhibits a Cs^+ block with an extremely steep voltage-dependency. The channel completely closes at negative voltages over a voltage window of less than 5 mV. Mutational studies, in which $Kcv_{Next\text{-}to\text{-}Smith}$ is mutated towards th sequence Kcv_{Smith}, show that the exchange of a single amino acid residue again in the first transmembrane domain of the protein already causes a dramatic change in the voltage dependence of the Cs^+ block. The results of this study imply a role of the outer transmembrane domain also in the mechanism of Cs^+ block.

3.2. Introduction

Chlorella viruses are large, plaque-forming dsDNA viruses, which infect certain types of unicellular green algae (VanEtten *et al.* 1983). They are large in physical size (~200 nm) and in genome size (>300 kbp). They are abundant all over the world in fresh waters with a high variety in plaque morphology and in their genetic features. Chlorella viruses have also been shown to encode for a couple of interesting genes, among which are a variety of membrane transport proteins such as an aquaglyceroporin (Gazzarrini *et al.* 2006), a Calcium-ATPase (Bonza *et al.* 2010), a potassium transporter (see chapter 3; Fitzgerald *et al*. 2007a) and a potassium channel (Plugge *et al.* 2000). Especially the potassium channels have been studied intensively. Three different types of this channel, the so-called Kcv (from $\underline{K}^+$ channel chlorella virus), have been found. The three different types of channels correspond to the three chlorovirus families studied so far (NC64A viruses, Pbi viruses and SAG viruses). Each of the three K^+ channel types has unique structural and functional features together with a high natural variability within each type of channel (Kang *et al.* 2004b; Gazzarrini *et al* 2004). Common to all three types of Kcv is that they contain the hallmarks of a potassium channel, i.e.

two transmembrane spanning domains (TMs), a pore region (pore), a filter region (filter) with the highly conserved signature sequence (TxxTxGF/YGD) and a turret domain (Gazzarrini *et al.* 2003). Also common to the three types of Kcv channels is their small size, meaning that a subunit is made of < 95 amino acids. The Kcv channel encoded by virus ATCV-1 – Kcv_{ATCV-1} - is so far the smallest of its kind; it has a size of 82 amino acids per monomer only (Gazzarrini *et al.* 2009). For comparison, K^+ channels found in eukaryotes, e.g. Kir 7.1 from *Homo sapiens* has a size of 375 amino acids per monomer (Krapivinski *et al.* 1998) and K^+ channels found in bacteria, e.g. KcsA from *Streptomyces lividans*, the reference channel for potassium channel structure, has a size of 160 amino acids per monomer (Schrempf *et al.* 1995).

In several studies it has been shown that the Kcv channels are functional and that they reveal many of the functional features of typical K^+ channels when expressed in a variety of heterologous expression systems, e.g. *Xenopus laevis* oocytes (Plugge *et al.* 2000, Kang *et al.* 2004a), chinese hamster ovary cells (CHO cells) (Gazzarrini *et al.* 2003), human embryonic kidney cells (HEK293 cells) (Hertel *et al.* 2010) and the *Saccharomyces cerevisiae* mutant strain SGY1528 (Chatelain *et al.* 2009).

The small size of the proteins combined with their robust function implies that the Kcv channels are representing the core unit of all known K^+ channels. An extensive phylogenetic comparison of the Kcv channels with the K^+ channels of the virus host *Chlorella* NC64A implies, that the viral channels make up a clade of their own, which is clearly separated from that of the host channels. This finding fosters the speculation that the miniature Kcv channels could even be the origin of all K^+ channel pores (see chapter 4; Hamacher *et al.* 2011).

The high natural variety of chlorella viruses together with the variability within the Kcv protein, makes the isolation of chlorella viruses from different environments interesting for structure-function studies. Both, isolation of the viruses and the isolation of the Kcv gene, are common lab procedures and are relatively easy to achieve. In the context of this study, viruses were isolated from several unique environments in central Nebraska, with a high amount of natural potassium. In the present study we choose the virus, which was isolated from the Smith lake (N 41° 47' 27.10", W 102° 31' 42.60", 3854 ft above sea level) and the virus that was isolated from a ditch running near the Smith lake (=Next-to-Smith). Initial characterizations of the two viruses showed that they are different in their plaque morphology (James Van Etten/USA, personal communication). This holds true for a mutual comparison between the two viruses, but also between these two viruses and other chlorella viruses. The main difference to other chlorella viruses is related to the fact, that the two new isolates generate a fuzzy plaque morphology (James Van Etten/USA, personal communication), while the majority of

the chlorella viruses forms round plaques. Because of the unique plaque morphology of the two viruses, it was already assumed that they might differ a lot also on the genetic level. Indeed, the isolation and sequencing of their Kcvs revealed that the two channel proteins differ in 11 out of 82 amino acids from each other.

Here we characterize the two channel proteins from the new virus isolates. It is expected that the structural variability in the channel proteins, as well as the extreme environment from which they were isolated, provide new insights in general and habitat specific structure-function correlates in K^+ channels.

3.3. Results

Sequence and structure

Smith Kcv (Kcv_{Smith}) and Next-to-Smith Kcv ($Kcv_{Next\text{-}to\text{-}Smith}$) homologues could be amplified using degenerated primers that were designed on the basis of $Kcv_{ATCV\text{-}1}$ and Kcv_{TN603} sequences. The PCR with both viruses, virus Smith and virus Next-to-Smith, resulted in a single band. The PCR products were cloned and sequenced. For both PCR products we found a sequence that is homologous to $Kcv_{ATCV\text{-}1}$ (**Fig. 6 A**). An alignment of the two proteins with other Kcv homologues is shown in **Fig. 6 A**, the differences between the two proteins can be seen in **Fig. 6 B**.

The alignment in **Fig. 6 A** shows the high similarity of the new channel isolates with other Kcvs. The latter were examined in earlier studies and several of them have already been shown to be functional (Gazzarrini *et al.* 2004; Gazzarrini *et al.* 2006; Gazzarrini *et al.* 2009; Kang *et al.* 2004a; Kang *et al.* 2004b).

Kcv_{Smith} and $Kcv_{Next\text{-}to\text{-}Smith}$ only differ in eleven amino acids (**Fig. 6 B**). Pore and filter region are identical; the majority of the deviations, which are all conservative or semiconservative exchanges, are found within the two transmembrane domains.

Fig. 7 shows an alignment of either Kcv_{Smith} or $Kcv_{Next\text{-}to\text{-}Smith}$ with $Kcv_{ATCV\text{-}1}$ and $Kcv_{PBCV\text{-}1}$ for comparisons, which will become important later.

A

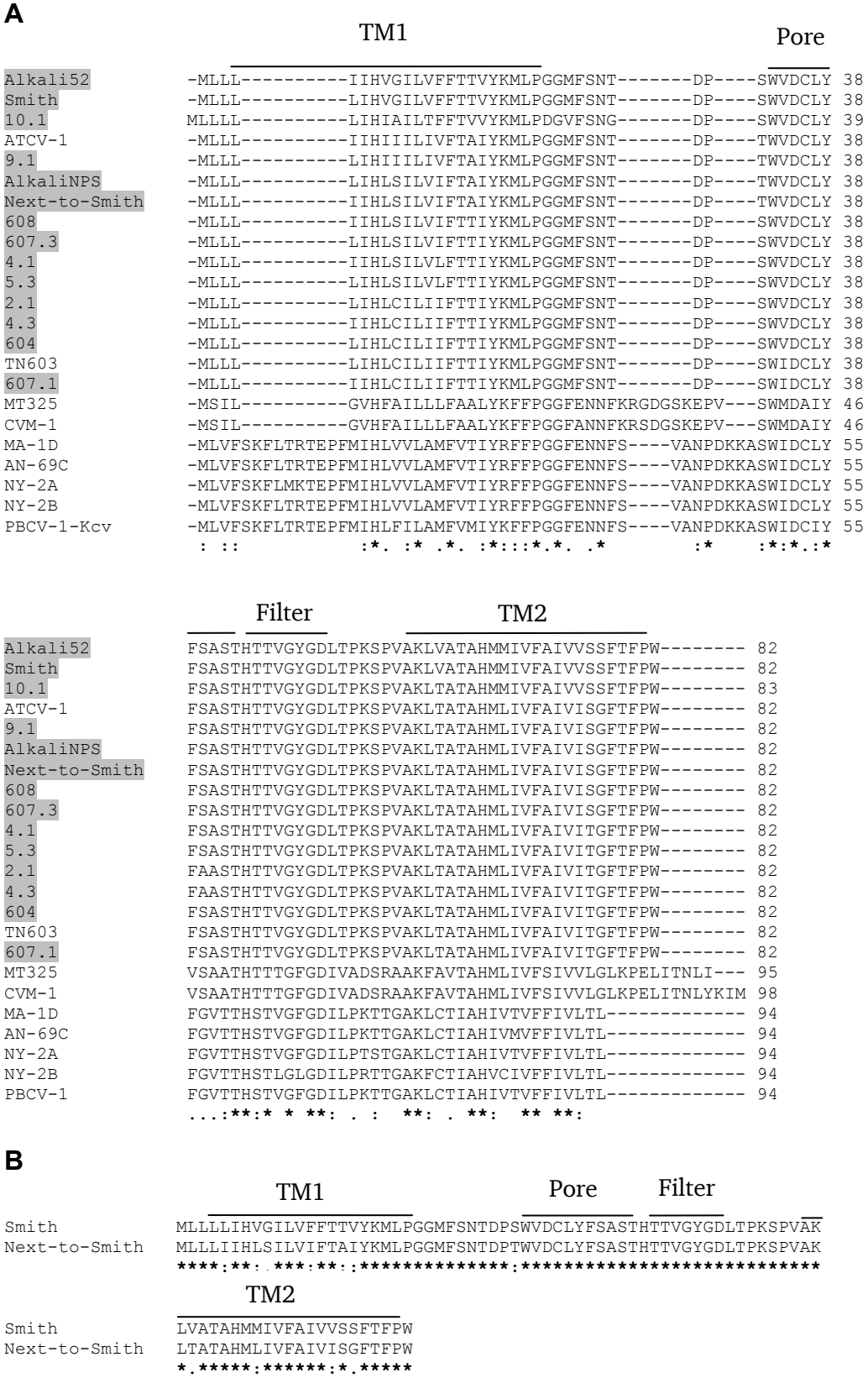

B

Figure 6: Sequence alignment of selected natural Kcv variants

(A) Sequence alignment of selected natural Kcv variants including the prototype chlorella virus K^+ channel Kcv_{PBCV-1} by ClustalW (http://www.ebi.ac.uk/Tools/clustalw2). First and second transmembrane domain (TM1 and TM2), pore helix (Pore) and selectivity filter (Filter) sequences are highlighted by horizontal lines. Assignment of these regions follows from a consensus among the prediction program TMHMM (http://www.cbs.dtu.dk/services/ TMHMM/) as well as structural data of

the molecular dynamics-refined model of Kcv_{PBCV-1} (Tayefeh *et al.* 2009). Asteriks and colons indicate identical and conserved residues respectively. Sequences derived from new virus isolates are highlighted in grey. **(B)** Sequence alignment of Kcv_{Smith} and $Kcv_{Next\text{-}to\text{-}Smith}$ for a direct comparison. Description is the same as in **(A)**.

A

```
Kcv_ATCV-1          MLLLIIHIIILIVFTAIYKMLPGGMFSNTDPTWVDCLYFSASTHTTVGYGDLTPKSPVAK 60
Kcv_Smith           MLLLLIHVGILVFFTTVYKMLPGGMFSNTDPSWVDCLYFSASTHTTVGYGDLTPKSPVAK 60
                    ****:**: **:.**::***************:*****************************

Kcv_ATCV-1          LTATAHMLIVFAIVISGFTFPW 82
Kcv_Smith           LVATAHMMIVFAIVVSSFTFPW 82
                    *.*****:******:*.*****
```

B

```
Kcv_ATCV-1          MLLLIIHIIILIVFTAIYKMLPGGMFSNTDPTWVDCLYFSASTHTTVGYGDLTPKSPVAK 60
Kcv_Next-to-Smith   MLLLIIHLSILVIFTAIYKMLPGGMFSNTDPTWVDCLYFSASTHTTVGYGDLTPKSPVAK 60
                    *******: **::**********************************************

Kcv_ATCV-1          LTATAHMLIVFAIVISGFTFPW 82
Kcv_Next-to-Smith   LTATAHMLIVFAIVISGFTFPW 82
                    **********************
```

C

```
Kcv_Next-to-Smith   MLLL----------IIHLSILVIFTAIYKMLPGG---MFSNTDP----TWVDCLYFSAST 43
Kcv_Smith           MLLL----------LIHVGILVFFTTVYKMLPGG---MFSNTDP----SWVDCLYFSAST 43
Kcv_PBCV-1          MLVFSKFLTRTEPFMIHLFILAMFVMIYKFFPGGFENNFSVANPDKKASWIDCIYFGVTT 60
                    **::          :**: **.:*. :**::***    ** ::*    :*:**:**..:*

Kcv_Next-to-Smith   HTTVGYGDLTPKSPVAKLTATAHMLIVFAIVISGFTFPW 82
Kcv_Smith           HTTVGYGDLTPKSPVAKLVATAHMMIVFAIVVSSFTFPW 82
Kcv_PBCV-1          HSTVGFGDILPKTTGAKLCTIAHIVTVFFIVLTL----- 94
                    *:***:**: **:. *** : **:: ** **::
```

Fig. 7: Kcv_{Smith} and $Kcv_{Next\text{-}to\text{-}Smith}$ aligned with $Kcv_{ATCV\text{-}1}$ and $Kcv_{PBCV\text{-}1}$

Sequence alignment of Kcv_{Smith} **(A)** and $Kcv_{Next\text{-}to\text{-}Smith}$ **(B)** with $Kcv_{ATCV\text{-}1}$ by ClustalW (http://www.ebi.ac.uk/Tools/clustalw2). **(C)** Sequence alignment of Kcv_{Smith}, $Kcv_{Next\text{-}to\text{-}Smith}$ and $Kcv_{PBCV\text{-}1}$. Amino residues of interest are highlighted in grey. Asteriks and colons indicate identical and conserved residues respectively.

General features of Kcv_{Smith} and $Kcv_{Next\text{-}to\text{-}Smith}$

Kcv_{Smith} and $Kcv_{Next\text{-}to\text{-}Smith}$ were heterologously expressed in human embryonic kidney (HEK293) cells as GFP-fusion proteins (Kcv_{Smith}::GFP and $Kcv_{Next\text{-}to\text{-}Smith}$::GFP) and studied with the patch-clamp technique in whole-cell configuration. Untransfected cells were used as negative control. Cells expressing $Kcv_{ATCV\text{-}1}$::GFP, a homologous Kcv derived from a virus found in Germany (Bubeck and Pfitzner 2005, Gazzarrini *et al.* 2009), was used as positive control. $Kcv_{ATCV\text{-}1}$ is from the same Kcv type as Kcv_{Smith} and $Kcv_{Next\text{-}to\text{-}Smith}$. It differs from Kcv_{Smith} in 12 amino acids and from $Kcv_{Next\text{-}to\text{-}Smith}$ in four amino acids (**Fig. 7 A** and **B**). The pipette solution contained 100 mM K^+ and the bath solution 50 mM K^+. Currents were elicited with a standard pulse protocol comprising steps of a holding voltage of 0 mV to test voltages between -160 mV and +80 mV with 20 mV increments and a post pulse to -80 mV (see Materials and Methods).

Fig. 8 summarizes exemplary current responses and I/V relations for the control and the examined channels. Untransfected HEK293 cells generated under the standard test conditions almost no inward current and only little outward current. This is typical for the endogenous currents of these cells (Jiang *et al.* 2002). Cells expressing $Kcv_{ATCV\text{-}1}$::GFP, in contrast, exhibited a large inward current with an inactivation at voltages < -100 mV and a significant increase in the outward currents. The characteristics of the $Kcv_{ATCV\text{-}1}$ generated current with the negative slope conductance at negative voltages is similar to that found in *Xenopus laevis* oocytes expressing the same channel (Gazzarrini *et al*. 2009). **Fig. 8** shows a typical recording of a HEK293 cell expressing $Kcv_{Next\text{-}to\text{-}Smith}$::GFP. The current response as well as the I/V relation shows that $Kcv_{Next\text{-}to\text{-}Smith}$ behaves very similar to $Kcv_{ATCV\text{-}1}$. This was the case in about 50 % of the measurements (n > 30 cells), whereas in other measurements no negative slope conductance at negative voltages appeared (**Fig. 9**). This effect appeared to be temperature-dependent and will be discussed below.

Kcv_{Smith} was examined under the same conditions. Cells expressing Kcv_{Smith}::GFP generated a conductance which is much larger than recorded in non-transfected cells. But while $Kcv_{Next\text{-}to\text{-}Smith}$ showed the voltage dependent inactivation at negative voltages, Kcv_{Smith} did not in 100 % of the cells examined (**Fig. 8**).

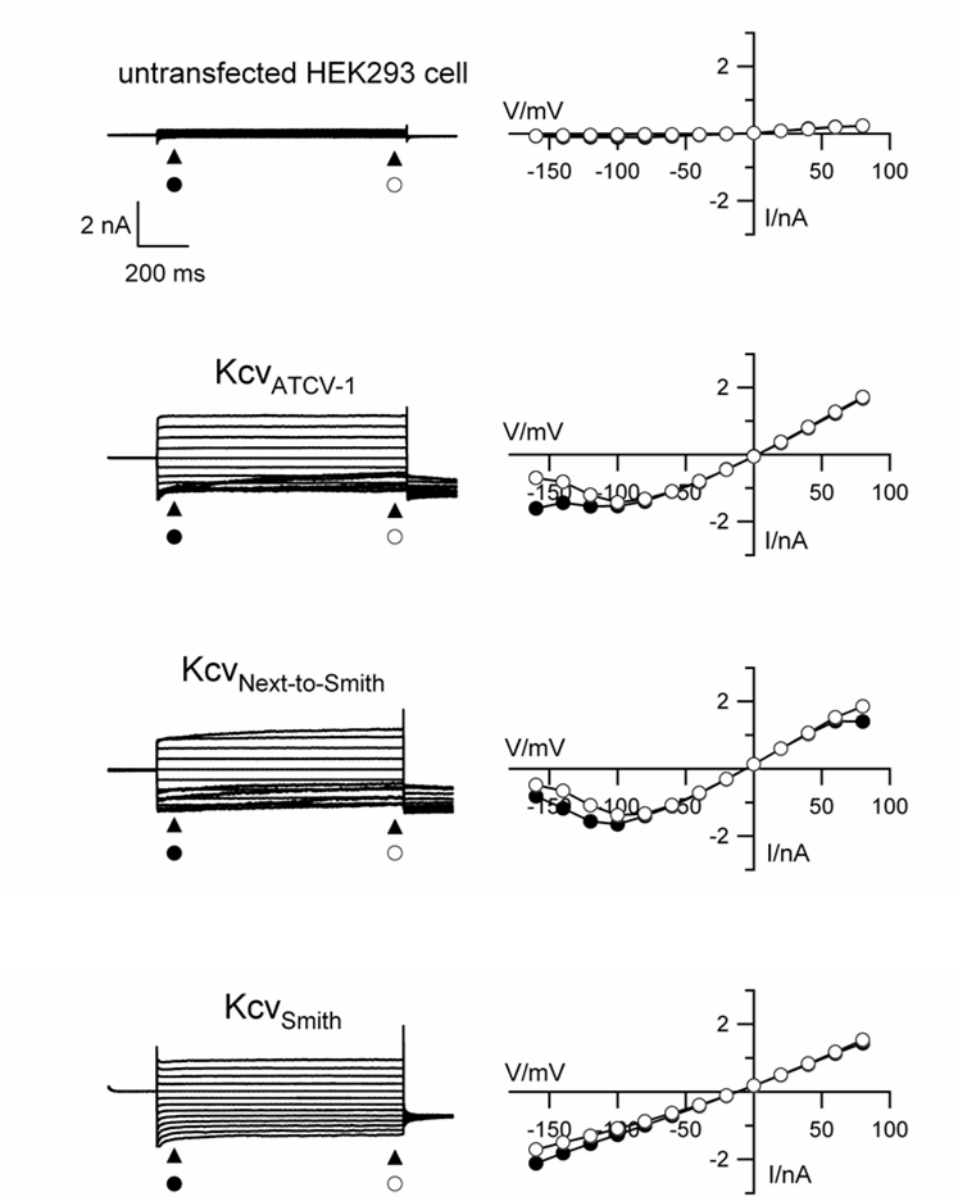

Figure 8: Kcv$_{Smith}$ and Kcv$_{Next-to-Smith}$ are functional ion channels

Exemplary current responses of an untransfected HEK293 cell and HEK293 cells transfected with either Kcv$_{ATCV-1}$::GFP, Kcv$_{Smith}$::GFP or Kcv$_{Next-to-Smith}$::GFP (left side) to a standard pulse protocol with test voltages between -160 mV and +80 mV with 20 mV increments. The corresponding I/V curves of the instantaneous (filled circles) and the steady-state (open circles) currents are shown on the right. Data were collected in a 50 mM K^+ bath solution.

Effect of temperature on the current generated by Kcv$_{Next-to-Smith}$

In about 50 % of HEK293 cells expressing Kcv$_{Next-to-Smith}$::GFP we observed a slow inactivation at negative voltages under standard conditions with 50 mM K^+ in the bath (**Fig. 9**). Previous studies have shown an effect of the temperature on the current of Kcv$_{PBCV-1}$ (Baumeister 2010). To test the effect of temperature on the kinetics of the current, we varied the temperature of the bath solution during the measurements. **Fig. 10** shows the current responses of a HEK293 cell expressing Kcv$_{Next-to-Smith}$::GFP to

a standard protocol at two different temperatures; the corresponding I/V relations at the temperature extremes (21 °C and 14 °C) are also shown. At 21 °C we observed a clear inactivation of the currents at negative voltages. This inactivation decreased towards lower temperatures and increased again with higher temperatures. This phenomenon was observed in three cells tested. In three other cells tested we observed almost no effect of the temperature on the current in a range from 14 °C to 40 °C (not shown).

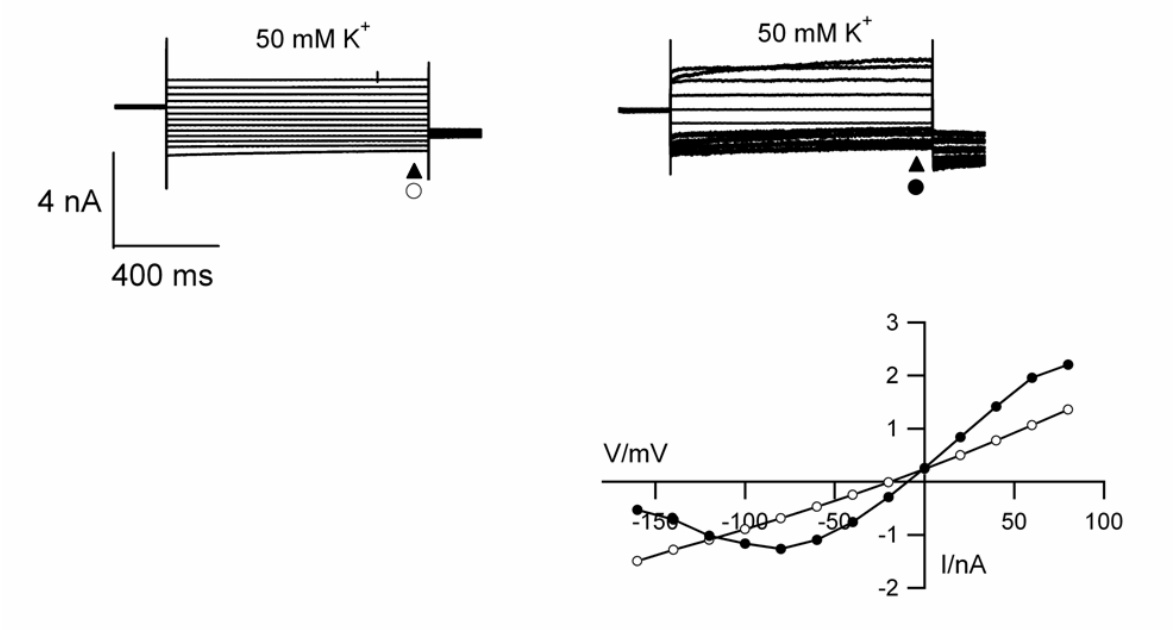

Fig. 9: $Kcv_{Next\text{-}to\text{-}Smith}$ shows two different current responses under the same conditions

Current responses from two different HEK293 cells expressing $Kcv_{Next\text{-}to\text{-}Smith}$::GFP in a 50 mM K^+ bath solution to a standard pulse protocol with test voltages between -160 mV and +80 mV with 20 mV increments. The corresponding I/V relations of the steady-state currents are shown in the right panel.

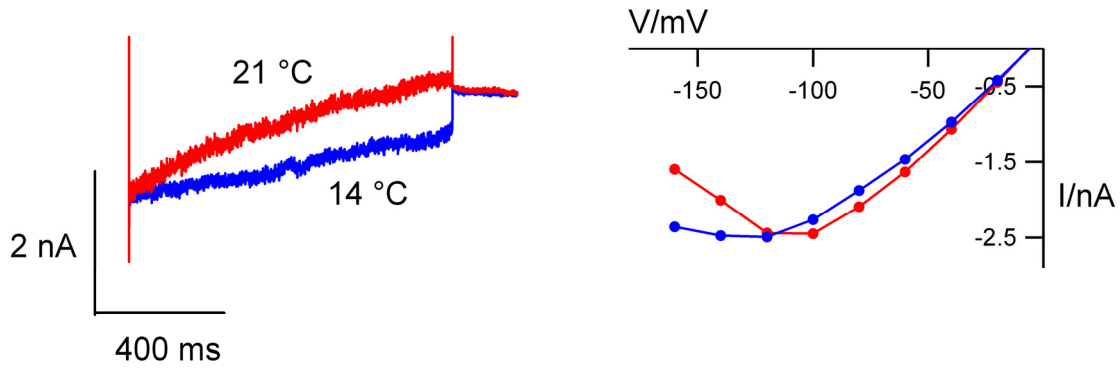

Fig. 10: Temperature-dependent inactivation of $Kcv_{Next\text{-}to\text{-}Smith}$

Exemplary current responses of a HEK293 cell expressing $Kcv_{Next\text{-}to\text{-}Smith}$::GFP in a 50 mM K^+ bath solution to a standard pulse protocol from 0 to -160 mV at 21 °C (red) and 14 °C (blue) (left side) and the corresponding I/V relation of the steady-state current (right side).

Selectivity

To test the ion selectivity of Kcv_{Smith} and $Kcv_{Next\text{-}to\text{-}Smith}$, HEK293 cells expressing either of the two channels were bathed in solutions with K^+ concentrations varying from 5 mM to 100 mM. An increase in K^+ concentration resulted in a progressive negative shift of the current reversal voltage for $Kcv_{Next\text{-}to\text{-}Smith}$ (**Fig. 11 A** and **C**). An interesting effect occurs at low K^+ concentrations (5 and 10 mM), where we observed a time dependent decrease of the current at negative voltages (**Fig. 11 B**). Linear fits of the reversal potential V_r versus $\log[K^+]_{bath}$ either with or without the values for 5 and 10 mM K^+ (**Fig. 11 D**) reveal different slopes: When we include the two low K^+ concentrations the slope is 24.5 mV per 10 fold difference in K^+ concentration. This low sub Nernstian slope is most likely due to the fact that low K^+ concentrations also affect the channel in a way which is not directly depending on the conductance only. A fit of the remaining data gives a slope of 76.1. This slope is higher than the theoretically expected slope of 59.2 mV. The reason for this high slope is probably related to the low number of data points which are used for the fit. For this reason we draw a line with the theoretical slope of 59 mV through the data. The resulting plot shows that this line is a good approximation of the data points and it demonstrates that the channel behaves like a K^+ channel.

The data for Kcv_{Smith} are shown in **Fig. 12**. The increase in K^+ concentration starting with 5 mM resulted in a progressive shift of the current reversal voltage (**Fig. 12 B** and **C**). A linear fit of the reversal potential versus $\log[K^+]_{bath}$ results in a linear relation (**Fig. 12 D**). The data were fitted either with or without the value at 5 mM K^+ to test if a depletion effect occurs at low K^+ concentrations. This resulted in two linear slopes with a slope of 36.7 (with the 5 mM K^+ value, red) and a slope of 45.2 (without the 5 mM K^+ value, blue) (**Fig. 12 D**). The two slopes do not differ as strong as in the case of $Kcv_{Next\text{-}to\text{-}Smith}$. The time dependent decrease of the current at low K^+ concentrations, which was observed for $Kcv_{Next\text{-}to\text{-}Smith}$ at negative voltages, did also not occur. Instead, we observed a slight inactivation at positive voltages > 40 mV (**Fig. 12 B**).

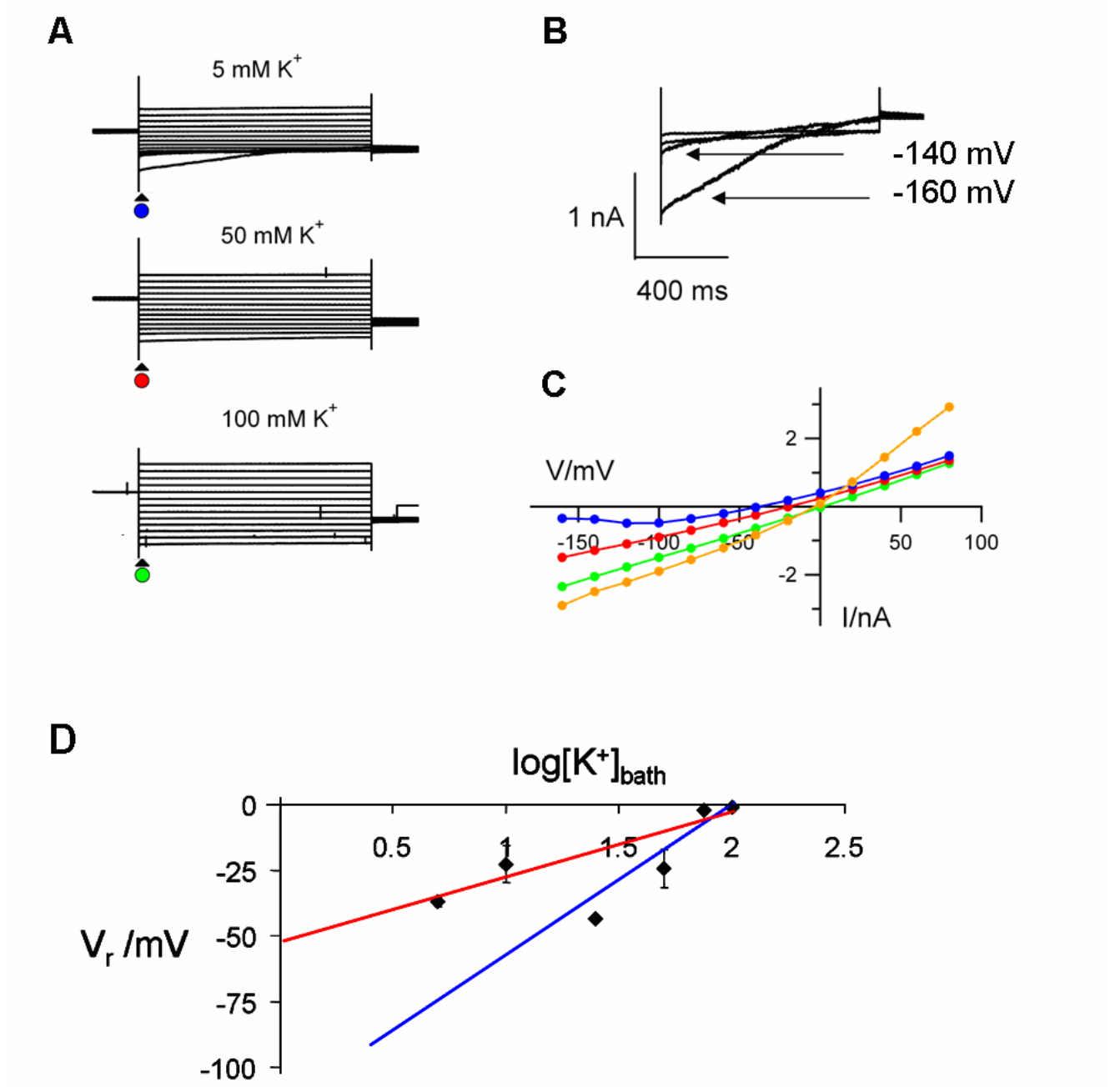

Fig. 11: Selectivity of $Kcv_{Next\text{-}to\text{-}Smith}$

(A) Current responses of a HEK293 cell expressing $Kcv_{Next\text{-}to\text{-}Smith}$::GFP in bath solutions containing 5 (blue circle), 50 (red circle) and 100 mM K^+ (green circle) to a standard pulse protocol by a standard pulse protocol as in **Fig. 8**. The corresponding I/V relations of the instantanous currents are plotted in **(C) (B)** Details of the current response with a decrease in current at negative voltages in 5 mM K^+ from **(A)**. **(D)** Mean values (n ≥ 5 ± S.D.) of reversal potential V_r plotted as a function of $\log[K^+]_{bath}$ with $[K^+]_{bath}$ = 5, 10, 25, 50, 75 and 100 mM K^+. The line is a linear fit of the data either with (red) or without (blue) the values obtained in 5 and 10 mM K^+ bath solutions.

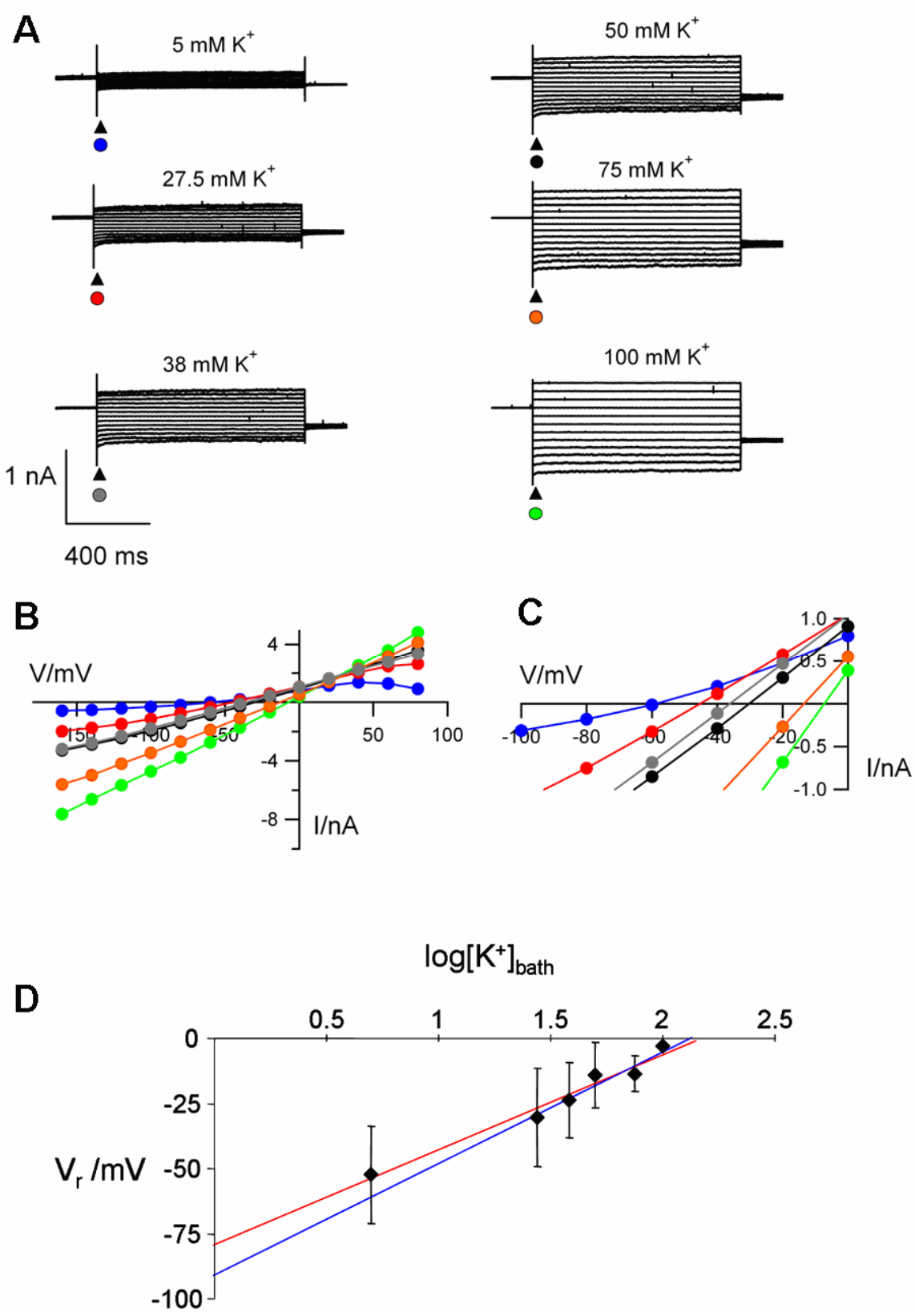

Fig. 12: Selectivity of Kcv_{Smith}

(A) Current responses of a HEK293 cell expressing Kcv_{Smith}::GFP in bath solutions containing 5 (blue circle), 27.5 (red circle), 38 mM (grey circle), 50 (black circle), 75 (orange circle) and 100 mM K^+ (green circle) to a standard pulse protocol by a standard pulse protocol with test voltages as in **Fig. 8**. The corresponding I/V relations of the instantanous currents are plotted in **(B)**. **(C)** Mean values (n ≥ 5 ± S.D.) of reversal potential V_r plotted as a function of $log[K^+]_{bath}$. The line is a linear fit to the data either with (red) or without (blue) the value in 5 mM K^+.

Selectivity of $Kcv_{Next\text{-}to\text{-}Smith}$

To study the permeability of $Kcv_{Next\text{-}to\text{-}Smith}$ to other cations, we exchanged the 50 mM K^+ in the bath solution for either 50 mM Na^+, Li^+, Rb^+ or NH_4^+. The replacement of K^+ by other cations resulted in the current responses shown in **Fig. 13 A** with the corresponding I/V relation (**Fig. 13 B** and **C**). Replacing K^+ for Rb^+ resulted in a shift of the reversal potential to more positive voltages. This means $Kcv_{Next\text{-}to\text{-}Smith}$ transports Rb^+ better than K^+. This is not in agreement with findings for $Kcv_{ATCV\text{-}1}$ expressed in *Xenopus laevis* oocytes, where the permeability for K^+ is higher than for Rb^+ (Gazzarrini *et al.* 2009). In a solution containing Li^+, Na^+ or NH_4^+ we found a shift of the reversal potential to more negative values and a corresponding decrease of the inward current, meaning that the permeability of the channel for these ions is lower than for K^+. Li^+ and NH_4^+also show a lower outward current, meaning the two ions also inhibit the channel. Na^+ on the other hand does not inhibit the channel. The estimated reversal potentials, summarized as mean value of $n \geq 5$ cells (**Fig. 13 D**) are comparable to those found for $Kcv_{ATCV\text{-}1}$ (Gazzarrini *et al*. 2009). From these data the permeability sequence of $Kcv_{Next\text{-}to\text{-}Smith}$ can be summarized as followed: $Rb^+ >> K^+ >> NH_4^+ > Li^+ > Na^+$.

For NH_4^+ an interesting effect occurred: **Fig. 14** shows the current response of a HEK293 cell transfected with $Kcv_{Next\text{-}to\text{-}Smith}$::GFP in a 50 mM NH_4^+ bath solution and the corresponding I/V relation. An inactivation of the channel occurs at positive voltages > 80 mV. This has not been seen with a 50 mM K^+ solution and was reversible after exchanging the 50 mM NH_4^+ bath solution for 50 mM K^+ bath solution.

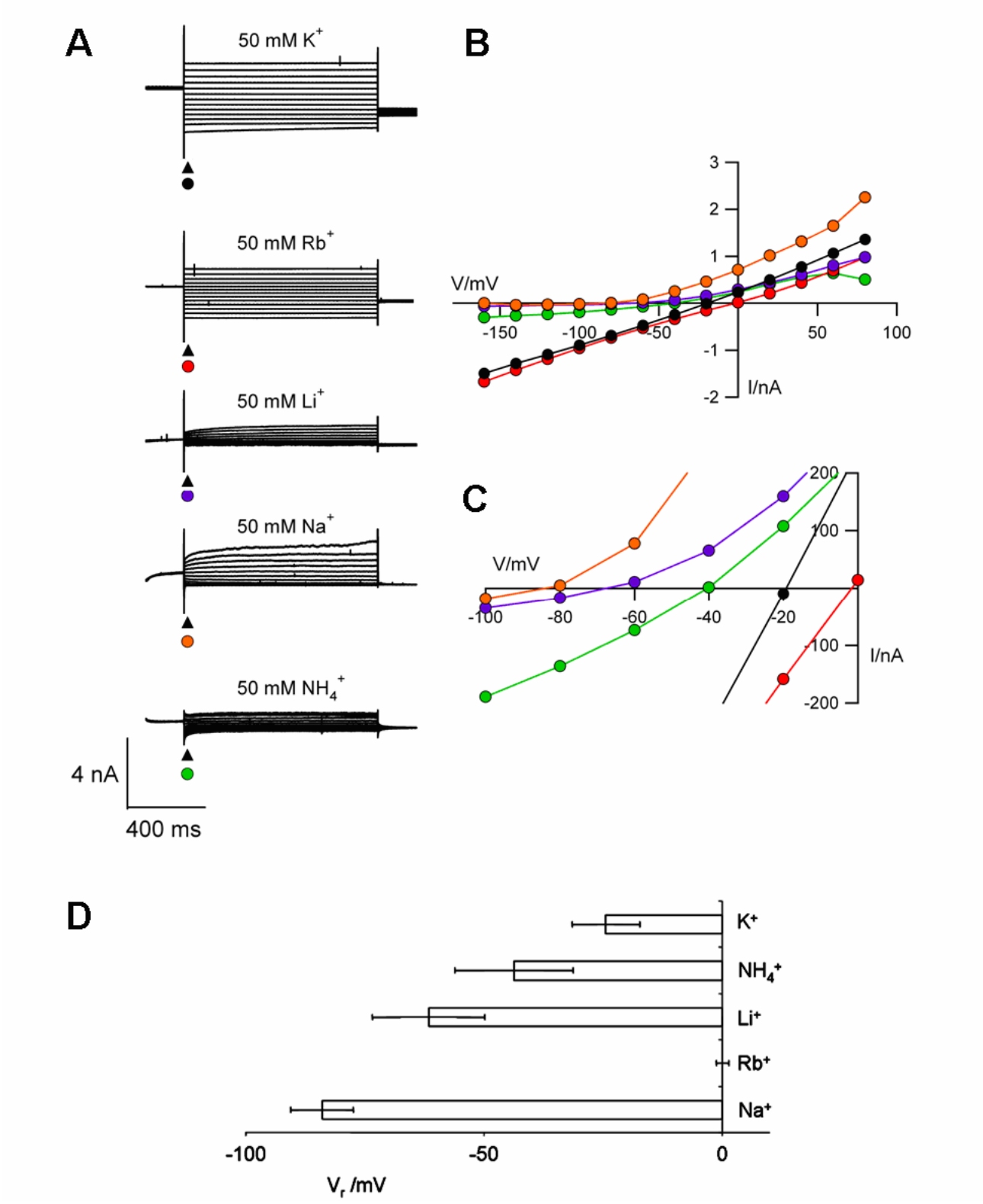

Fig. 13: Selectivity of $Kcv_{Next\text{-}to\text{-}Smith}$

(A) Exemplary current responses of a HEK293 cell transfected with $Kcv_{Next\text{-}to\text{-}Smith}$::GFP in bath solution with different cations (50 mM) to a standard pulse protocol as in **Fig. 8**. **(B)** I/V relation of the instantanous currents measured in **(A)** with an enlargement in **(C)**. **(D)** summarizes the mean values (n ≥ 5 ± S.D.) of V_r for the cations tested.

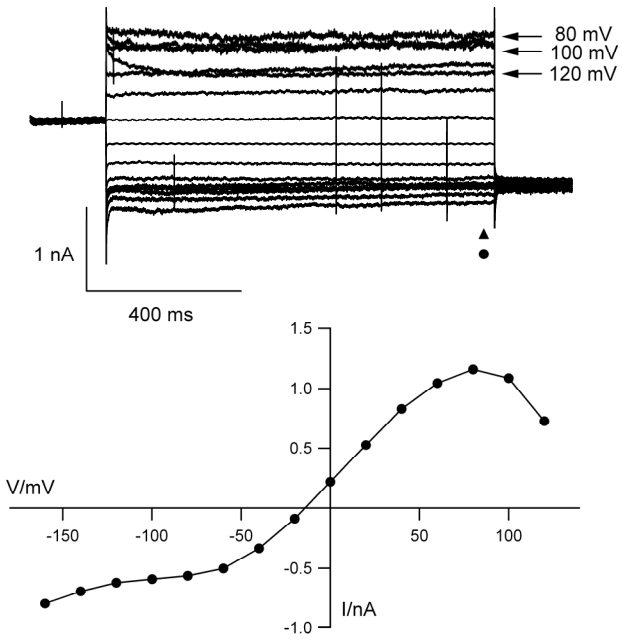

Fig. 14: $Kcv_{Next\text{-}to\text{-}Smith}$ shows inactivation at high positive voltages with ammonium

Exemplary current response of a HEK293 cell transfected with $Kcv_{Next\text{-}to\text{-}Smith}$::GFP in a bath solution containing 50 mM NH_4^+ to a standard pulse protocol with test voltages as in **Fig. 8** and the corresponding I/V relation of the steady-state currents.

Selectivity of Kcv_{Smith}

To study the Selectivity of Kcv_{Smith} to other cations, we exchanged the 50 mM K^+ in the bath solution for either 50 mM Na^+, Li^+, Rb^+ or NH_4^+ in the same way as for $Kcv_{Next\text{-}to\text{-}Smith}$. The Replacement of K^+ by other cations resulted in the current responses shown in **Fig. 15**. Replacing K^+ for Rb^+ did not result in a shift of the reversal potential. This means Kcv_{Smith} transports both, Rb^+ and K^+ with the same preference. In a solution containing Li^+, Na^+ or NH_4^+ we found a shift of the reversal voltage to more negative values and a corresponding decrease of the inward current, meaning that the permeability of the channel for these ions is lower than for K^+. This is in agreement with the findings for other Kcv variants (Gazzarrini *et al.* 2009). As for $Kcv_{Next\text{-}to\text{-}Smith}$ we observed the highest reversal potential for Na^+ followed by Li^+ and then NH_4^+.Also, it can be seen that Li^+ and Na^+ drastically reduce the outward current, meaning that the two ions inhibit the channel, whereas NH_4^+ did not inhibit it. This is different to the situation observed for $Kcv_{Next\text{-}to\text{-}Smith,}$ where Li^+ and NH_4^+, but not Na^+ inhibited the channel. The estimated reversal potentials, summarized as mean value of $n \geq 5$ cells, are shown in **Fig. 15 D**. The permeability sequence for Kcv_{Smith} can be summarized as followed: $Rb^+ \approx K^+ >> NH_4^+ \approx Li^+ \approx Na^+$.

The different selectivities found for Kcv_{Smith} and $Kcv_{Next\text{-}to\text{-}Smith}$ together with the data for $Kcv_{ATCV\text{-}1}$ were surprising, since the three channels have an identical pore and filter region (**Fig. 6 B** and **Fig. 7 A/B**). $Kcv_{ATCV\text{-}1}$ and $Kcv_{Next\text{-}to\text{-}Smith}$ differ in only four amino acids within the outer transmembrane domain, but the channels differ strongly in their permeation for Rb^+ and K^+. Whereas $Kcv_{ATCV\text{-}1}$ was more

permeable for K^+ than for Rb^+, the situation was reversed in the case of $Kcv_{Next\text{-}to\text{-}Smith}$. To examine the molecular basis for this difference in permeability we tested the I5L mutant of $Kcv_{Next\text{-}to\text{-}Smith}$ for its permeability. The mutant, which was made for another purpose (see below), mimics Kcv_{Smith}. The data show that the mutation affects the selectivity of the channel for Rb^+ and K^+. The estimated reversal potentials are shown as mean of ≥ 5 cells in **Fig. 16**. The mutant is slightly more permeable for K^+ (V_r = -5.62 ± 2.11) than for Rb^+ (V_r = -10.86 ± 2.06).

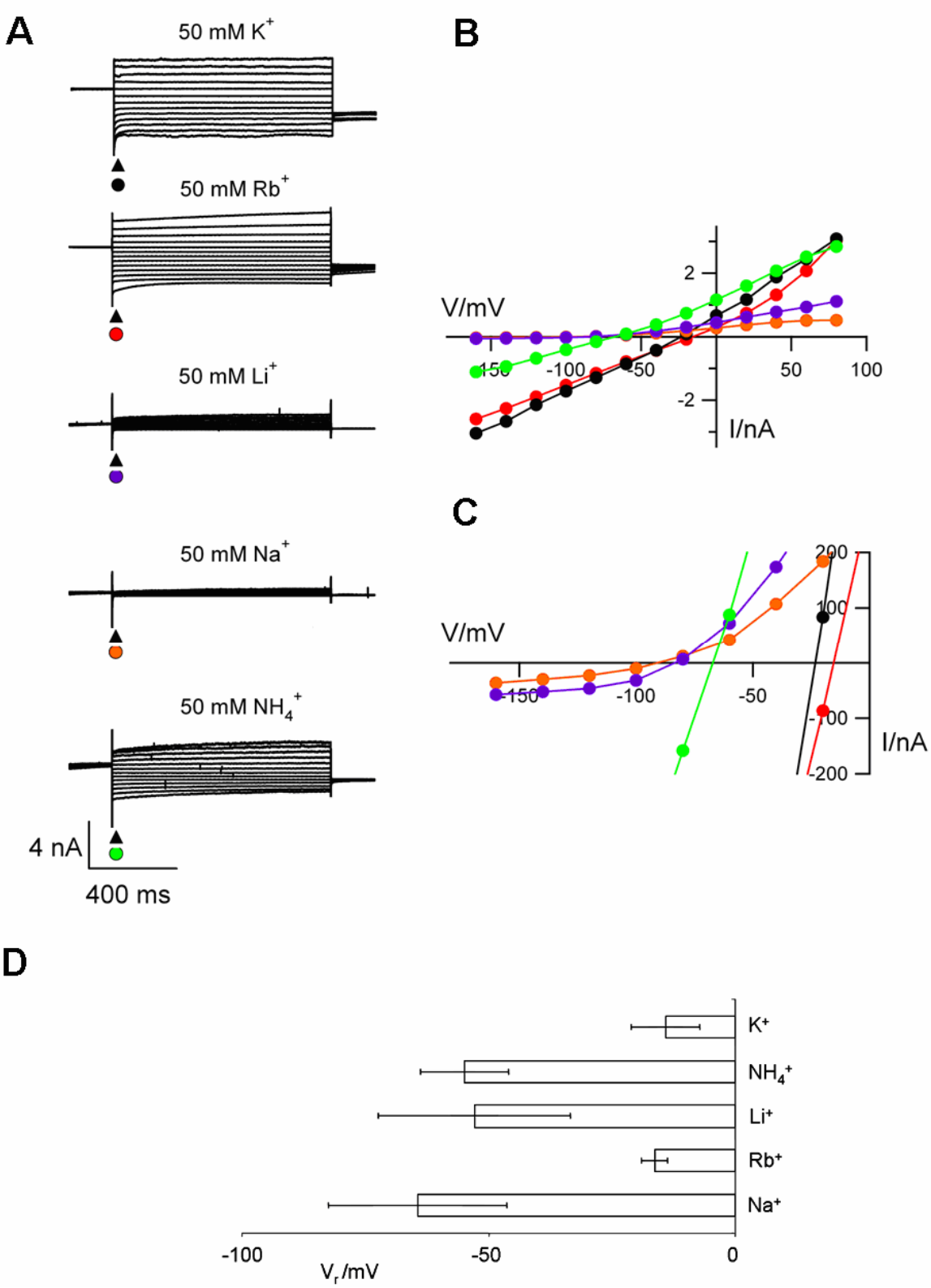

Fig. 15: Selectivity of Kcv_{Smith}

(A) Exemplary current responses of a HEK293 cell transfected with Kcv_{Smith}::GFP in bath solution with different cations (50 mM). Currents were elicited by a standard pulse protocol as in **Fig. 8**. **(B)** I/V relation of the instantanous currents measured in **(A)** with an enlargement of the reversal voltage in **(C)**. **(D)** summarizes the mean values (n ≥ 5 ± S.D.) of V_r for the cations tested.

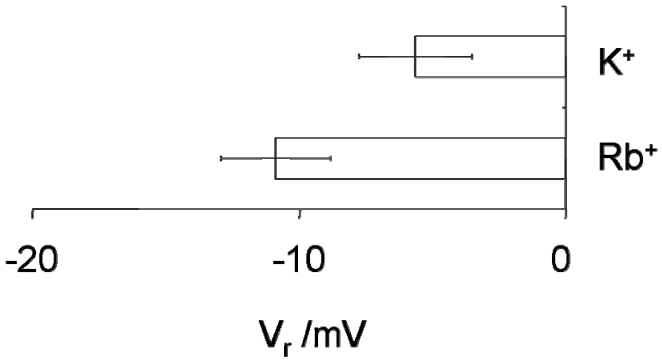

Fig. 16: Selectivitity of $Kcv_{Next\text{-}to\text{-}Smith}$-I5L
Reversal potentials of HEK293 cells transfected with $Kcv_{Next\text{-}to\text{-}Smith}$-I5L::GFP in either a 50 mM K^+ or a 50 mM Rb^+ bath solution to a standard pulse protocol as in **Fig. 8**. Values are means (n ≥ 5 ± S.D.).

Pharmacology

To test the pharmacology of Kcv_{Smith} and $Kcv_{Next\text{-}to\text{-}Smith}$, we added 10 mM of a blocking agent, i.e. either Ba^{2+}, Cs^+, TEA or Amantadine, to the bath solution with 50 mM K^+.

Fig. 17 summarizes the current response of a HEK293 cell transfected with either Kcv_{Smith}::GFP or $Kcv_{Next\text{-}to\text{-}Smith}$::GFP with (black) and without (blue) 10 mM of a blocking agent at a membrane potential of -140 mV.

Neither TEA nor Amantadine had any appreciable effect on either Kcv_{Smith} or $Kcv_{Next\text{-}to\text{-}Smith}$. In previous studies, it has been shown that the antiviral drug amantadine blocks the current of the homologous $Kcv_{PBCV\text{-}1}$ ($Kcv_{ATCV\text{-}1}$ was not tested with amantadine) (Chatelain *et al.* 2009). In the case of Kcv_{Smith} and $Kcv_{Next\text{-}to\text{-}Smith}$ we found no effect of amantadine on the K^+ currents of these channels (**Fig. 17**).

Also for the homologous $Kcv_{PBCV\text{-}1}$ an effect of TEA has been found. The inward current of this channel was reduced by 10 mM TEA by 30 - 40 % (Gazzarrini *et al*. 2003). For Kcv_{Smith} and $Kcv_{Next\text{-}to\text{-}Smith}$ we found a weak reduction of the inward current by ~10 – 20 % (**Fig. 17**).

Kcv_{Smith} and $Kcv_{Next\text{-}to\text{-}Smith}$ are blocked by Ba^{2+}

The addition of 10 mM Ba^{2+} to the 50 mM K^+ bath solution resulted in a total, but reversible block of the inward current carried by Kcv_{Smith} and $Kcv_{Next\text{-}to\text{-}Smith}$ (**Fig. 17** and **Fig. 18**). Ba^{2+} also generated an effect on the outward current, where an activating component appeared in the presence of the bivalent blocker (**Fig. 18)**. The same effect has been seen for $Kcv_{PBCV\text{-}1}$ and $Kcv_{ATCV\text{-}1}$ (Gazzarrini *et al*. 2009, Rosenberg-Lipinsky 2006).

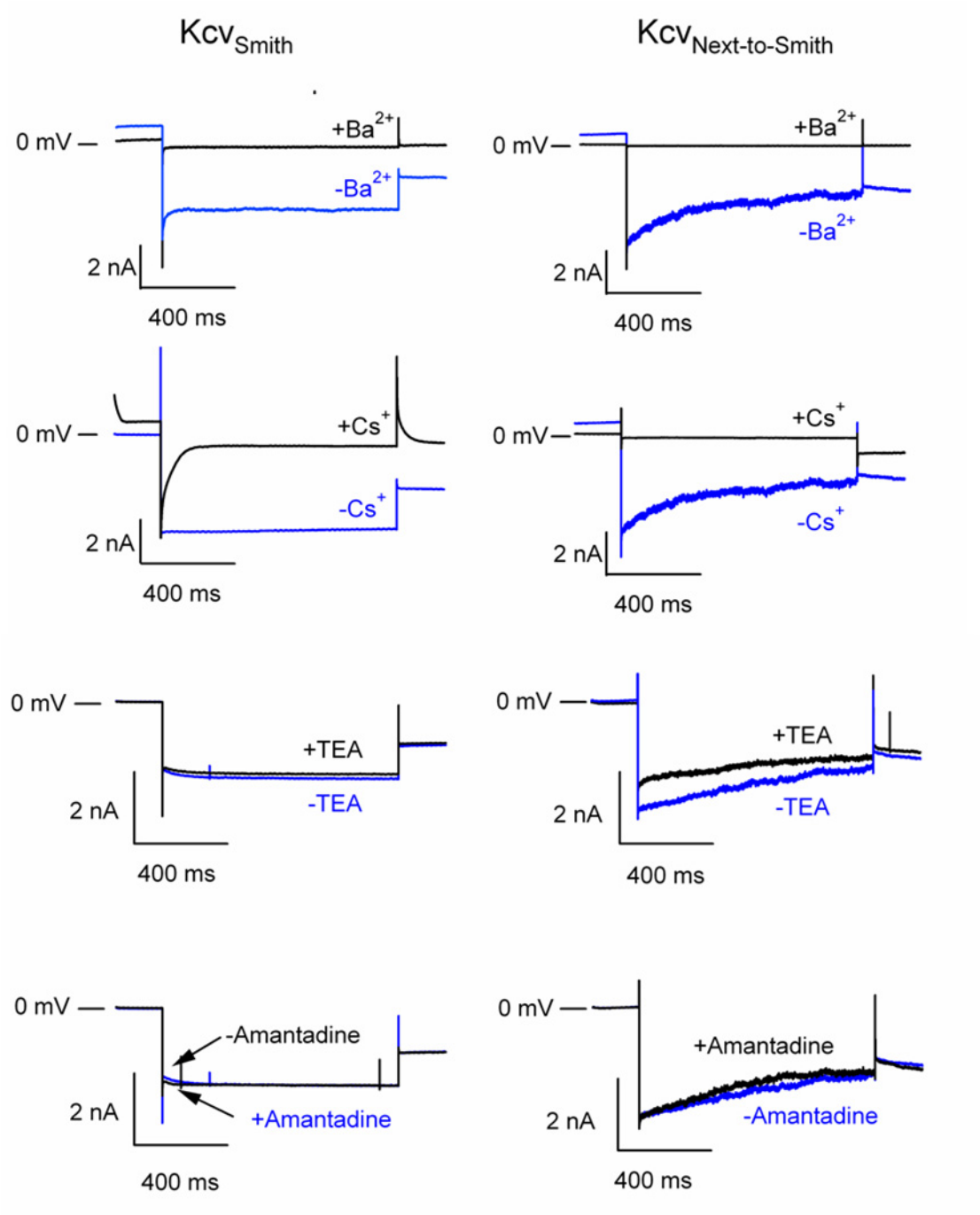

Fig. 17: Pharmacology of Kcv$_{Smith}$ and Kcv$_{Next-to-Smith}$

Comparison of currents with (black) and without 10 mM blocking agent (blue) in bath solutions with 50 mM K^+. Currents were elicited by voltage steps from 0 mV to -140 mV in HEK293 cells transfected with either Kcv$_{Smith}$::GFP (left side) or Kcv$_{Next-to-Smith}$::GFP (right side).

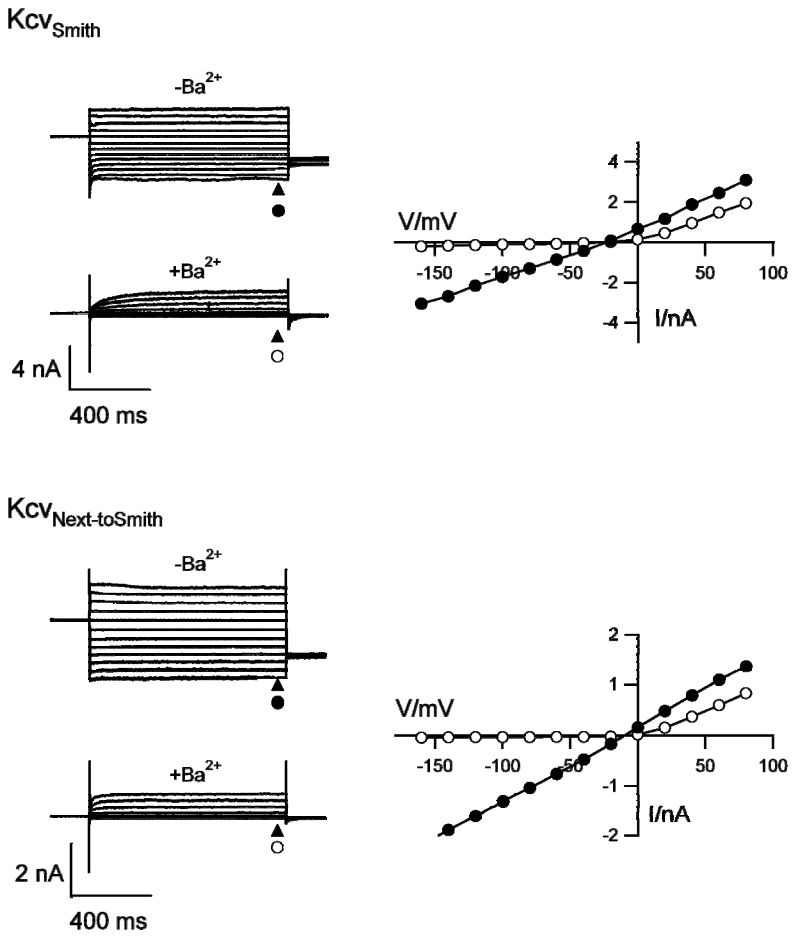

Fig. 18: Barium blocks Kcv$_{Smith}$ and Kcv$_{Next-to-Smith}$

Current responses of HEK293 cells transfected with either Kcv$_{Smith}$::GFP or Kcv$_{Next-to-Smith}$::GFP in a 50 mM K^+ bath solution with and without 10 mM $BaCl_2$ (left side) to a standard pulse protocol as in **Fig. 8**. The respective I/V relations of the steady-state currents are plotted on the right.

For Kcv$_{PBCV-1}$ it was found that the responsible site for the barium sensitivity is threonine at position 63 in the filter region (**Fig. 7 C**; Chatelain *et al*. 2009). A mutation of this residue to a serine resulted in a loss of barium sensitivity. To test if the same site is responsible in the new channels, we created an analogous T46S mutant for Kcv$_{Next-to-Smith}$.

Fig. 19 shows the current response of a HEK293 cell transfected with the T46S mutant of Kcv$_{Next-to-Smith}$::GFP to a standard pulse protocol in a 50 mM K^+ bath solution. The current generated by the mutant is comparable to that of the wildtype channel (**Fig. 8** and **Fig. 9**). The addition of 10 mM Ba^{2+} to the bath solution resulted in a strong inhibition of the inward current. Barium has an effect on the channel, but there are differences compared to the barium block of the wildtype: (a) The inward current is reduced by ~ 57.3 ± 16.7 % (n = 5 cells) at -140 mV and not fully blocked and (b) the activating component in the outward currents, which has been seen for the wildtype, does no longer

occur. The effect of Ba^{2+} was, like in the case of the wildtype, reversible upon exchanging the bath solution for 50 mM K^+ bath solution. Thus, the single mutation within the selectivity filter, which has been proposed as binding site for barium ions in the case of Kcv_{PBCV-1}, resulted in a significant change to the barium block of $Kcv_{Next\text{-}to\text{-}Smith}$.

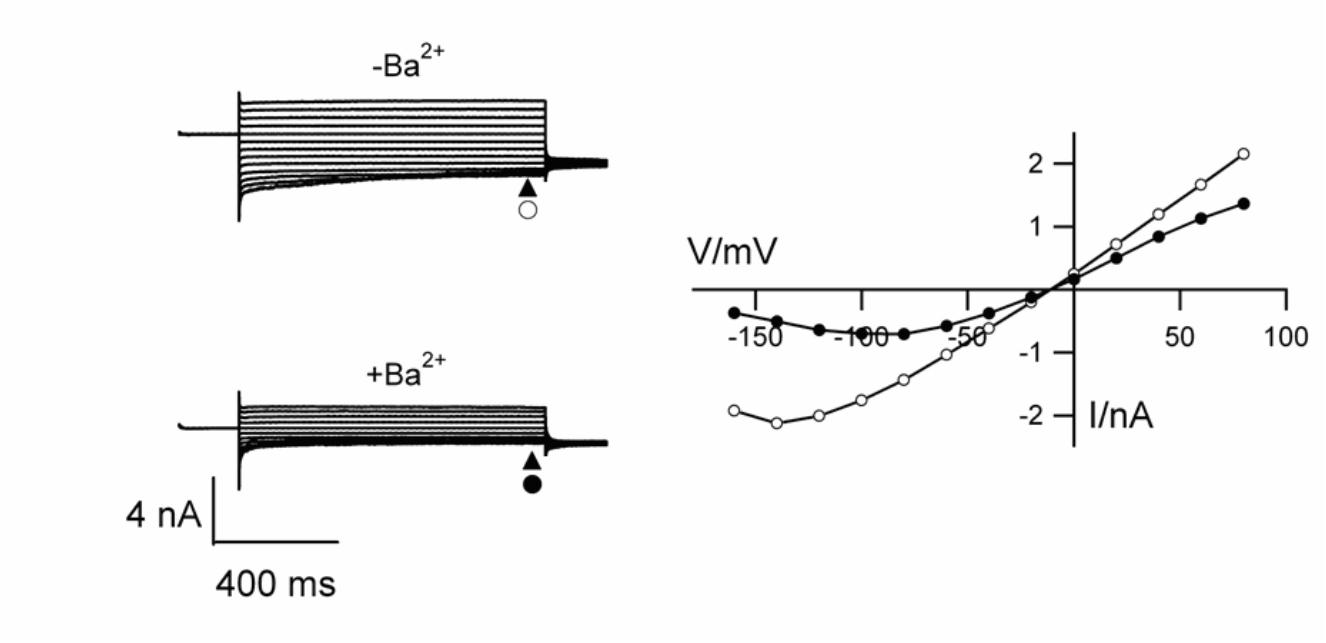

Fig. 19: Threonine at position 46 in the filter region of $Kcv_{Next\text{-}to\text{-}Smith}$ is important for barium block
Current responses of a HEK293 cell transfected with $Kcv_{Next\text{-}to\text{-}Smith}$-T46S::GFP in a 50 mM K^+ bath solution with and without the addition of 10 mM $BaCl_2$ (left side). Currents were elicited by a standard pulse protocol as in **Fig. 8**. The respective I/V relations of the steady-state currents are plotted on the right.

Kcv_{Smith} and $Kcv_{Next\text{-}to\text{-}Smith}$ are blocked by Cs^+

Kcv_{Smith} is fully blocked by cesium at negative voltages. **Fig. 20** shows the current response of a HEK293 cell transfected with Kcv_{Smith}::GFP in a 50 mM K^+ bath solution either with or without 10 mM CsCl. The channel is blocked in a voltage-dependent manner. This block is comparable to the cesium block observed with Kcv_{ATCV-1} expressed in *Xenopus laevis* oocytes (Gazzarrini *et al.* 2009). To test if the block depends on the Cs^+ concentration a HEK293 cell transfected with Kcv_{Smith}::GFP was examined in a 50 mM K^+ bath solution with varying CsCl concentration. The current responses and the corresponding I/V relations can be seen in **Fig. 21**. The block shifts to more negative voltages with decreasing Cs^+ concentration (**Fig. 21**). Also the reversal potential is shifted to more positive voltages with Cs^+ (all concentrations tested) meaning that Cs^+ is passing the channel and blocking it at the same time (**Fig. 20** and **21**). At low Cs^+ concentration it can be seen that the instantanous current is unaffected (**Fig. 21**). A fast closing of the channel can be observed. Higher Cs^+ concentrations, on the other hand, also block the instantanous current.

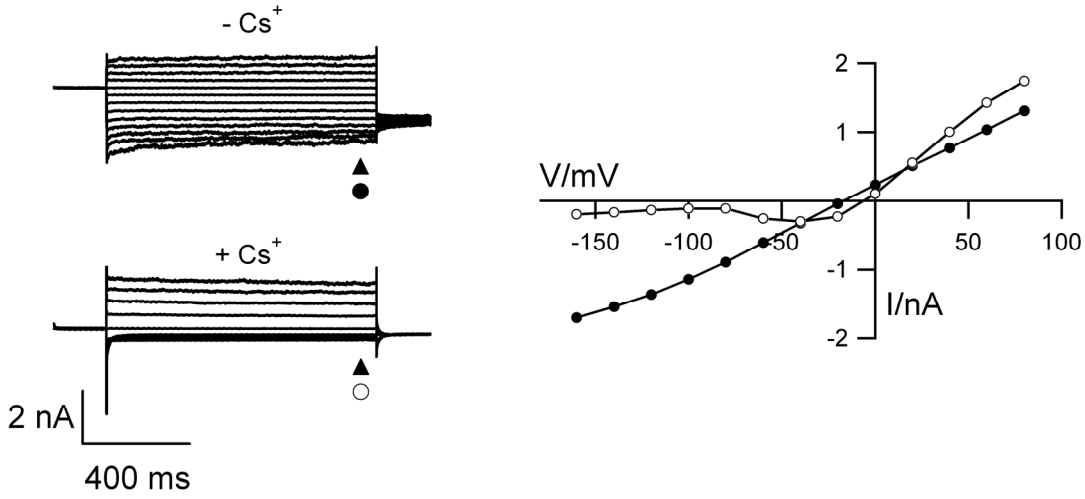

Fig. 20: Kcv_{Smith} is blocked by cesium ions

Exemplary current responses of a HEK293 cell expressing Kcv_{Smith}::GFP with and without 10 mM CsCl in the bath solution (left side). Currents were elicited by a standard pulse protocol as in **Fig. 8**. The corresponding I/V relation of the steady-state currents are plotted on the right.

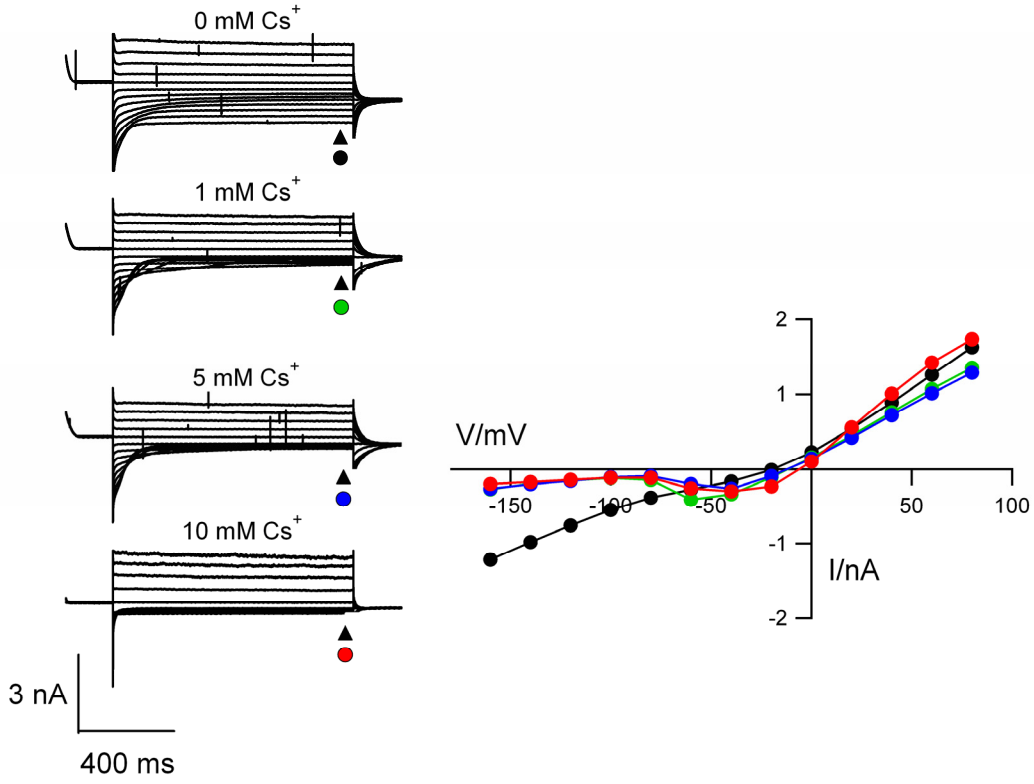

Fig. 21: Kcv_{Smith} is blocked by cesium ions

Exemplary current responses of a HEK293 cell expressing Kcv_{Smith}::GFP in a 50 mM K^+ bath solution without and with varying concentrations of Cs^+ (left side). Currents were elicited by a standard pulse protocol as in **Fig. 8**. The corresponding I/V relations of the steady-state currents are plotted on the right.

$Kcv_{Next\text{-}to\text{-}Smith}$ is also blocked by 10 mM Cs^+ (**Fig. 22**) in surprisingly steep voltage-dependent manner. Fig. **23 A** shows the current response of a HEK293 cell transfected with $Kcv_{Next\text{-}to\text{-}Smith}$::GFP to a standard pulse protocol. Here the block occurs only at voltages < -120 mV. To analyze this block further, the pulse protocol was modified by a) using shorter pulses (40 ms) (**Fig. 22 B**) and b) increasing the number of pulses (from 12 to 47) with smaller voltage increments (5 mV) (**Fig. 23**). The high temporal resolution of the initial phase of the current response (**Fig. 22 B**) shows the kinetics of the block better. A close scrutiny of the single current traces (**Fig. 22 C**) reveals that the channel is blocked by Cs^+ with a complex kinetics. At very negative voltages (-220 mV) the channel is blocked with a single exponential kinetics. At less negative voltages (-160 mV) the single exponential closure of the channel occurs only after a short lag time. At -140 mV the channel is barely inhibited.

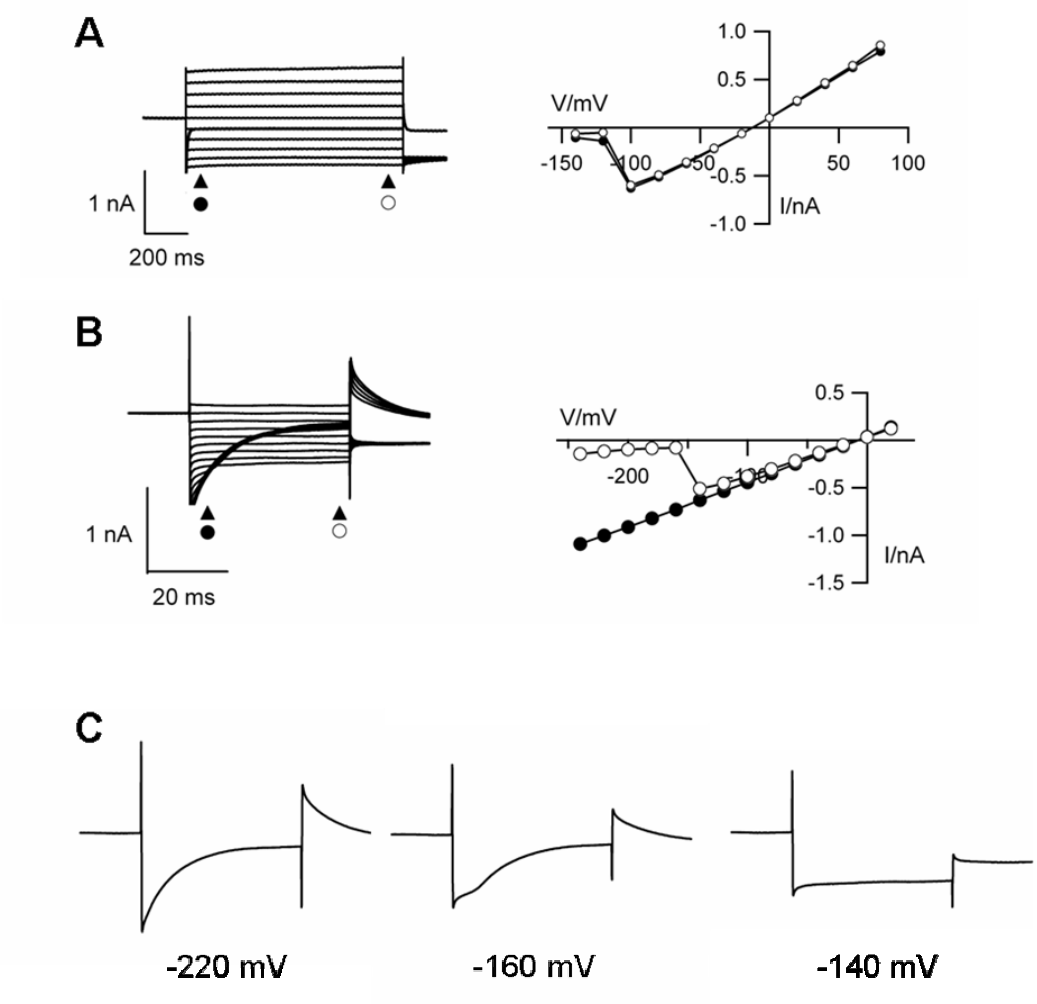

Fig. 22: $Kcv_{Next\text{-}to\text{-}Smith}$ shows unusual cesium block

(A) Exemplary current response of a HEK293 cell expressing $Kcv_{Next\text{-}to\text{-}Smith}$::GFP (left side) in a 50 mM K^+ bath solution containing 10 mM CsCl. Currents were elicited by a standard pulse protocol as in **Fig. 8**. The corresponding I/V relations of the instantanous currents (filled circles) and of the steady-state currents (open circles) are plotted on the right. **(B)** Current response of the same cell as in **(A)** to a modified pulse protocol with short 40 ms long test pulses (left side). The corresponding I/V relations are shown on the right side. **(C)** Shows single current traces at different clamp voltages from **(B)**.

By decreasing the voltage increments in the pulse protocol (**Fig. 23**), the complexity of the closing kinetics can be better resolved. The data show that increase in channel closing at negative voltages is best explained by a shortening of the lag time preceding the exponential decrease in current. The exponential decrease in current is rather insensitive to the voltage. The lag time can be resolved by superimposing the current traces (**Fig. 24 A**). **Fig. 24 A** also confirms that the exponential decrease in current is not affected by the voltage. **Fig. 24 B** shows the lag time of the block as a function of the voltage. It can be seen that the lag time decreases exponentially with more negative voltages.

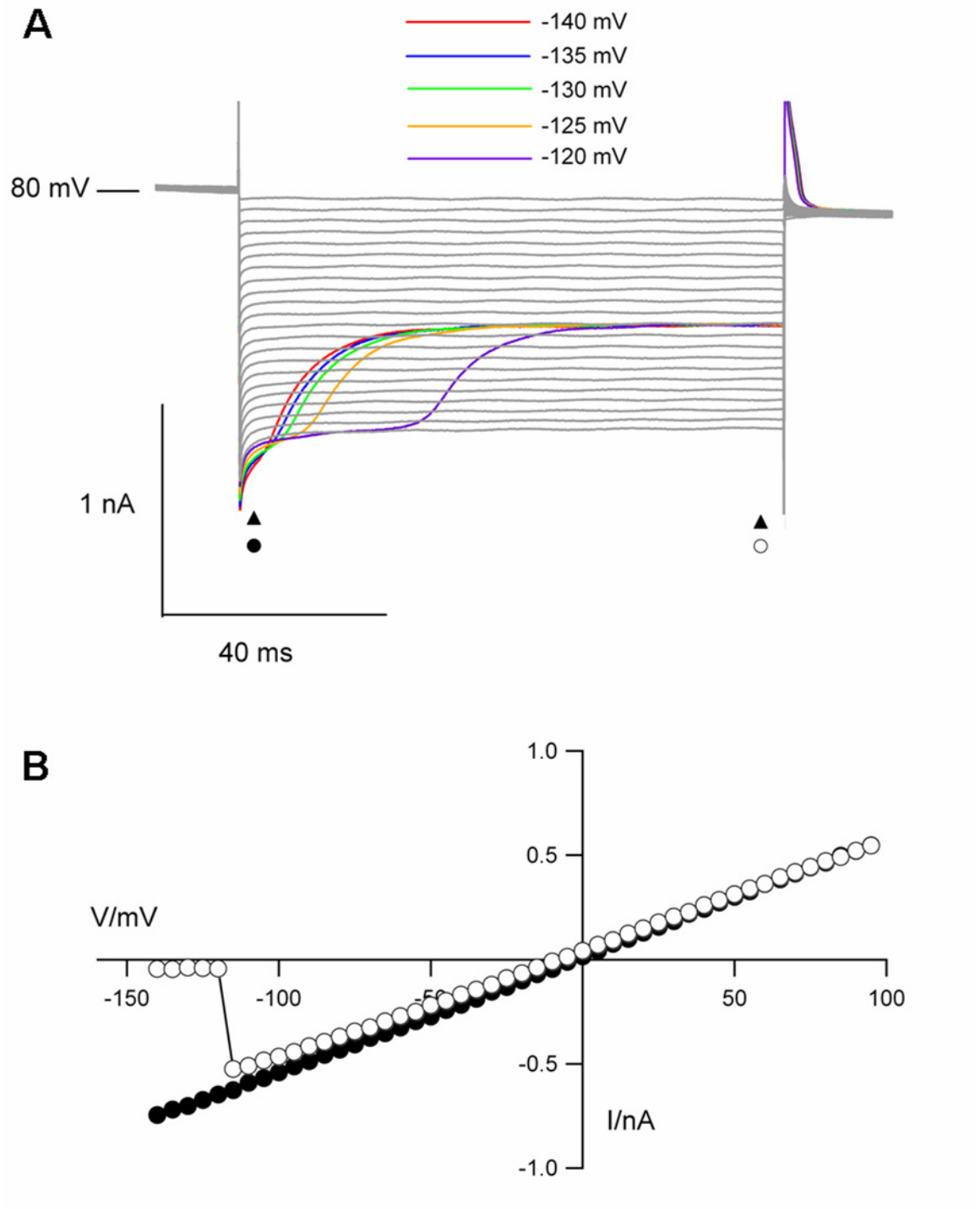

Fig. 23: Sharp voltage-dependent cesium block of $Kcv_{Next\text{-}to\text{-}Smith}$

Current response of the HEK293 cell expressing $Kcv_{Next\text{-}to\text{-}Smith}$ (same cell as in **Fig. 22**) to a modified pulse protocol with small 5 mV voltage step increments and an increased number of test pulses **(A)**. The corresponding I/V relation of the instantanous currents (filled circles) and the steady-state currents (open circles) are shown in **(B)**.

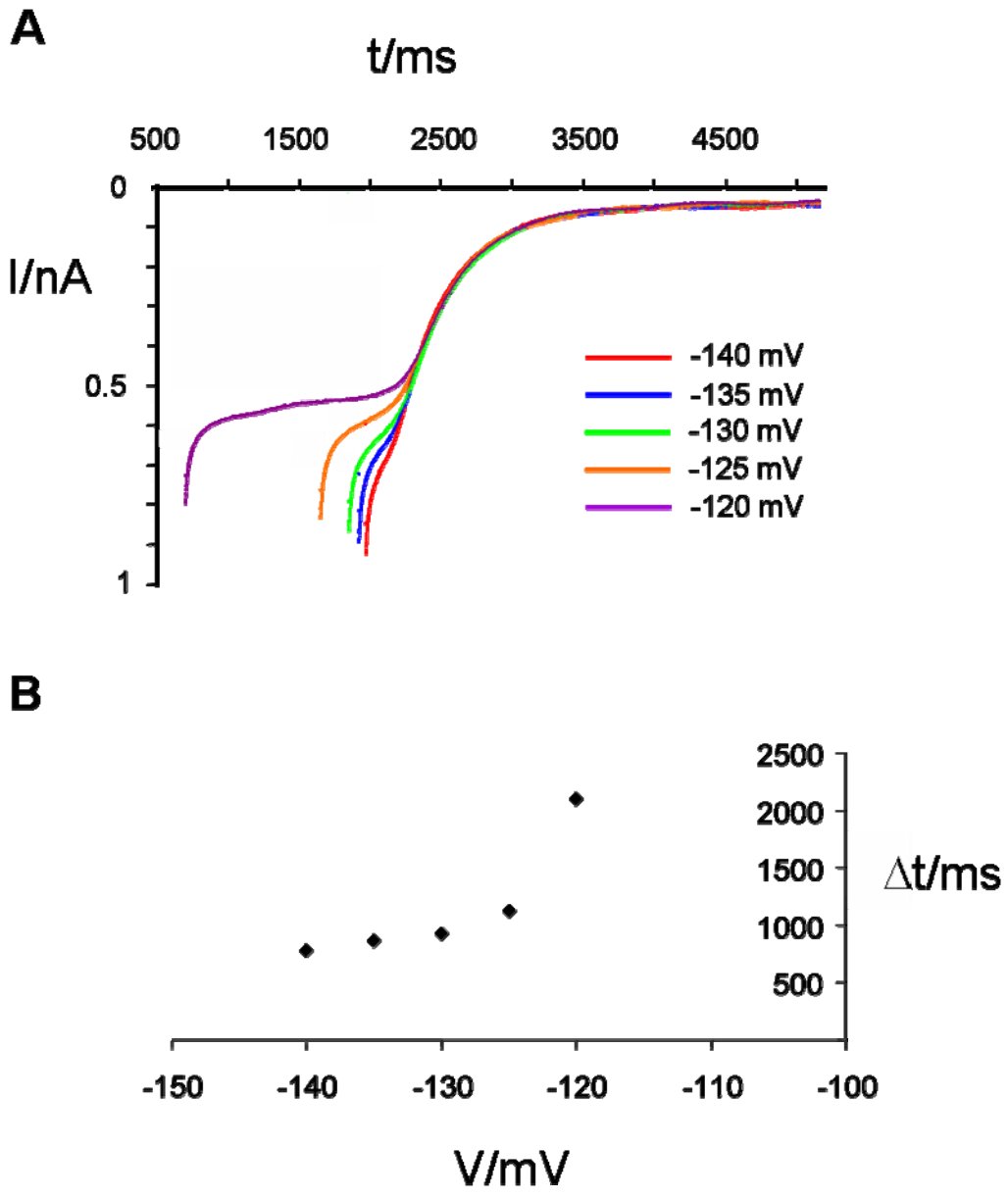

Fig. 24: Details of the cesium block of $Kcv_{Next\text{-}to\text{-}Smith}$

(A) Superimposed current responses at different clamp voltages from **Fig. 24 A**. **(B)** Plot of the block lag time of **(A)** versus the membrane voltage.

For an estimation of the relative block, the non-blocked part of the I/V relation was extrapolated and the blocked current was subtracted (**Fig. 25 A** and **B**). This procedure provides a measure for the blocked channel as a function of voltage. The data can be fitted by a Boltzmann equation (**eqn. 1**):

$$y = \frac{\text{max rel. Block}}{1 + e^{(V-V_{1/2})/dx}}$$

(**eqn. 1**)

In the equation max rel. block is the maximal relative block (see **Fig. 25**), $V_{1/2}$ the half maximal voltage at which the block occurs, i.e. the inflection point, and dx is the slope in the inflection point as a measure of the steepness of the curve.

A fit of the present data with eqn. 1 yields a dx of 0.71 ± 0.16 (n = 9 cells ± S.D.) as a measure of the steepness of the block of the steady-state current (**Fig. 25 B**). For comparison, the same analysis was performed with Kcv_{Smith}. For this channel a dx value of 14.12 ± 1.35 (n = 3 cells ± S.D.) was calculated. The comparison shows how much steeper the Cs^+ block of $Kcv_{Next\text{-}to\text{-}Smith}$ is compared to Kcv_{Smith}; the difference is nearly one order of magnitude.

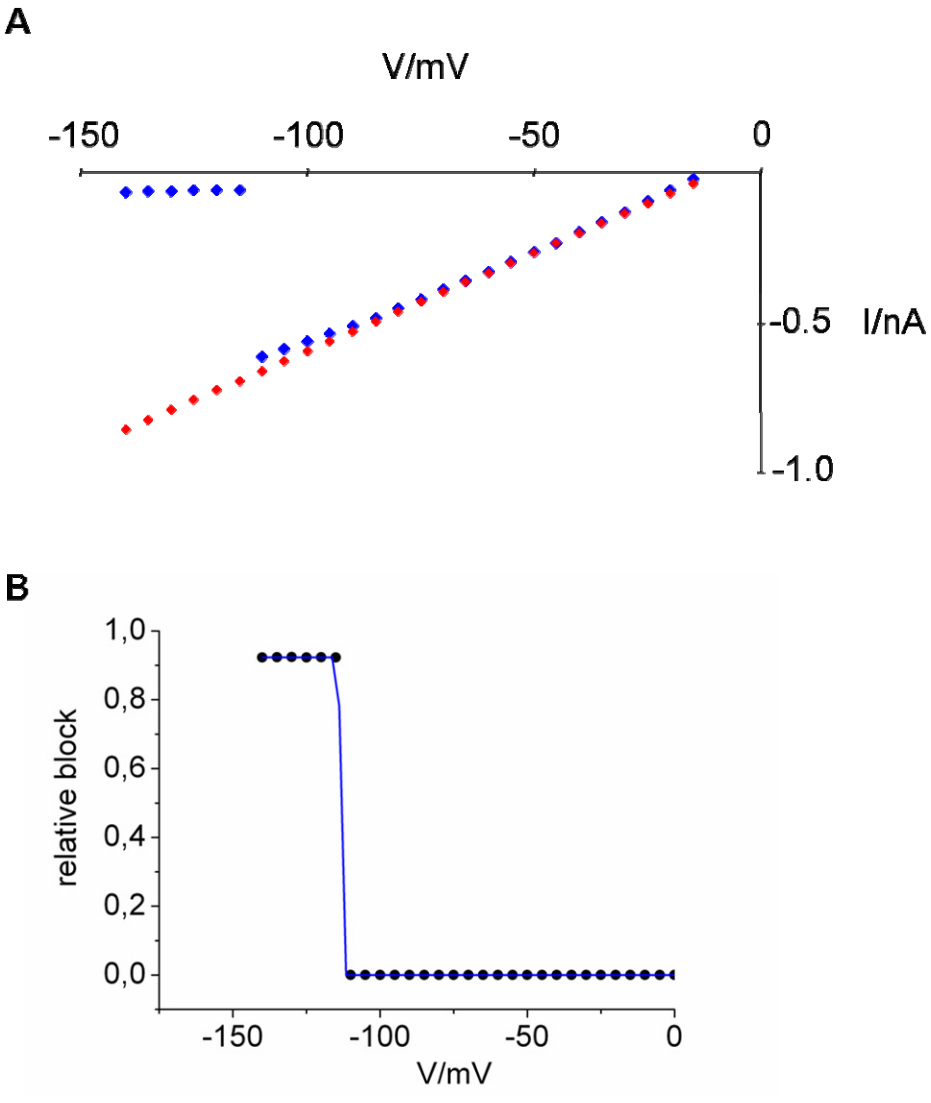

Fig. 25: Relative Block of $Kcv_{Next\text{-}to\text{-}Smith}$

Determination of the relative block: (A) the non-blocked part of the I/V relation (blue) at voltages positive of ca. -100 mV was fitted with a regression and extrapolated to negative voltages (red). the difference between unblocked (= 0) and fully blocked (= 1) currents is plotted as a function of the clamp voltage. (B) The resulting relative block was then fitted (blue line) with a Boltzmann function (**eqn. 1**) yielding a steepness of the block of 0.79.

In another experiment, the Cs^+ concentration was varied between 1 and 10 mM to determine the concentration dependence of the block. **Fig. 26 A** shows the I/V relations of a cell expressing $Kcv_{Next\text{-}to\text{-}Smith}$ in a 50 mM K^+ bathing solution with different Cs^+ concentrations. The voltage at which the channel closes in a voltage dependent manner is shifted to more negative voltages with decreasing amounts of Cs^+. Also, in this case, the steepness of the block differs as a function of the Cs^+ concentration; the higher the blocker concentration the steeper the transition between unblocked and blocked channels. The results of these experiments show that not only the voltage at which the channel is blocked by Cs^+ is concentration dependent, but also the blocking kinetics. **Fig. 26 B** shows the half maximal voltage $V_{1/2}$ at which the block occurs as a function of the Cs^+ concentration. The plot shows that there is an exponential relation between the half maximal voltage and the Cs^+ concentration.

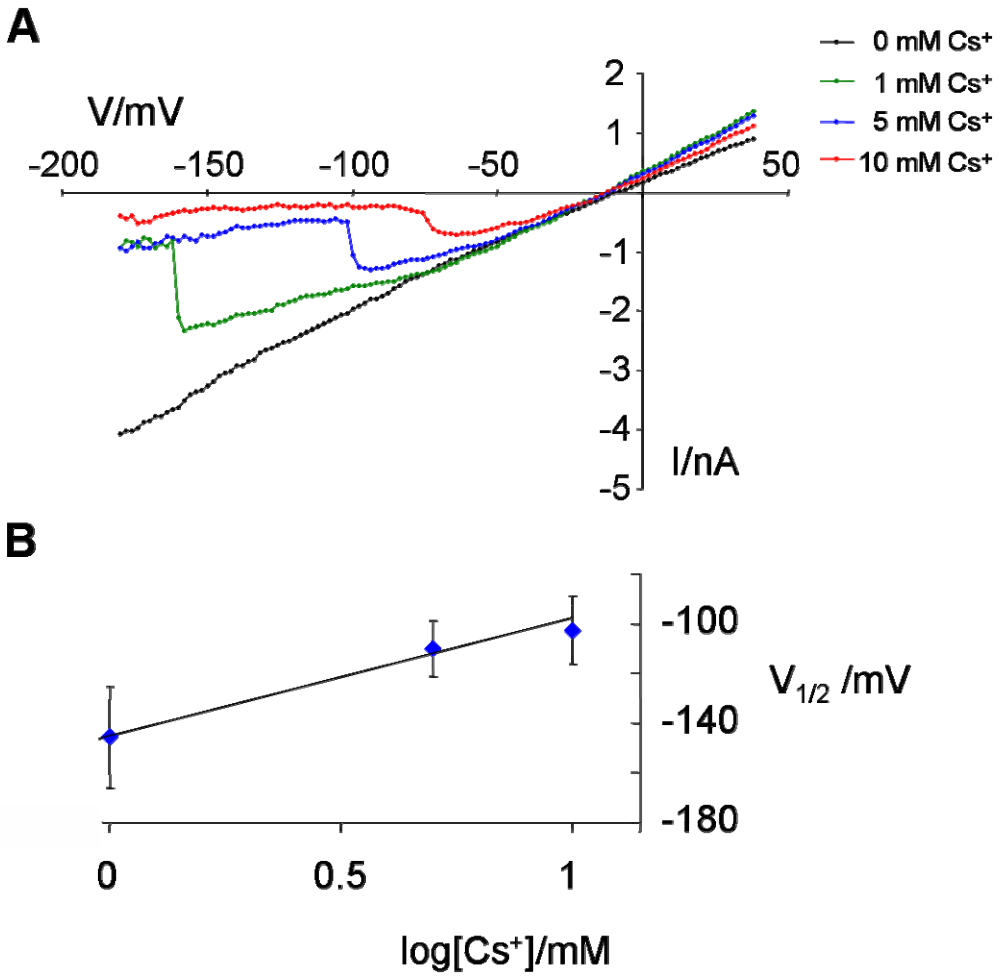

Fig. 26: The cesium block of $Kcv_{Next\text{-}to\text{-}Smith}$ is voltage- and concentration dependent
(A) Steady-state I/V relations of a cell expressing $Kcv_{Next\text{-}to\text{-}Smith}$ with different amounts of Cs^+ in the 50 mM K^+ bath solution. Currents were elicited with the modified pulse protocol of **Fig. 23**. **(B)** Plot of the half maximal voltage $V_{1/2}$ versus log[Cs^+] representating the voltage at which half of the current is inhibited . Values are means of n = 3 to 6 cells ± S.D.

Cs^+ sensitivity of $Kcv_{Next\text{-}to\text{-}Smith}$ related to its structure

To determine the amino acid residues, which are responsible for the unusual difference in Cs^+ sensitivity in the two channels, we sequentially mutated $Kcv_{Next\text{-}to\text{-}Smith}$ in order to mimic Kcv_{Smith}. For a start we were choosing two positions in the first TMD (Ile5 and Ser9). The rational behind this decision results from the comparison of $Kcv_{Next\text{-}to\text{-}Smith}$ with the channels, which show a slow cesium block: Kcv_{Smith} and $Kcv_{ATCV\text{-}1}$. Kcv_{Smith} has a leucine at position 5, while $Kcv_{Nextto\text{-}Smith}$ and $Kcv_{ATCV\text{-}1}$ have an isoleucine at this position. At position 9 Kcv_{Smith} has a glycine and $Kcv_{ATCV\text{-}1}$ has an isoleucine (**Fig. 6 B**).

Using site-directed mutagenesis, we generated the following $Kcv_{Next\text{-}to\text{-}Smith}$ mutants: I5L, S9G (both in order to mimic Kcv_{Smith}), S9A (to exchange the Ser9 for another small amino acid) and S9F (in order to mimic the cesium resistant $Kcv_{PBCV\text{-}1}$). All of the respective mutants generated a $Kcv_{Next\text{-}to\text{-}Smith}$ like current when expressed in HEK293 cells (**Fig. 27**). In case of the $Kcv_{Next\text{-}to\text{-}Smith}$-S9G mutant the addition of 10 mM Cs^+ to the bath solution resulted in the same steep voltage-dependent block, which was observed in the wildtype (**Fig. 27**). In case of the three other mutants, $Kcv_{Next\text{-}to\text{-}Smith}$-I5L, -S9A and S9F, the channels are like Kcv_{Smith} blocked over the entire negative voltage range. The steep voltage-dependent block observed at the wildtype does no longer occur (**Fig. 27**).

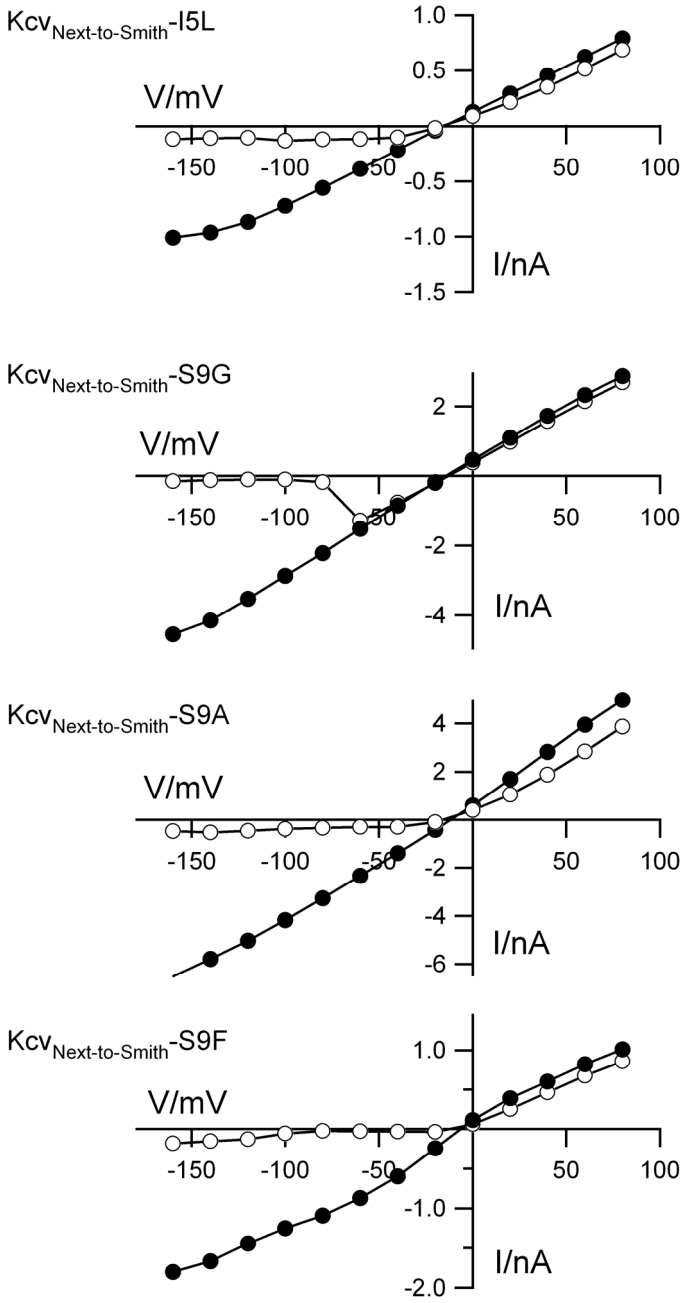

Fig. 27: Mutations in the outer TM of $Kcv_{Next\text{-}to\text{-}Smith}$, which make this channel similar to Kcv_{Smith}, affect the mode of Cs^+ block

Exemplary steady-state I/V relations of HEK293 cells expressing different $Kcv_{Next\text{-}to\text{-}Smith}$-mutants. Currents were elicited in cells bathed in 50 mM K^+ bath solution without (filled circles) and with 10 mM Cs^+ (open circles) by a standard pulse protocol with test voltages as in **Fig. 8**.

3.4. Discussion

Different chlorella viruses code for small membrane proteins with many of the hallmarks of K^+ channels. With a monomer size of less than 100 amino acids these Kir like channels correspond, from a structural point of view, to the "pore module" of all known potassium channels (Kang *et al.* 2003). Structure-function correlates in this model channel can be examined by exploiting the known evolutionary pressure on viruses. In this context the channel can be seen as undergoing a quasi-unlimited statistical complexity of naturally evolved proteins in which each spontaneous mutation has been selected through millions of years in the context of the surrounding sequence to generate a

modified variant of the original sequence. Because a functional Kcv channel is apparently required for the virus to replicate (Thiel *et al*. 2010a), it does not come as a surprise, that all the Kcv variants, generated by the long evolutionary history of these viruses (Kang *et al.* 2004a), are functional. They constitute a pool of pre-screened and therefore functional genetic diversity in which selection has removed non-advantageous diversity from the pool of functional channels. Previous studies have already identified natural Kcv variants containing 4 – 12 amino acid substitutions; these variants exhibited different kinetics and permeability properties relative to the reference channel Kcv_{PBCV-1} (Plugge *et al*. 2000; Kang *et al.* 2004a).

With Kcv_{Smith} and $Kcv_{Next-to-Smith}$ we found two further Kcv variants from a unique environment. The characterization of the two proteins, which differ basically only within their transmembrane domains, revealed similarity with well-known Kcv variants, such as Kcv_{PBCV-1}, but also unexpected properties. First of all, Kcv_{Smith} and $Kcv_{Next-to-Smith}$ have shown to be functional potassium channels. Expressed in HEK293 cells both channel proteins show a significant increase in current with selectivity for K^+. This is expected from the sequence homology to other Kcv variants (**Fig. 6A**) and the bulk of studies done with several of these variants (Plugge *et al.* 2000; Kang *et al* 2004a; Kang *et al*. 2004b; Gazzarrini *et al.* 2003; Gazzarrini *et al*. 2009; Thiel *et al*. 2010b). The variation of the K^+ concentration and the resulting plots in **Fig. 11 D** and **Fig. 12 D** show a linear relation with slopes of 45.2 (Kcv_{Smith}) and 59.2 ($Kcv_{Next-to-Smith}$). This means, that both channels show selectivity for K^+, but that Kcv_{Smith} is less close to the theoretical value of 59.2 mV calculated with the Nernst equation (Hille 2001; Gazzarrini *et al.* 2009). At low K^+ concentrations it can be seen that the respective reversal potentials are in both cases more positive than expected. The two linear fits in **Fig. 11 D** and **Fig. 12 D** show that the data point for 5 mM K^+ has a strong effect on the slope of the fit if it is incorporated into the regression or not. This effect is most dramatic in the case of $Kcv_{Next-to-Smith}$, which also shows a large time-dependent decrease of the inward current at very negative voltages (**Fig. 11 B**). We assume that the low K^+ concentration causes a depletion of K^+ ions within the filter region, which further leads to a destabilization of the protein and a decrease of conductance. Studies with KcsA have shown that a depletion of K^+ ions in the filter region leads to a collapse of the pore; the channel is therefore in a non-conducting state (**Fig. 3 E**; MacKinnon, 2004). An effect of K^+ depletion has also been observed in more complex potassium channels, such as KAT1 (Hertel *et al.* 2005). The authors hypothesize that the inactivation due to low $[K^+]$ is a safety mechanism to prevent K^+ leakage. This is probably not the case for the viral channel, but might be based on the same mechanism.

The hypothesis that low $[K^+]$ leads to destabilization of the channel is consistent with the finding on the stability of the Kcv_{PBCV-1} tetramer: it has been shown in a SDS-PAGE analysis that K^+ in the buffer stabilizes the tetrameric form of the protein, whereas the replacement of K^+ with Na^+ results in a

disaggregation of the tetramer (Shim *et al*. 2007; Chatelain *et al*. 2009). Here we evidence that $Kcv_{Next\text{-}to\text{-}Smith}$ is more sensitive to a depletion of K^+ in the filter than Kcv_{Smith} (**Fig. 12 D**). This fosters the hypothesis that the stability of the protein tetramer is not only determined by the filter region, since both channels do not differ in this region (**Fig. 6 A**).

The canonical view is that several channel properties such as selectivity and block by cationic inhibitors is intimately related to the structure of the selectivity filter. The present data show that this is, at least in the three viral channels, not the case. The data support a model according to which also the outer transmembrane domain is able to modify properties of the selectivity filter. One of the surprising findings is that the three channels $Kcv_{ATCV\text{-}1}$, Kcv_{Smith} and $Kcv_{Next\text{-}to\text{-}Smith}$ have an identical filter sequence. Nonetheless the three channels differ in their selectivity between K^+ and Rb^+. $Kcv_{Next\text{-}to\text{-}Smith}$ has a higher permeability for Rb^+ than for K^+. This is opposite to the situation in $Kcv_{ATCV\text{-}1}$, which is more permeable for K^+ than for Rb^+ (Gazzarrini *et al.* 2009). Kcv_{Smith} on the other hand does not discriminate between K^+ and Rb^+. The difference in selectivity between the channels extends also to other cations. While $Kcv_{Next\text{-}to\text{-}Smith}$ shows a clear preference for cations ($NH_4^+ > Li^+ > Na^+$), Kcv_{Smith} is less distinctive and conducts NH_4^+, Li^+ and Na^+ equally well. This means three homologous potassium channels, $Kcv_{ATCV\text{-}1}$, Kcv_{Smith} and $Kcv_{Next\text{-}to\text{-}Smith}$, which have identical filter regions show three distinctly different cation selectivities. We must, therefore, conclude that not only the selectivity filter determines the permeability of at least these potassium channels.

The same conclusion can be drawn in relation to the differential Cs^+ block of the channels. Cs^+ has a similar size to K^+ and is conducted by many K^+ channels. Because the conductance of Cs^+ is lower than that of K^+ it effectively blocks the K^+ channel. In the present study we find that again the two channels, Kcv_{Smith} and $Kcv_{Next\text{-}to\text{-}Smith}$, with the identical selectivity filter are blocked in a distinctly different mode by Cs^+. While Kcv_{Smith} was blocked in the same shallow voltage-dependent manner as $Kcv_{ATCV\text{-}1}$, $Kcv_{Next\text{-}to\text{-}Smith}$ showed an extremely steep voltage-dependent block (**Fig. 22 - 25**). The different block modes can be interpreted in a sense that Kcv_{Smith} has a Cs^+ binding site, which is occupied by the blocking ion already at moderate negative voltages. The same binding site in $Kcv_{Next\text{-}to\text{-}Smith}$ on the other hand is only binding Cs^+ at much higher negative voltages. The negative voltage seems to force Cs^+ into this binding site, which explains the very steep voltage dependency.

Again the difference in Cs^+ block cannot be explained on the basis of different binding sites in the filter, because the three channels are on a sequence basis identical in this region. The interpretation that a binding of Cs^+ is not soleley coupled to the selectivity filter is also supported by the complex kinetics of the Cs^+ block in $Kcv_{Next\text{-}to\text{-}Smith}$. The data in **Fig. 23** and **Fig. 24** show that the blocking kinetics consists of at least two components: an exponential component that is identical for several

voltages tested and a lag time component, which preceeds the exponential component in a voltage-dependent manner. The kinetics of this block shows that Cs^+ can initially pass the selectivity filter for several ms before the block becomes manifested. This observation is consistent with the interpretation that the block is not directly governed by the selectivity filter.

The alignments of Kcv_{Smith}, $Kcv_{Next\text{-}to\text{-}Smith}$ and $Kcv_{ATCV\text{-}1}$ (**Fig. 7 A** and **B**) show that the three proteins differ mostly in amino acids within the first transmembrane domain. The experimental data support the hypothesis that the deviation in this domain is responsible for their difference in Cs^+ block and selectivity. The I5L mutant of $Kcv_{Next\text{-}to\text{-}Smith}$ for instance has a clear effect on the selectivity of the channel for K^+ versus Rb^+. As a result of the mutation the reversal potential for K^+ shifted to more positive values and the reversal potential for Rb^+ shifted to more negative values, meaning that the general selectivity of the channel became more similar to Kcv_{Smith}. This means that the channel mutant discriminates less between the two ions. Thus, the conclusion here is that the permeability of the channels is not only determined by the filter sequence, but is also largely affected by the outer transmembrane domain of the channel. The results of these experiments are indeed remarkable if we consider that the exchange of isoleucine into leucine is basically just an exchange of two stereoisomeres of the same molecule. Hence, only a minute change in the amino acid composition of the channel in a domain distant from the selectivity filter is able to profoundly affect a key property of a K^+ channel.

The importance of the outer transmembrane domain for the channel performance is further supported by the analysis of Cs^+ block in mutants. The fact that the S9F mutant in $Kcv_{Next\text{-}to\text{-}Smith}$ reveals the same phenotype as Kcv_{Smith} underscores the structural importance of the outer transmembrane domain. The data, which shows that other mutations in this region are not affecting the Cs^+ block of $Kcv_{Next\text{-}to\text{-}Smith}$, furthermore show that this effect is very site specific and not a global property of the outer transmembrane domain.

The present results and interpretations are not completely surprising. Previous investigations of $Kcv_{PBCV\text{-}1}$ and natural variants of it, especially $Kcv_{MA\text{-}1D}$ had already shown that an amino acid in the outer transmembrane domain, namely Phe19, drastically affects the Cs^+ sensitivity of these channels. Mutational studies with these channels revealed Phe19 interacts in some yet unknown manner with a residue in the pore (Ile54) (see **Fig. 7 C**; Gazzarrini *et al*. 2004). These two synergistically interacting residues showed a dramatic influence of several properties of the channels, i.e. inactivation of K^+ current and permeation of Rb^+ (Gazzarrini *et al*. 2004). A crude superposition of $Kcv_{PBCV\text{-}1}$, Kcv_{Smith} and $Kcv_{Next\text{-}to\text{-}Smith}$ shows that the respective residues in Kcv_{Smith} and $Kcv_{Next\text{-}to\text{-}Smith}$ are Gly9 (in Kcv_{Smith}) and Ser9 (in $Kcv_{Next\text{-}to\text{-}Smith}$) and Leu37 (in both channels). Hence, the previous findings with $Kcv_{PBCV\text{-}1}$ are

also on a structural basis consistent with the findings here: a single amino acid within the upstream part of the outer TM (Ile5 and Leu5 respectively) seems to interact with the distant pore region. In following studies it would be interesting to test further, if Leu37 is indeed the residue, which is interacting with Ile5 and Leu5 respectively, and if the effect caused by the single mutation in TM1, i.e. the change in permeability, can be reversed as was the case for Kcv_{PBCV-1} (Gazzarrini *et al*. 2004).

The present data show that the mechanism of Cs^+ block is definitely different from the block by Ba^{2+}. So far, all known natural Kcv variants are blocked by Ba^{2+} (Plugge *et al.* 2000; Kang *et al.* 2004a; Gazzarrini *et al*. 2004; Gazzarrini *et al.* 2009; Chatelain *et al.* 2009). This holds true for Kcv_{Smith} and $Kcv_{Next\text{-}to\text{-}Smith}$, which are both clearly blocked in a reversible manner (**Fig. 17** and **Fig. 18**). This is consistent with the findings for Kcv_{ATCV-1}, which is also totally blocked under the same conditions and shows the same activating component at the outward current. This activation is not fully understood. The assumption is that few barium ions enter the cell and then slightly block the channel while the potassium ions get pulled out in a voltage-dependent manner.

The filter region of the two examined channels contains a threonine residue in position 46, which is analogous to the threonine 63 in the filter region of Kcv_{PBCV-1}. This position had been determined as the binding site for barium. A mutation into a serine by a randomized approach resulted in an insensitivity to barium in the case of Kcv_{PBCV-1} (Chatelain *et al.* 2009). To test, if the analogous Thr46 in Kcv_{Smith} and $Kcv_{Next\text{-}to\text{-}Smith}$ is the respective binding and blocking site for barium, we made the analogous mutation T46S of $Kcv_{Next\text{-}to\text{-}Smith}$. The data show that the mutation causes a decrease in barium sensitivity (**Fig. 19**); the channel is not totally blocked like the wildtype (**Fig. 18**) and the activation at the outward currents disappeared. Thus, the threonine at position 46 is analogous to the threonine at position 63 in Kcv_{PBCV-1}, and it shows that two potassium channels, which heavily differ in size and amino acid composition, exhibit not only similar properties, but also contain key amino acid residues, which have homologous properties.

Ion channels facilitate the transport of charges across a non-conducting medium, the membrane. If the channels are voltage-dependent, then a comparison to the field-effect transistors from electronics is possible as described in “Life´s transistors” (Sigworth 2003). Transistors are electronic elements, in which the flow of electrons through a semiconductor is controlled by two voltages: the source-drain-voltage, which causes electrons to flow through the semiconductor, and the gate-voltage, which permits the electrons to flow (Horowitz 1998). In a voltage-dependent ion channel an applied voltage fulfils both functions. Ion channels are therefore most interesting candidates for bio-engineered electronic elements. Interestingly, ion channels show a sharper voltage-dependency than a technical semiconductor (Fig. 1 from Sigworth 2003). Hence, it is conceivable to use channels as transistor

switch. However, before realizing such a device, several challenges have to be handled. This includes the finding of channels with physical stability and high currents. The viral potassium channels seem to be ideal candidates. They are minimal in size with a large unitary conductance. Furthermore, they are voltage dependent and they show a high resistance to temperature and detergents, i.e. a relatively high physical robustness (Shim *et al.* 2007). In particular, $Kcv_{Next\text{-}to\text{-}Smith}$ seems to be the most interesting candidate because of its extremely steep voltage-dependent block by cesium. The channel behaved under these conditions like a transistor switch when expressed in HEK293 cells. Thus, the utilization of $Kcv_{Next\text{-}to\text{-}Smith}$ coupled with other organic compounds in bioelectronic circuits, such as described in Huang *et al.* 2010, is conceivable. In this publication, the authors describe a bionanoelectric transistor. It consists of a carbon nanotube and a purified Na^+/K^+-ATPase; both are incorporated in a lipid bilayer. The control over this circuit is facilitated by the addition of ATP, thus, the ATPase works as a transistor gate. $Kcv_{Next\text{-}to\text{-}Smith}$, therefore, could function as cesium controlled gate.

In summary, both channels, Kcv_{Smith} and $Kcv_{Next\text{-}to\text{-}Smith}$, have shown to be functional potassium channels, which differ largely in their properties. Most striking are the differences in cation selectivity and Cs^+ block. The channels demonstrate the importance of the outer transmembrane on both, permeability and block, and imply a site specific interaction between parts of the outer TM and the pore. Most notable is the cesium block of $Kcv_{Next\text{-}to\text{-}Smith}$ with a, to date, unobserved steepness in its voltage dependency.

3.5. Methods

Virus isolation

Smith Lake virus was isolated from Smith Lake in central Nebraska N 41 47.148 W 102 31.412, 3854 ft above sea level. Next-to-Smith virus was isolated from a ditch running near Smith Lake (David D. Dunigan, personal communication). *Chlorella* SAG 3.83 culture, virus isolation and virus purification were done as described in Van Etten *et al.* 1983 and Bubeck and Pfitzner 2005.

Isolation of Kcv genes and sub-cloning

Kcv homologous genes were amplified using degenerated primers that were designed on the basis of $Kcv_{ATCV\text{-}1}$ (ORF Z585R; NCBI Accession #YP_001427066) and Kcv_{TN603} (ORF Y02_007R; http://greengene.uml.edu/database/php/get_orf.php?genome_name=TN603) sequences and cloned into the vector pSGEM (a modified version of pGEM-HE, courtesy of M. Hollmann, Max Planck Institute for Experimental Medicine, Göttingen, Germany) at BamHI and XhoI sites for sequencing.

For the expression in HEK293 cells, the Kcv genes were subcloned into the expression vector pEGFP-N2 ((Clontech-Takara Bio Europe, Saint-Germain-en-Laye, France)) in frame with and upstream of the EGFP gene at BglII and EcoRI sites ($Kcv_{Next\text{-}to\text{-}Smith}$) and XhoI and EcoRI sites (Kcv_{Smith}), respectively, using the primer sequences Next-to-Smith-BglII-for: 5'- TAT AGA TCT ATG TTG CTG CTT MTC ATA -3' and Next-to-Smith-EcoRI-rev: 5'- TAT GAA TTC CCA CGG GAA CGT GAA GCT -3' (for $Kcv_{Next\text{-}to\text{-}Smith}$), and Smith-XhoI-for TAT CTC GAG ATG TTG CTG CTT CTC ATA and Next-to-Smith-EcoRI-rev (see above, for Kcv_{Smith}). The stop codons of the Kcv genes were deleted for the fusion with the EGFP gene.

Site-directed mutagenesis

Point mutations were made with the QuickChange Site-directed Mutagenesis method (Stratagene). Primers were synthesized by Eurofins MWG GmbH, Ebersberg, Germany. Resulting constructs were checked by sequencing (Eurofins MWG GmbH, Ebersberg, Germany).

Electrophysiological Measurements

HEK293 (Human Embryonic Kidney 293) cells were grown in 35 mm culture dishes at 37 °C and 5 % CO_2 in DMEM/F12 medium with 2.5 mM glutamine, 10 % FCS and 10 mL/L Penicilline/Streptomycine for one or two days until they reached ~ 70 to 80 % confluence. The cells were then transiently transfected with Kcv::EGFP constructs with the help of the liposomal transfection reagent TurboFect™ (Fermentas, St. Leon Rot, Germany). After one day, the cells were washed with PBS (140 mM NaCl, 3 mM KCl, 8 mM Na_2HPO_4, 1.4 mM KH_2PO_4, pH 7.05), dispersed with Accutase® (SIGMA-Aldrich, Schnelldorf, Germany) and sowed into new culture dishes with lower density. The cells were allowed to settle down for at least five hours.

For the electrophysiological measurements, the culture medium was removed and replaced by different bath solutions. The solutions contained 1.8 mM $CaCl_2$, 1 mM $MgCl_2$ and 5 mM 4-(2-hydroxyethyl)-1-piperazineethanesulfonic acid (HEPES) and either KCl (up to 100 mM) or 50 mM NaCl, RbCl, NH_4Cl, LiCl or 50 mM KCl with the addition of a blocking agent (10 mM $BaCl_2$, 10 mM CsCl, 10 mM Amantadine-HCl or 10 mM Tetraethylammonium chloride (TEA)). The pH was adjusted to 7.4 with the respective hydroxide, i.e. KOH for the KCl solution, LiOH for the LiOH solution, etc. The osmolarity was adjusted to 330 mOsmol with mannitol. The Pipette solution contained 130 mM D-potassium-gluconic acid, 10 mM NaCl, 5 mM HEPES, 0.1 mM guanosine triphosphate (Na salt), 0.1 μM $CaCl_2$, 2 mM, $MgCl_2$, 5 mM phosphocreatine and 2 mM adenosine triphosphate (ATP, Na salt); the pH was adjusted to 7.4 with KOH, the osmolarity was adjusted to 330 mOsmol with mannitol.

Single cell patch-clamp measurements were performed in whole-cell configuration under standard methods (Hamill et al., 1981) with a EPC-9 patch-clamp amplifier (HEKA, Lamprecht, Germany) at room temperature. As standard pulse protocol we used a holding voltage of 0 mV with test voltages between -160 mV and +80 mV with 20 mV increments and a post pulse of -80 mV (**Fig. 28**). The data were acquired with the Pulse software (HEKA, Lamprecht, Germany). A change of bath solutions was achieved by a perfusion pipette, which was positioned close to the cell under investigation.

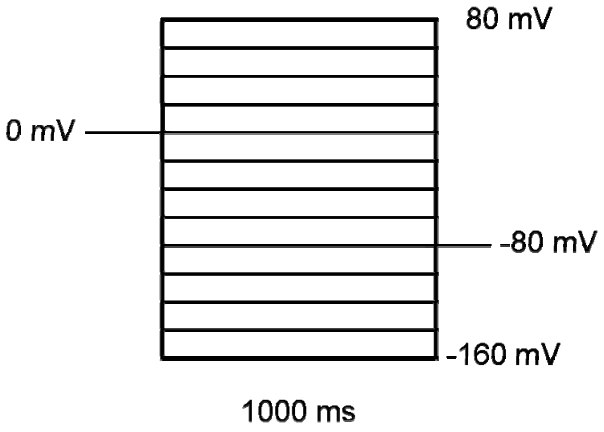

Fig. 28: Standard pulse protocol for the examination of Kcv channel proteins

3.6. References

Baumeister, D. (2010): Struktur-Funktions-Beziehung viraler Kaliumkanäle: Einfluss der Transmembrandomänen auf die Funktion und Sortierung von Kaliumkanälen. Dissertation at the Technische Universität Darmstadt.

Bonza, M. C., Martin, H., Kang, M., Lewis, G., Greiner, T., Giacometti, S., Van Etten, J. L., De Michaelis, M. I., Thiel, G., Moroni, A. (2010): A functional calcium-transporting ATPase encoded by chlorella viruses. *Journal of General Virology*, **91**, 2620. doi:10.1099/vir.0.021873-0

Bubeck, J. A., Pfitzner, A. J. P (2005): Isolation and characterization of a new type of chlorovirus that infects an endosymbiotic Chlorella strain of the heliozoon Acanthocystis turfacea. *Journal of General Virology*, **86**, 2871. doi:10.1099/vir.0.81068

Chatelain, F. C., Gazzarrini, S., Fujiwara, Y., Arrigoni, C., Domigan, C., Ferrara, G., Pantoja, C., Thiel, G., Moroni, A., Minor, D. L. (2009): Selection of Inhibitor-Resistant Viral Potassium Channels Identifies a Selectivity Filter Site that Affects Barium and Amantadine Block. *PLoS ONE*, **4**, e7496. doi:10.1371/journal.pone.0007496

Fitzgerald, L.A., Graves, M. V., Li, X., Feldblyum, T., Hartigan, J., and Van Etten, J. L. (2007a): Sequence and annotation of the 314-kb MT325 and the 321-kb FR483 viruses. *Virology*, **358,** 459. doi:10.1016/j.virol.2006.08.034

Gazzarrini, S., Severino, M., Lombardi, M., Morandi, M., DiFrancesco, D., Van Etten, J. L., Thiel, G., Moroni, A. (2003): The viral potassium channel Kcv: structural and functional features. *FEBS Lett.*, **552**, 12.

Gazzarrini, S., Kang, M., Van Etten, J. L., Tayefeh, S., Kast, S. M., DiFrancesco, D., Thiel, G., Moroni, A. (2004): Long Distance Interactions within the Potassium Channel Pore Are Revealed by Molecular Diversity of Viral Proteins. *The Journal of Biological Chemistry*, **279**, 28443. doi:10.1074/jbc.M401184200

Gazzarrini, S., Kang, M., Epimashko, S., Van Etten, J. L., Dainty, J., Thiel, G. and Moroni, A. (2006): Chlorella virus MT325 encodes water and potassium channels that interact synergistically. *PNAS*, **103,** 5355. doi:10.1073/pnas.0600848103

Gazzarrini, S., Kang, M., Abenavoli, A., Romani, G., Olivari, C., Gaslini, D., Ferrara, G., Van Etten, J. L., Kreim, M., Kast, S. M., Thiel, G., Moroni, A. (2009): Chlorella virus ATCV-1 encodes a functional potassium channel of 82 amino acids. *Biochem. J.*, **420**, 295. doi:10.1042/BJ20090095

Hamacher, K., Greiner, T., Van Etten, J. L., Gebhardt, M., Villareal, L. P., Moroni, A., Thiel, G. (2011): Diverse but Conserved Phycodnavirus Potassium Ion Channel Proteins Question the Viral Molecular Piracy Hypothesis. Submitted.

Hamill, O. P., Marty, A., Neher, E., Sakmann, B., Sigworth, F. J. (1981): Improved patch-clamp techniques for high-resolution current recording from cells and cell-free membrane patches. *European Journal of Physiology*, **391**, 85. doi:10.1007/BF00656997

Hertel, B., Horváth, F., Wodala, B., Hurst, A., Moroni, A., Thiel, G. (2005): KAT1 inactivates at sub-millimolar concentrations of external potassium. *Journal of Experimental Botany*, **56**, 3103. doi:10.1093/jxb/eri307

Hertel, B., Tayefeh, S., Kloss, T., Hewing, J., Gebhardt, M., Baumeister, D., Moroni, A., Thiel, G., Kast, S. M. (2010): Salt bridges in the miniature viral channel Kcv are important for function. *Eur Biophys J*, **39**, 1057. doi:10.1007/s00249-009-0451-z

Hille, B. (2001): Ion Channels of Excitable Membranes. Third Edition. Sinauer Associates, Inc., Sunderland, Massachusetts, USA.

Horowitz, G. (1998): Organic Field-Effect Transistors. *Adv. Mater.*, **10**, 365.

Huang, S.-C. J., Artyukhin, A. B., Misra, N., Martinez, J. A., Stroeve, P. A., Grigoropoulos, C. P., Ju, J.-W. W., Noy, A. (2010): Carbon Nanotube Transistor Controlled by a Biological Ion Pump Gate. *Nano Letters*, **10**, 1812. doi:10.1021/nl100499x

Jiang, B., Sun, X., Cao, K., Wang, R. (2002): Endognous K_v channels in human embryonic kidney (HEK293) cells. *Molecular and Cellular Biochemistry*, **238**, 69. doi:10.1023/A:1019907104763

Kang, M., Moroni, A., Gazzarrini, S., Van Etten, J. L. (2003): Are chlorella viruses a rich source of ion channel genes? *FEBS Letters*, **552**, 2. doi:10.1016/S0014-5793(03)00775-0

Kang, M., Moroni, A., Gazzarrini, S., DiFrancesco, D., Thiel, G., Severino, M., Van Etten, J. L. (2004a): Small potassium ion channel proteins encoded by chlorella viruses. *PNAS*, **101**, 5318. doi:10.1073/pnas.0307824100

Kang, M., Graves, M., Mehmel, M., Moroni, A., Gazzarrini, S., Thiel, G., Gurnon, J. R., Van Etten, J. L. (2004b): Genetic diversity in chlorella viruses flanking *kcv*, a gene that encodes a potassium ion channel protein. *Virology*, **326**, 150. doi:10.1016/j.virol.2004.05.023

Krapivinski, G., Medina, I., Eng, L., Krapivinsky, L., Yang, Y., Clapham, D. (1998): A Novel Inward Rectifier K^+ Channel with Unique Pore Properties. *Neuron*, **20**, 995.

MacKinnon, R. (2004): Potassium Channels and the Atomic Basis of Selective Ion Conduction. *Bioscience Reports*, **24**, 75.

Plugge, B., Gazzarrini, S., Nelson, M., Cerana, R., Van Etten, J. L., Derst, C., DiFrancesco, D., Moroni, A., Thiel, G. (2000): A Potassium Channel Protein Encoded By Chlorella Virus PBCV-1. *Science*, **287**, 1641. doi:10.1126/science.287.5458.1641

Rosenberg-Lipinsky, H. Dissertation (2006): Funktionelle Rolle von Oberflächenladungen in der Turret-Domäne des viralen Miniatur-Kaliumkanals Kcv. Dissertation at the Technische Universität Darmstadt.

Schrempf, H., Schmidt, O., Kümmerlen, R., Hinnah, S., Müller, D., Betzler, M., Steinkamp, T., Wagner, R. (1995): A prokaryotic potassium ion channel with two predicted transmembrane segments from *Streptomyces lividans*. *The EMBO Journal,* **14**, 5170.

Shim, J. W., Yang, M., Gu, L.-Q. (2007): In vitro synthesis, tetramerization and single channel characterization of virus-encoded potassium channel Kcv. *FEBS Letters*, **581**, 1027. doi:10.1016/j.febslet.2007.02.005

Sigworth, F. J. (2003): Life´s transistors. *Nature*, **423**, 21.

Tayefeh, S., Kloss, T., Kreim, M., Gebhardt, M., Baumeister, D., Hertel, B, Richter, C., Schwalbe, H., Moroni, A., Thiel, G., Kast, S. M. (2009): Model development for the viral Kcv potassium channel. *Biophys. J.*, **96**, 485-498. doi:10.1016/j.bpj.2008.09.050

Thiel, G., Moroni, A., Dunigan, D., Van Etten, J. (2010a): Initial Events Associated with Virus PBCV-1 Infection of *Chlorella* NC64A. *Progress in Botany*, **71**, 169. doi:10.1007/978-3-642-02167-1_7

Thiel, G., Baumeister, D., Schroeder, I., Kast. S. M., Van Etten, J. L., Moroni, A. (2010b): Minimal art: Or why small viral K^+ channels are good tools for understanding structure function relations. *Biochimica et Biophysica Acta*, **1808**, 580. doi:10.1016/j.bbamem.2010.04.008

Van Etten, J. L., Burbank, D. E., Kuczmarski, D., Meints, R. H. (1983): Virus infection of culturable chlorella-like algae and development of a plaque assay. *Science*, **219**, 994.

4. Chapter 3 – A functional potassium transporter encoded by Chlorella viruses

4.1. Abstract

Chlorella viruses have shown to be source for interesting membrane transport proteins. Here we examine a putative potassium transporter encoded by Pbi virus Fr483 and few related chlorella viruses. The protein shares sequence and structural features with HAK/KUP/KT-like potassium transporters from plants, bacteria and fungi. Yeast complementation assays and Rb^+-uptake experiments show that the viral protein is functional with transport characteristics comparable to known potassium transporters. Due to its overall function we termed the protein HAKCV-1 for High Affinity K^+ transporter Chlorella Virus-1. Expression studies reveal that the protein is expressed early during the viral replication cycle and proteomics data show that it is probably not part of the virion. The function of the transporter during replication is still unclear. The data are not in agreement with the idea that the transporter substitutes for the role of the K^+ channels in infection.

4.2. Introduction

Chlorella viruses are a large family of plaque-forming dsDNA viruses, which infect certain unicellular exsymbiotic green algae of the chlorella type (Van Etten *et al.* 1983). They are large in genome size (280 to 370 bp), structurally similar, but they exhibit a high diversity with regard to their proteins (Van Etten *et al.* 2010). These viruses are abundant all over the world in fresh waters and have been studied intensively in the last 30 years (Van Etten *et al.* 2010). They encode for a variety of unexpected proteins, e.g. a hyaluronan synthase (De Angelis *et al.* 1997), an aquaglyceroporin (Gazzarrini *et al.* 2006), a Calcium-ATPase (Bonza *et al.* 2010) and a small potassium channel named Kcv, which has been studied intensively (Plugge *et al.* 2000, Gazzarrini *et al.* 2003; Kang *et al* 2004a; Kang *et al.* 2004b). Especially the potassium channel Kcv occurs to be essential for the replication of the viruses. The current view is that the virus particle incorporates this channel into the plasma membrane of the host early during infection (Thiel *et al* 2010a). This leads to a depolarization of the host plasma membrane and finally in a loss of K^+ from the host. In this way the virus can reduce the turgor pressure of the host and ease the ejection of its large genome into the alga cell (Thiel *et al.* 2010a). Surprisingly one virus, namely the Pbi virus Fr483, does not encode for a Kcv ortholog. Instead a putative potassium transporter gene was found in the genome of virus Fr483 and it was speculated that this protein might take over the role of Kcv (Fitzgerald *et al.* 2007a).

Potassium transporters differ from potassium channels in two respects: they have a lower transport rate and their transport can be coupled to that of other ions. The general turnover rate of transporters is in the range of 10^2 to 10^4 ions per second (Hick and Hick 2009). Hence the transporters are conducting potassium up to four orders of magnitude slower than channels; channels have, for

reference, a transport rate of 10^7 to 10^8 ions per second (Hille 2001). The transport mechanism of transporters differs from that of channels in that they can catalyze the flux of K^+ in form of a symport or antiport with other ions against a concentration gradient. The energy for this uphill transport of K^+ is derived frequently from a coupling to a downhill transport of H^+. In this way, plant potassium transporters for example can take up K^+ from an environment with μmolar K^+ content into the cytosol with 100 mM K^+ (Epstein *et al.* 1963; Kim *et al.* 1998; Rodríguez-Navarro and Rubio 2006).

The putative potassium transporter from Pbi virus Fr483 is homologue to the HAK/KUP/KT-like potassium transporters from plants, bacteria and fungi (Grabov 2007). Hence, we termed it HAKCV-1 for High Affinity K^+ transporter Chlorella Virus-1. There are only limited data about the structure of HAK/KUP/KT-like potassium transporters since there is as yet no crystal structure available.

Hydrophobicity plots of the amino acid sequences of HAK/KUP/KT-like potassium transporters suggest that they consist of 10 to 14 transmembrane domains with a large hydrophylic loop between the second and the third transmembrane. The second transmembrane domain contains a sequence (VFGD/IYGD), which is conserved among all HAK/KUP/KT K^+ transporters and is discussed as putative filter sequence (Rigas *et al.* 2001). It is not yet clear of how many subunits the functional transporter is composed (Rigas *et al.* 2001).

Recently, a crystal structure was published for VbTrkH from *Vibrio parahaemolyticus* (Cao *et al.* 2011), another kind of potassium tranporter proteins from the Ktr/TRK/HKT family. The members of this family are structurally different from HAK/KUP/KT-like potassium transporters: they form homodimers, which contain four pore forming domains including four different selectivity filter sequences – TTTGAT, AIGGFS, TTAGFT and NNLGPG in the case of VbTrkH (Cao *et al.* 2011). Like other potassium transporting proteins, including potassium channels, the respective filter sequences contain glycine residues.

HAK/KUP/KT-like potassium transporters do not discriminate between K^+ and Rb^+, a fact, which made it possible to use the Rb^+ for flux experiments. Since the turnover rate of transporters is too low for electrophysiological recording of the transporter activity, the use of Rb^+ has proved to be a powerful tool for the characterization of the transport properties of these proteins (Kim *et al.* 1998; Rigas *et al.* 2001). The general picture, which emerges from these studies, is that HAK/KUP/KT-like potassium transporters preferentially transport potassium. Like K^+ channels they also transport Cs^+ (Zhu and Smolders 2000), but they do not transport NH_4^+ and they are even inhibited by this cation (Rodriguez-Navarro and Rubio 2006). Na^+ is also transported by them albeit with a low affinity (Rodriguez-

Navarro and Rubio 2006). HAK/KUP/KT-like potassium transporters facilitate the transport of the ion by a symport with H^+ (Szcserba *et al*. 2009).

Unlike K^+ channels HAK/KUP/KT K^+ transporters are not encoded by all organisms. They can be found in plants (e.g. the Tiny Root hair -1 K+ transporter (TRH1) in *Arabidopsis thaliana* (Rigas *et al.* 2001)), in fungi (e.g. the High Affinity K+ transporter 1 (HAK1) in yeast (Banuelos *et al* 1995)) and in bacteria (e.g. the K^+ Uptake Protein 1 (KUP1) (Schleyer and Bakker 1993)). To date, no animal encoded HAK/KUP/KT-like K^+ transporter is known.

A closer look at the sequence and the predicted structure of the viral protein motivated us to examine the function of the protein and its potential role in the viral life cycle.

4.3. Results

Sequence and structure of putative viral potassium transporters

The genome of Pbi virus Fr483 was fully sequenced and annotated (Fitzgerald *et al.* 2007a). The annotation revealed a putative potassium transporter, encoded by ORF N110R, which was homologue to HAK transporters from *Arabidopsis thaliana*, e.g. TRH1 or HAK5 (Rigas *et al.* 2001). To further investigate this similarity, we made an alignment of N110R with HAK5 from *Arabidopsis thaliana*. The alignment shows the high similarity of the two proteins (**Fig. 29**); they share 37 % sequence identity.

The prediction of transmembrane domains (TMs) for HAKCV-1 by the TMHMM algorithm shows that it contains at least 12 TMs (**Fig. 30 A**). For comparison we also analyzed the HAK5 transporter from *Arabidopsis thaliana.* For this protein, which is 125 amino acids longer than HAKCV-1, we also found 12 predicted TMs. For both proteins the structural prediction implies a large gap between the second and the third TM and a long cytoplasmic C-terminus. The main difference between the two proteins lies in the length of the C-terminus, which is about 100 amino acids longer in the case of HAK5. **Fig. 30 B** shows a schematic representation of the protein based on the predictions by the TMHMM algorithm.

```
HAK5            MDGEEHQIDGDEVNNHENKLNEKKKSWGKLYRPDSFIIEAGQTPTNTGRRSLMSWRTTMS 60
N110R           ------------------------------MSETGVVTIEQEEKILELGRKNIRGWS-LVI 30
                                             : ... . **  :.  : **:.: .*   :

HAK5            LAFQSLGVVYGDIGTSPLYVYASTFTDGINDKDD--VVGVLSLIIYTITLVALLKYVFIV 118
N110R           LSLASLGVVFGDIGTSPLYVLPAIFGELRHQPTENFILGVFSTIFWTITLMVLVKYVWFT 90
                *:: *****:********** .: * :  ::  :  ::**:* *::****:.*:***::.

HAK5            LQANDNGEGGTFALYSLICRYAKMGLIPNQEPEDVELSNYTLELPTTQLRRAHMIKEKLE 178
N110R           LAIDDHGEGGVFALYSIIRRAITS------KPSDFGVDTQEEKIPS-------KTKDFLE 137
                *  :*:****.*****:* *  .       :*.*. :..   ::*:         *: **

HAK5            NSKFAKIILFLVTIMGTSMVIGDGILTPSISVLSAVSGIKSLG---QNTVVGVSVAILIV 235
N110R           NNKWARKVIMGIVITCASLTMADGILTPSISVISATEGIQFHTGISHDTVIFITIGILVG 197
                *.*:*: ::: :.*  :*:.:.**********:**..**:      ::**: :::.**:

HAK5            LFAFQRFGTDKVGFSFAPIILVWFTFLIGIGLFNLFKHDITVLKALNPLYIIYYFRRTG- 294
N110R           LFSIQFLGTGKVGVIFGPTMLVWFVFNLSVGVYNVTKMPG-VFRAFSPHYMYYFWEEFGS 256
                **::* :**.***. *.* :****.* :.:*::*: *    *::*:.* *: *::.. *

HAK5            RQGWISLGGVFLCITGTEAMFADLGHFSVRAVQISFSCVAYPALVTIYCGQAAYLTKHTY 354
N110R           WEAFKLLGEVFLAITGVEALYADMGHLNAMSIRISFSAIVYPSLVMNYLGQTAVVLLDYN 316
                 :.:  ** ***.***.**::**:**:.. :::****.:.**:**  * **:* :  .

HAK5            NVSNTFYDSIPDPLYWPTFVVAVAASIIASQAMISGAFSVISQSLRMGCFPRVKVVHTSA 414
N110R           TSSSLYWSSIPAKLAWPSLAIAASAAVIASQALITGTFTIVQQAMHANVFPRVAIFQTNK 376
                . *. ::.***  * **::.:*.:*::*****:*:*:*:::.*::: . **** :.:*.

HAK5            KYEGQVYIPEINYLLMLACIAVTLAFRTTEKIGHAYGIAVVTVMVITTLMVTLIMLVIWK 474
N110R           KHAGQIYIPVVNFALLVGSISVVLIFQSSSKIVSAYGFAVSIVVVLTHIFFCIVLHIQGR 436
                *: **:*** :*: *::..*:*.* *:::.**  ***:**  *:*:* ::. ::: :  :

HAK5            TNIVWIAIFLVVFGSIEMLYLSSVMYKFTSGGYLPLTITVVLMAMMAIWQYVHVLKYRYE 534
N110R           -NKLFSFVFSSFFGVISIAFAASLTIKIPKGAWFSAAIGSALIFVSLVWHRGHRMKVRYI 495
                 * ::  :*  .** *.: : :*:  *:..*.::. :*  .*: :  :*:  * :* **

HAK5            LREKISRENAIQMATSPDVNRVPGIGLFYTELVNGITPLFSHYISNLSSVHSVFVLISIK 594
N110R           KINRLSARQVFSKPSNNSKN-----IVFYNELTDGIVPAYNQLENLITISGTNNIVLSVR 550
                  :::* .:.:. .:. . *      :**.**.:**.* :.:  . ::   :  :::*::

HAK5            TLPVNRVTSSERFFFRYVGPKDSGMFRCVVRYGYKEDIEEPDEFERHFVYYLKEFIHHEH 654
N110R           KMTIPRVREDQRFLITGYD----GVYHVVARYGYAEIIDHGNCFARKLCQAVN------- 599
                .:.: ** ..:**::   .    *::: *.**** * *:. : * *::   ::

HAK5            FMSGGGGEVDETDKEEEPNAETTVVPSSNYVPSSGRIGSAHSSSSDKIRSGRVVQVQSVE 714
N110R           ------------------------------------------------------------


HAK5            DQTELVEKAREKGMVYLMGETEITAEKESSLFKKFIVNHAYNFLKKNCREGDKALAIPRS 774
N110R           --------AESSDVVFVMGRTKLLTTNTS--FYNKAVIAMYSLLVKLSSWTTDTFNTPTS 649
                        *....:*::**.*:: : : *  * :  *   *.:* * .    .::  * *

HAK5            KLLKVGMTYEL 785
N110R           KLIIFEASYEI 660
                **: .  :**:
```

Fig. 29: Alignment of the putative potassium Transporter HAKCV-1encoded by virus Fr483 ORF N110R with the High Affinity K+ Transporter 5 (HAK5) of *Arabidopsis thaliana*. Alignment was done with ClustalW (http://www.ebi.ac.uk/Tools/msa/clustalw2/). Asteriks and colons indicate identical and conserved residues respectively.

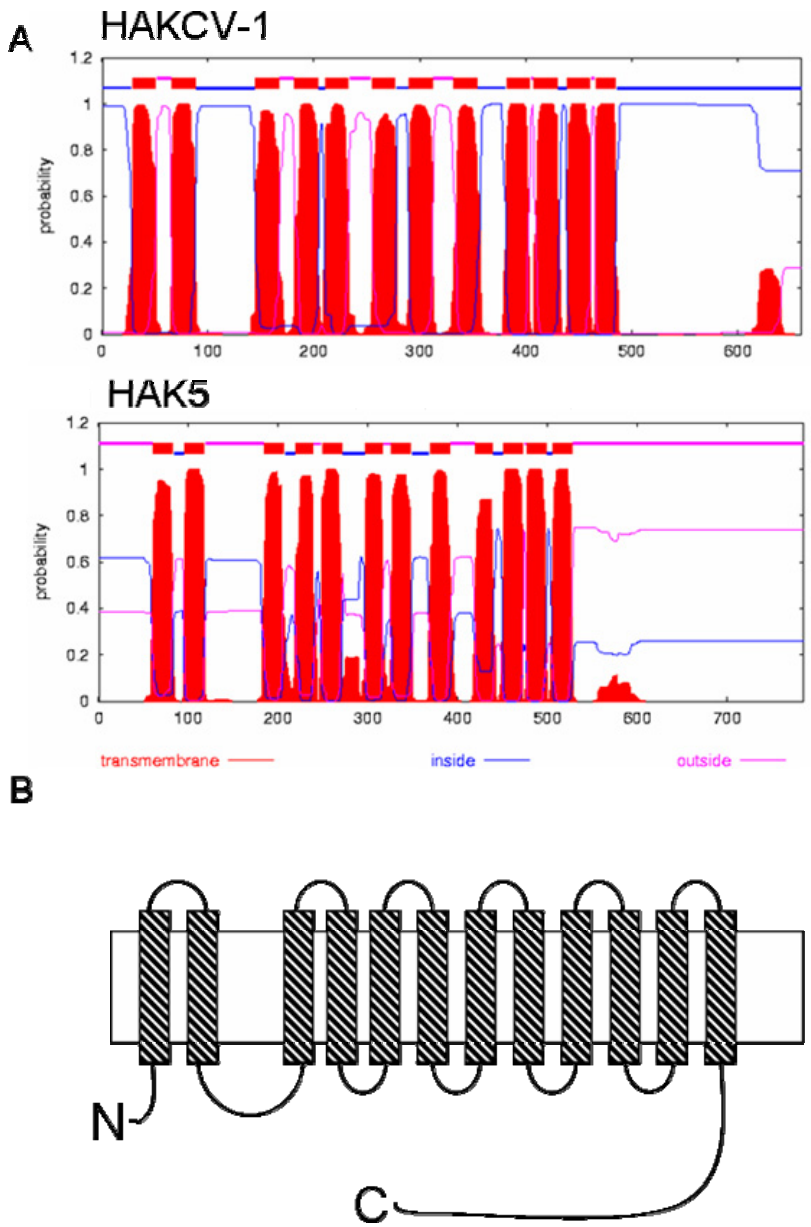

Fig. 30: The putative viral potassium transporter HAKCV-1 has the structure of a HAK-like potassium transporter

(A) Predicted transmembrane domains of the putative potassium transporter HAKCV-1 compared HAK5 transporter from Arabidopsis thaliana. Transmembrane domain prediction was done with TMHMM (http://www.cbs.dtu.dk/services/TMHMM/).

(B) Schematic representation of a HAK-like transporter.

To get an idea about the origin and evolution of the viral transporter HAKCV-1, we used potassium transporter homologs of plants, fungi, bacteria and archaea for a phylogenetic tree (**Fig. 31**). Here we found a clear separation between a prokaryal group and a eukaryal group including the viral transporters. The prokaryal transporters are separated into a eubacterial and an archaeal branch. The eukaryal branch is separated into a viral branch on the one side and a plant/fungi branch on the other side with strong statistical support. From the clear separation of the viral branch from the plant/fungal branch we assume that the viral transporters were not obtained from their hosts by molecular piracy.

So far, this interpretation is speculative since there is no genomic data available for the hosts *Chlorella* Pbi and *Chlorella* SAG 3.83. A blast search against the genome of the fully sequenced related *Chlorella* NC64A revealed a small protein (CDS: fgenesh3_pg.C_scaffold_30000010) with similarities to HAKCV-1. **Fig. 32** shows an alignment of HAKCV-1 with the respective algal protein from *Chlorella* NC64A. The *Chlorella* NC64A protein (CNP) has a size of only 282 amino acids and five predicted TMs (not shown). It is, thus, not a HAKT/KUP/KT-like potassium transporter from a structural point of view. These data support the interpretation of the phylogenetic tree in that the HAKCV-1 gene was not picked up from the host.

This interpretation is also in agreement with a more detailed study in which the relation between viral K^+ channels and their host was examined. In this study it was found that the potassium channel Kcv is not related to the channels from the host and it was suggested that the respective genes are of viral origin (see chapter 5; Hamacher *et al.* 2011).

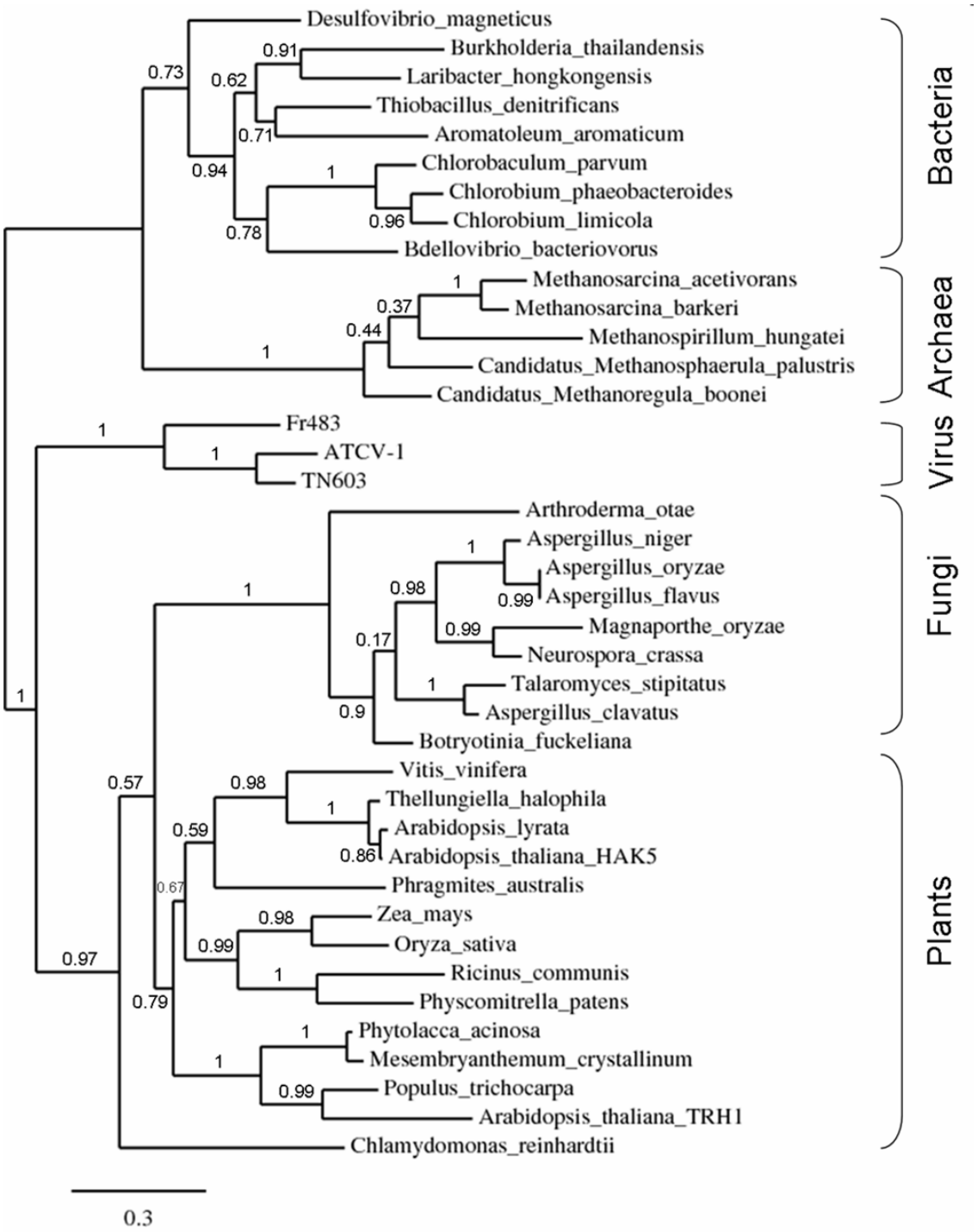

Fig. 31: Phylogenetic tree of HAK/KUP/KT-like potassium transporters

Phylogenetic tree of potassium transporters from several organisms (plants, fungi, archaea, bacteria and viruses). Tree was made by using the server at www.phylogeny.fr with the default parameters. Rooting was done at mid-point (Dereeper and Guignon *et al.* 2008). The scale bar indicates the number of substitutions per position.

```
HAKCV-1         ------MSETGVVTIEQEEKILELGRKNIRG--WSLVILSLASLGVVFGDIGTSPLYVLP 52
CNP             MAGQLTVSSLWAHDADLQKQVEEAHRKRMGVGTWSLLAMAFSTLGIVYGDIGTSPLYVFA 60
                      :*.  .   : :::: *  **.:    ***: ::::::*:*:**********:.

HAKCV-1         AIFGELRHQPTENFILGVFSTIFWTITLMVLVKYVWFTLAIDDHGEGGVFALYSIIRRAI 112
CNP             SIFPDG--PPSAEVTLGAASTIFWSITGIVVVKYIVFTLQADDNGEGGIFALYALLCRAV 118
                :** :    *: :. **. *****:** :*:***: ***  **:****:****::: **:

HAKCV-1         TSK-----------------------------PSDFGVDTQ----------EEKIPSKT 132
CNP             SIRSGSLLHEADLSLSQYQAPDPPAQARASPSPPHTSGAGTCGGPGAAYTRWRQSVVARA 178
                : :                                *   *..*           .:.: :::

HAKCV-1         KDFLENNKWARKVIMGIVITCASLTMADGILTPSISVISATEGIQFHTGISHDTVIFITI 192
CNP             RASLEGSRAAQGILLAVVLLAANMILSDGVLTPAISVVSAVEGIEYQTGISRGTVVGIAV 238
                :  **..: *: ::::.:*: .*.: ::**:***:***:**.***:::****:.**: *::

HAKCV-1         GILVGLFSIQFLGTGKVGVIFGPTMLVWFVFNLSVGVYNVTKMPGVFRAFSPHYMYYFWE 252
CNP             GILVCLFAVQPWGTQRVAVMFSPLVFLWFAS---------------------------- 269
                **** **::*  ** :*.*:*.* :::**.

HAKCV-1         EFGSWEAFKLLGEVFLAITGVEALYADMGHLNAMSIRISFSAIVYPSLVMNYLGQTAVVL 312
CNP             -----------------------------LSGIGEALGLAA------------------ 281
                                              *.::.  :.::*

HAKCV-1         LDYNTSSSLYWSSIPAKLAWPSLAIAASAAVIASQALITGTFTIVQQAMHANVFPRVAIF 372
CNP             ------------------------------------------------------------


HAKCV-1         QTNKKHAGQIYIPVVNFALLVGSISVVLIFQSSSKIVSAYGFAVSIVVVLTHIFFCIVLH 432
CNP             ------------------------------------------------------------


HAKCV-1         IQGRNKLFSFVFSSFFGVISIAFAASLTIKIPKGAWFSAAIGSALIFVSLVWHRGHRMKV 492
CNP             ------------------------------------------------------------


HAKCV-1         RYIKINRLSARQVFSKPSNNSKNIVFYNELTDGIVPAYNQLENLITISGTNNIVLSVRKM 552
CNP             ------------------------------------------------------------


HAKCV-1         TIPRVREDQRFLITGYDGVYHVVARYGYAEIIDHGNCFARKLCQAVNAESSDVVFVMGRT 612
CNP             ------------------------------------------------------------


HAKCV-1         KLLTTNTSFYNKAVIAMYSLLVKLSSWTTDTFNTPTSKLIIFEASYEI 660
CNP             -------------------------------------------------
```

Fig. 32: Alignment of HAKCV-1 encoded by virus Fr483 with an uncharacterized protein encoded by the alga *Chlorella* NC64A (CNP). Alignment was done with ClustalW (http://www.ebi.ac.uk/Tools/msa/clustalw2/). Asteriks and colons indicate identical and conserved residues respectively.

A recent genome-sequencing project involving 50 chlorella viruses from 3 different families has discovered a total of six potassium transporter homologs. One was found in a Pbi virus and five were found in SAG viruses. **Tab. 1** shows the new genes together with the two known genes from Pbi virus

Fr483 and SAG virus ATCV-1. The occurrence of the potassium transporter within the diverse chlorella viruses can be summarized as followed:

i) NC64A viruses encode for a potassium channel only, no potassium transporter was found up to date.
ii) All SAG viruses encode all for a potassium channel and several (six) of them encode in addition also for a potassium transporter.
iii) Two Pbi viruses encode for a potassium transporter (Fr483 and NW665.2); except for virus Fr483 they do all encode for a potassium channel.

To get an idea about the distribution of the transporter gene among the chlorella viruses, we made a phylogenetic tree based on the DNA polymerase gene exploiting the data from the aforementioned sequencing project. The DNA polymerase gene has shown to be useful as genetic marker in several studies of phycodnaviruses, because all members contain the gene (Chen and Suttle 1995; Chen *et al.* 1996; Hanson *et al.* 2006). **Fig. 33** shows a phylogenetic tree based on amino acid sequences of the DNA polymerase gene from all known chlorella virus genomes. The analysis is complemented by the DNA polymerase genes from other members of the Phycodnaviridae, namely *Ostreococcus tauri* virus-5 (OsV5), *Emiliana huxleyi* virus-86 (EhV86) and *Ectocarpus siliculosus* virus-1 (EsV-1) as outgroups. It can be seen that the three different chlorella virus families are clearly separated. The potassium transporter protein occurs in several viruses without a pattern. Hence the transporter is not virus species specific or related to a particular host.

Tab. 1: Predicted potassium transporter proteins encoded by chlorella viruses

Virus	Family	Length (aa)	ORF
Fr483	Pbi viruses	660	N110R
NW665.2	Pbi viruses	660	R1M11_755R
TN603	SAG viruses	644	R1M1_2359R
Br0604L	SAG viruses	644	R2M1_1283L
MN0810.1	SAG viruses	644	R2M5_1262R
GM0701.1	SAG viruses	676	R2M4_1084R
OR0704.3	SAG viruses	644	R2M10_35R
ATCV-1	SAG viruses	644	Z696R

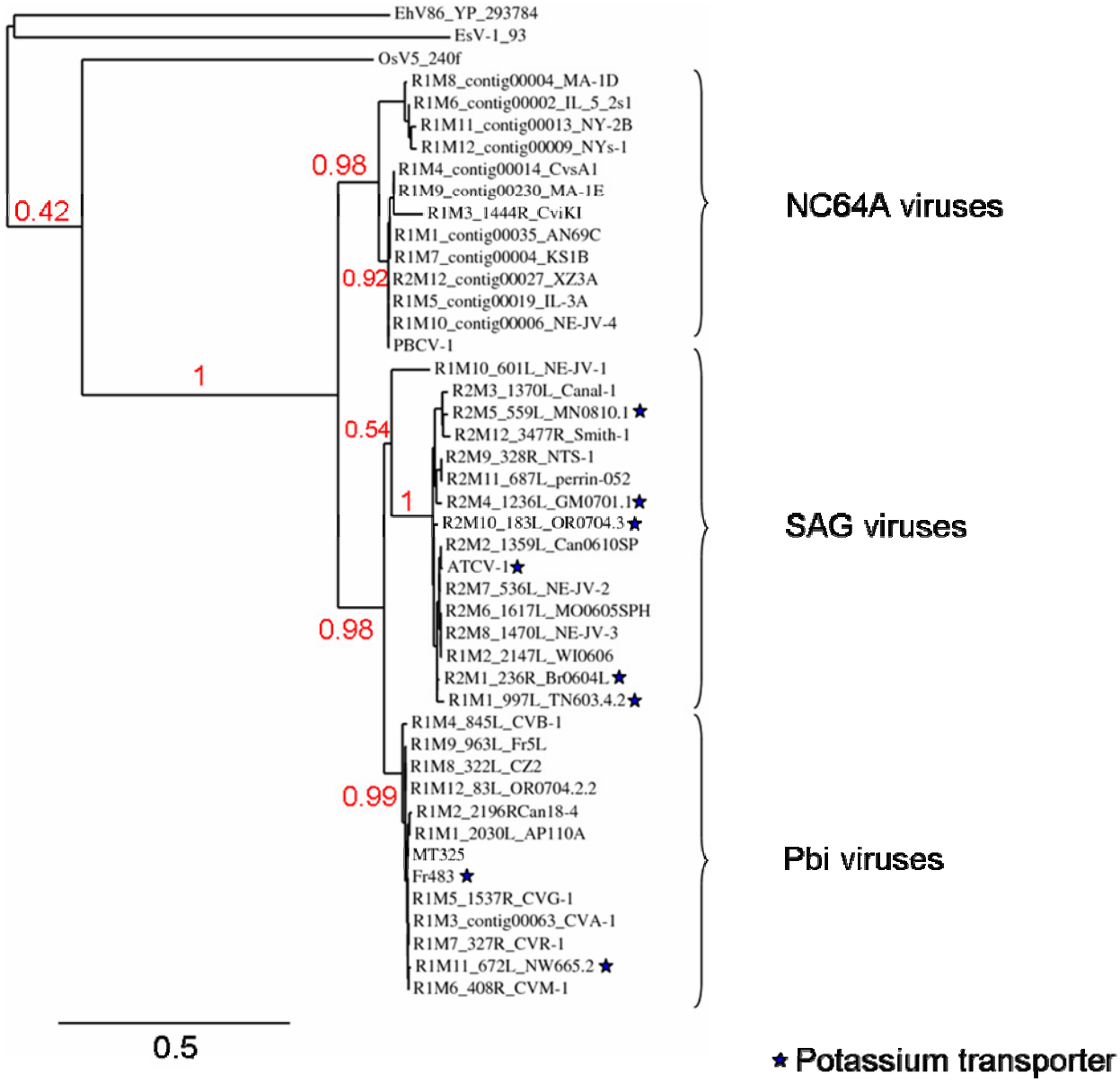

Fig. 33: Potassium transporting proteins among chlorella viruses

Tree was generated by using the DNA polymerase genes of all fully sequenced chlorella viruses including the polymerase genes of *Ostreococcus tauri* virus-5 (OsV5), *Emiliana huxleyi* virus-86 (EhV86) and *Ectocarpus siliculosus* virus-1 (EsV-1) as outgroups. Tree was made using the server at www.phylogeny.fr with the default parameters. Rooting was done at mid-point (Dereeper and Guignon *et al.* 2008). The scale bar indicates the number of substitutions per position.

Functional characterization of the putative potassium transporter HAKCV-1 in heterologous expression systems

To test the putative potassium transporter HAKCV-1 for functionality, we used the Δtrk1 Δtrk2 mutant of *Saccharomyces cerevisiae* as expression systems. This yeast strain lacks endogenous K^+ uptake systems (Minor *et al.* 1999) and is, therefore, not able to grow on media with low K^+ (Ko and Gaber 1991). For the experiment we transformed yeasts with either HAKCV-1, the functional potassium channel Kcv from chlorella virus PBCV-1 (Chatelain *et al.* 2009; Gebhardt *et al.* 2011a; Gebhardt *et al.* 2011b) as positive control or empty vector pYES2 as negative control. The yeast cells were grown in

liquid transformation medium, washed twice with water and diluted to an optical density at 600 nm (OD600) of 1. Cells were spotted on a non-selective plate containing 100 mM K^+ to test whether the protein is toxic for the yeasts. Cells were also spotted on selective plates with 1 and 0.5 mM K^+ respectively, to test for functionality. Subsequent dilutions were performed to avoid artefactual growth. **Fig. 34** shows that all yeasts were growing on the 100 mM K^+ control plate at all dilutions. Hence none of the expressed proteins is deleterious for the cells. Cells expressing HAKCV-1 and PBCV-1 Kcv clearly grow in all dilutions on the selective plates whereas yeasts transformed with the empty vector do not. The results of these experiments suggest that HAKCV-1 is functional and complements the K^+ uptake defect of the yeast mutants. For a more quantitative analysis the experiment was repeated in liquid media containing 0.5 mM K^+. The growth of the cells was determined from the OD600 after 0, 6, 24, 48 and 72 hours; the OD600 value was in this case normalized to zero at $t = 0$ and the data are shown as normalized increase in OD600. Again, cells expressing HAKCV-1 and the positive control Kcv_{PBCV-1} show growth, whereas the negative control does not. The results of these experiments show that HAKCV-1 can complement the deficiency in K^+ uptake transport in this yeast mutant. This indicates that HAKCV-1 is a functional potassium transporter. The efficiency for complementation is similar to that of the viral K^+ channel.

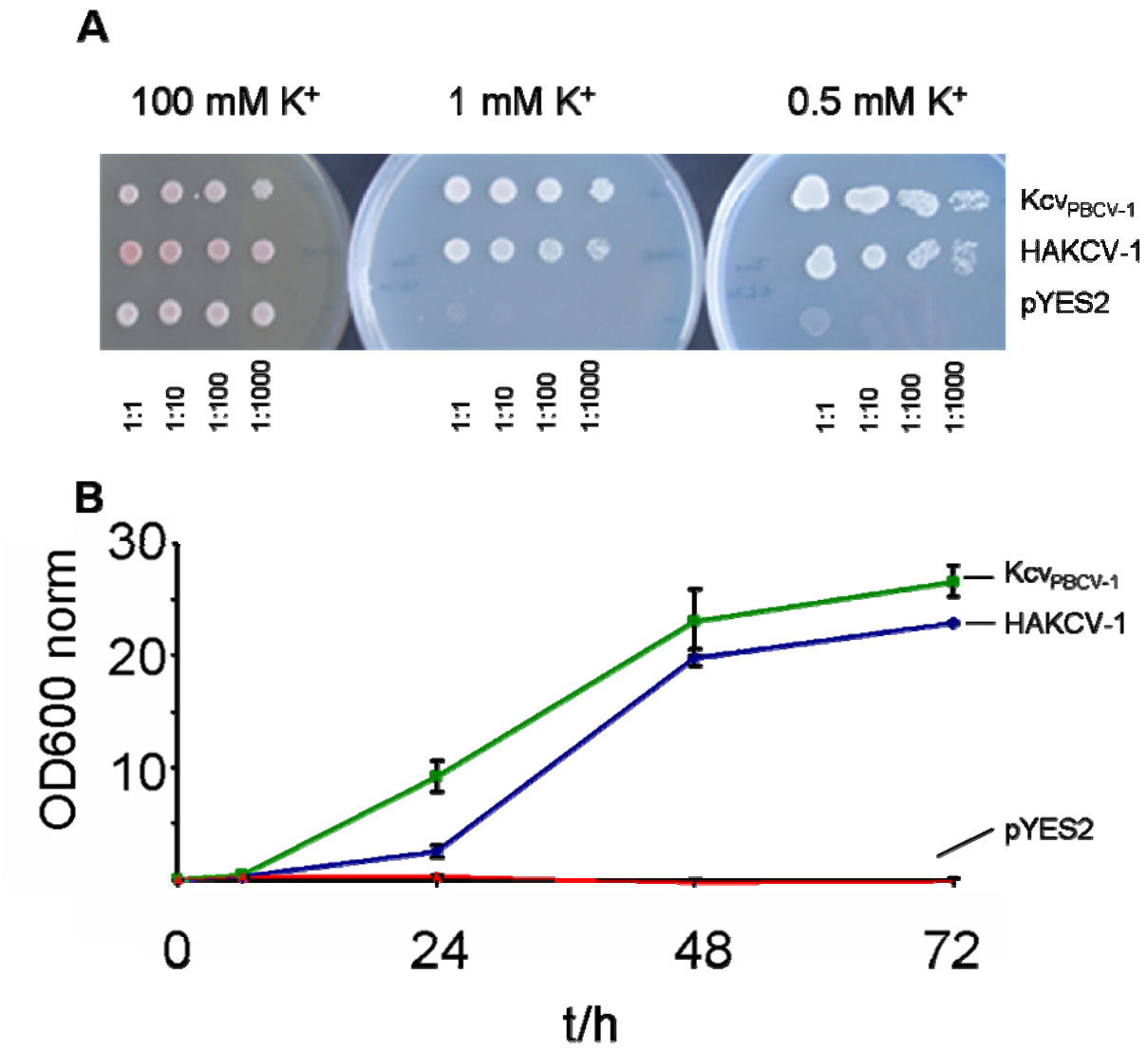

Fig. 34: The putative potassium transporter HAKCV-1 can rescue a Δtrk1, Δtrk2 mutant of *Saccharomcyes cerevisiae*

(A) Complementation of a Δtrk1, Δtrk2 mutant of *Saccharomyces cerevisiae* with Kcv_{PBCV-1} (positive control), HAKCV-1 and empty vector (negative control). The transformed yeasts were grown under non-selective conditions (100 mM K^+) and under selective conditions (1 and 0.5 mM K^+). Subsequent dilutions (1:1 – 1:1000) were done to avoid artifactual growth. (B) Growth of a Δtrk1, Δtrk2 mutant of *Saccharomyces cerevisiae* carrying the HAKCV-1 gene, Kcv_{PBCV-1} or empty vector pYES2. Cells were grown in liquid –ura –met 0.5 mM K^+ medium for 3 days (30 °C, 220 rpm). OD600 was determined after 0, 6, 24, 48 and 76 hours.

For a closer look at the kinetics and mechanisms of transport, we performed uptake experiments with Rb^+ as substitute for K^+. This assay has been established for several HAK/KUP/KT-like transporter proteins (Rodriguez-Navarro and Ramos 1984; Rodriguez-Navarro and Rubio 2006). Yeast cells were transformed with either HAKCV-1 or with empty vector pYES2 as negative control and grown in 50 mM K^+ synthetic medium. At time zero 50 mM RbCl was added to the medium and the time course of Rb^+ was followed. The same experiment was repeated with starved cells: cells were grown in 50 mM K^+ synthetic medium and starved for two hours in K^+ free synthetic medium. This was done to show that enhanced Rb^+ uptake is due to the expressed protein and not due to the upregulation of

endogenous transport proteins (Ramos *et al.* 1985). After the two hours 0.5 mM RbCl was added to the medium and the time course of Rb^+ was followed. **Fig. 35** shows the results of the uptake experiments. In both cases the amount of Rb^+ within the cells increased during the experiment showing that the cells were able to take up the Rb^+. Also in both cases the cells expressing HAKCV-1, show about three to four times higher Rb^+ uptake than the empty vector control. Again, the results of these experiments underscore the fact that HAKCV-1 is a functional K^+ transporter.

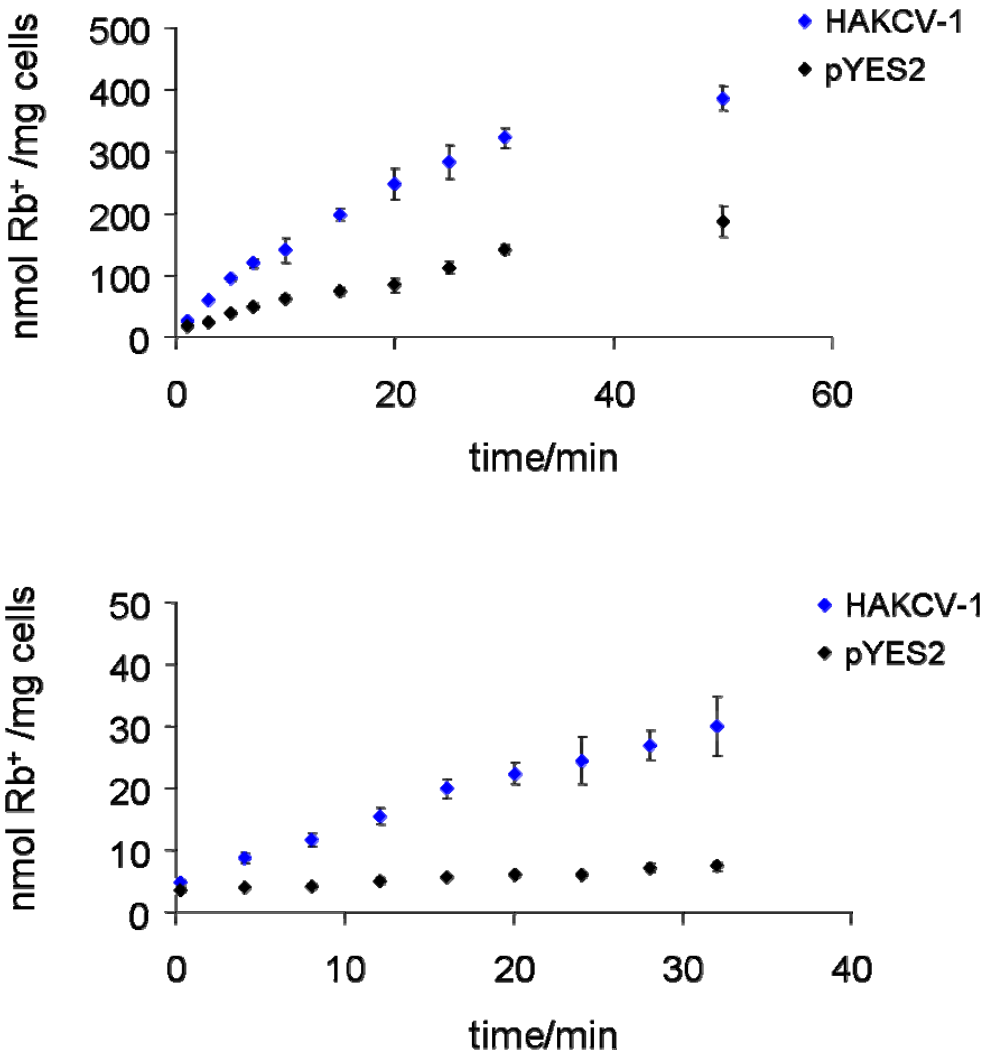

Fig. 35: HAKCV-1 has enhanced Rb^+ uptake

(A) Yeast cells transfected with either empty vector pYES2 or HAKCV-1 were grown in 50 mM K^+ synthetic medium. At time zero 50 mM Rb^+ was added to the medium. **(B)** Yeast cells transfected with either empty vector pYES2 or HAKCV-1 were grown in 50 mM K^+ synthetic medium and then starved in K^+ free synthetic medium. At time zero 0.5 mM Rb^+ was added to the medium.

Expression studies in *Xenopus laevis* oocytes were also performed, but no enhanced conductance was found (not shown).

Role of the putative viral potassium transporters during replication

We used Northern hybridization to determine if and when the Pbi virus Fr483 and SAG virus ATCV-1 express the HAKCV transporters. For this purpose we constructed probes for the *hakcv* genes N110R (FR483) and Z696R (ATCV-1) and hybridized them with RNA extracted from infected *Chlorella* Pbi and *Chlorella* SAG 3.83 respectively. The resulting Nothern blot (**Fig. 36**) shows, that in both cases a strong band appears at ~ 2000 bp, i.e. the size expected for the transporter. In both cases the expression is transient. For Fr483, the first visible signal becomes appearent at 20 minutes p.i. (post infection), with the strongest band at 45 minutes p.i.; later the signal fades out and disappears at times >180/360 minutes p.i.. In the case of virus ATCV-1 the expression is slightly shifted to earlier times: the first visible band appears at 10 minutes and peaks at 30 minutes before disappearing after 90 minutes. Thus, we conclude, that the transporter of ATCV-1 is an early/late gene, which is expressed only for a short time (~80 minutes) during replication. In the case of the prototype chlorella virus PBCV-1 genes are classified according to their expression in either early genes (0 - 60 min p.i.), early/late genes (10 - 360 min p.i.) or late genes (60 - 360 min p.i.) (Yanai-Balser *et al.* 2010). Early genes are usuallly involved in DNA sysnthesis and host DNA degradation. Late genes on the other hand are usually part of the virus capsid or packaged within it (Yanai-Balser *et al.* 2010).

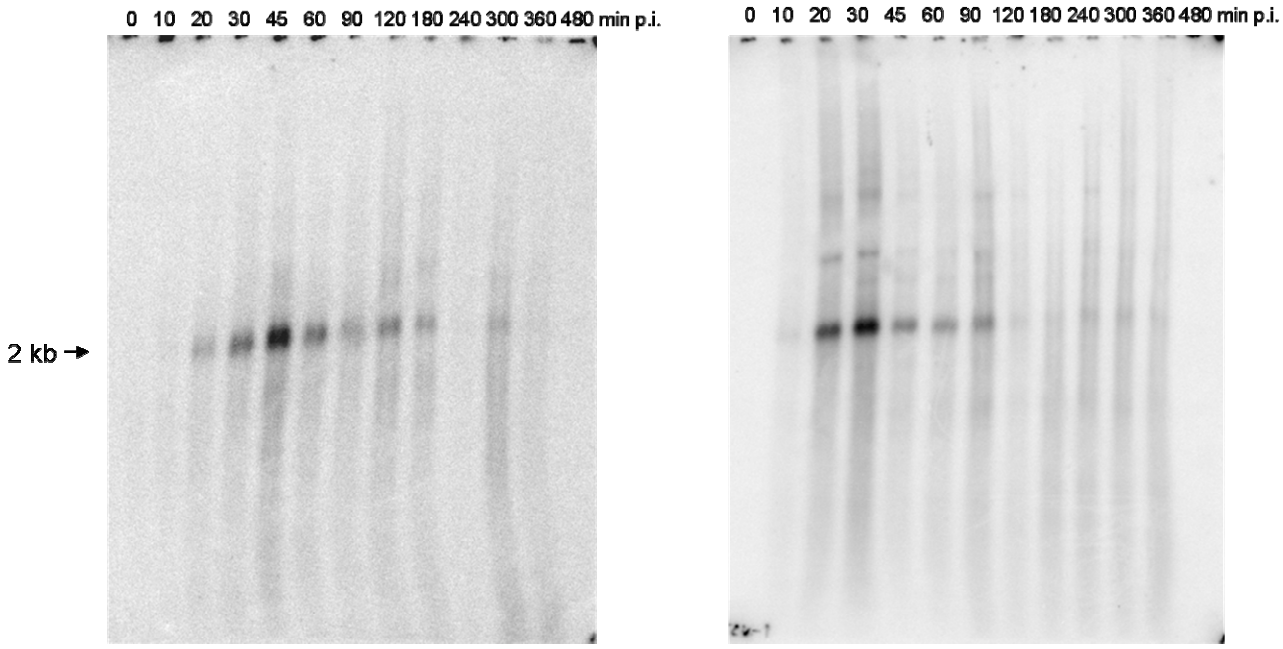

Fig. 36: The putative viral potassium transporters are expressed as early genes during replication
Northern hybridization of the putative potassium transporter genes encoded by Pbi virus FR483 (left side) and SAG virus ATCV-1 (right side).

In virus Fr483, the expression of the transporter gene spans over a much longer time than in virus ATCV-1. This might be explained by the different replication times of the two viruses. The ATCV-1

virus takes only ~ 5 hours for replication whereas Fr483 takes ~ 8 hours. Thus, the potassium transporter of Fr483 can also be seen as an early/late gene.

Taken together the results of these experiments stress that the transporter genes are expressed and used by the virus during replication; they seem not to be part of the virion itself, because they were not detected in a proteomics analysis of both viruses (Dunigan et al., unpublished data).

4.4. Discussion

Collectively, the data show, that the viral protein HAKCV-1 encoded by Pbi virus Fr483 ORF N110R is a fully functional potassium transporter, which is expressed early during the replication cycle of the Pbi virus Fr483.

The topology prediction shows that the protein consists of twelve transmembrane domains with a larger gab between the second and the third transmembrane domain. In this respect the viral protein has in addition to a sequence homology also the same structural architecture as other HAK/KUP/KT-like potassium transporters (**Fig. 29**). Like the latter transporters the viral protein also contains the conserved putative filter sequence in the second transmembrane domain VFGD (Rigas *et al.* 2001). This sequence - VFGD - strongly reminds of the potassium channel filter sequence TxxTxGYGD and will be a good target for mutational studies on functionality and selectivity of the protein in future studies.

The viral protein does also not differ much in size from related proteins. This finding is interesting since the size of viral genes is usually small compared to gene homologs from eukaryotes or prokaryotes (Van Etten *et al*. 2010). The potassium channels encoded by the chlorella viruses for example are minimal in size, resembling only the “core” of other potassium channels (Thiel *et al.* 2010b). This is apparently not the case for the potassium transporters. With 660 amino acids HAKCV-1 is even slightly larger than the potassium transporters encoded, e.g. by *Methanospirillum hungatei* JF-1 (611 amino acids) or by *Desulfovibrio magneticus* RS-1 (635 amino acids).

A phylogenetic comparison with potassium transporter proteins from other organisms shows that the viral transporters make up their own clade. This is especially interesting, because for the viral potassium channels it was shown that these genes were not acquired from their respective host (see chapter 5; Hamacher *et al*. 2011). The transporter is hence another candidate for analyzing the relationship between viral and host genes. The problem here is that there are as yet no genomic data available for the hosts – *Chlorella* Pbi and *Chlorella* SAG 3.83 – so we do not know if it encodes for a similar protein. The full genomic sequencing of *Chlorella* NC64A, which is closely related to *Chlorella*

Pbi and *Chlorella* SAG 3.83 revealed a small protein with some sequence similarity to HAKCV-1. However, this protein is much smaller than the viral HAKCV-1 protein. This implies that *Chlorella* algae are not encoding for a *hakcv*-like gene. But without the genomic data from the host it cannot be fully excluded that the two *Chlorella* species *Chlorella* Pbi and *Chlorella* SAG 3.83 encode for the same length putative potassium transporters.

Only two of the three chlorella virus families, namely Pbi viruses and SAG viruses, encode for a HAKCV ortholog. The phylogenetic tree based on the viral DNA polymerase gene in **Fig. 33** suggests that the common ancestor of Pbi viruses and SAG viruses aleady carried the HAKCV gene, and that a repeated loss occurred mostly within the Pbi viruses. The repeated loss of a gene is more likely than repeated acquisition of the gene in analogy to Dollo´s law of irreversibility (Dollo 1893).

To test the protein for functionality we performed yeast complementation assays and Rb^+ flux experiments. Both experiments have shown that HAKCV-1 is a functional potassium transporter. Cells expressing HAKCV-1 clearly grew under selective conditions while the negative control did not (**Fig. 34**). The cells expressing the transporter grew as much as the positive control, i.e. cells expressing the viral potassium channel Kcv_{PBCV-1}. The latter has been shown to be a functional potassium channel in a bulk of studies (Plugge *et al.* 2000; Gazzarrini *et al.* 2003; Thiel *et al.* 2010b). The data of the flux experiments demonstrate that cells transformed with HAKCV-1 have an about three to four times higher transport rate for Rb^+ than the negative control (**Fig. 35**). The experiment with the K^+-starved cells shows that the uptake of Rb^+ is due to the expressed protein and not the result of an up-regulated endogenous transport protein. A comparable Rb^+ uptake was also reported for yeast cells expressing other HAK/KUP/KT-like potassium transporters, e.g. HAK1 from barley - *Hordeum vulgar*e - (Fig. 4 in Santa-Maria *et al.* 1997) and HAK1 from the yeast *Debaryomyces hansenii* (Fig. 5 in Martínez *et al.* 2011*)*. This means that the viral transporter is also from its transport capacity comparable to other known transporters of the same kind.

Several attempts were made to obtain an insight into the role and function of the viral potassium transporter during the life cycle of the virus. There is ample evidence for a mandatory role of viral potassium channels in the infection of the host (see introduction, Thiel *et al*. 2010). In analogy to the role of the channels it was hypothesized that the viral transporter might substitute for the potassium channel Kcv in the case of virus Fr483. This virus is the only virus known so far, which is lacking a Kcv gene (Fitzgerald *et al*. 2007). The present data are not in agreement with this hypothesis. If the transporter substitutes for the channel the protein should be part of the virion. Proteomics data of Fr483 virions however revealed no signal for HAKCV-1 (Dunigan *et al.*, unpublished data), which

suggests that it is not part of the virion. This argument is not fully excluding the aforementioned hypothesis since it is possible that the protein is not detected due to a very low abundance.

Another strong argument against the hypothesis under discussion comes from the northern blot hybridization experiments with the *hakcv* genes N110R and Z696R. They show that the transporters are expressed other than the channels not as late genes but as early/late genes (**Fig. 36**). Early genes most likely fulfil functions during virus DNA synthesis within the host cells (e.g. polymerases, nucleases, etc), whereas, in most cases, late genes are part of the virion (e.g. capsid proteins). These data support the notion that the protein is most likely not part of the virion. The transporter probably has a function, which is different from that of the channels, which are expressed as late genes (Mehmel *et al.* 2003; Gazzarrini *et al.* 2003; Yanai-Balser *et al.* 2010). A further argument against the view that the transporters substitute for channels derives from the fact that only few viruses encode for a potassium transporter. This suggests that the protein may not be essential for the viruses. A knock-out mutant could give more information on this, but to date, it is not possible to generate knock-out mutants of chlorella viruses (J. L. Van Etten, personal communication). The SAG viruses, which encode for the transporter, also encode for Kcv gene (**Fig. 33**). This also supports the assumption that the transporters do not substitute the channels. They must have another, more supportive function than the channels. On another token it is also questionable, if a potassium transporter can substitute for a potassium channel during the infection process. The transport rate of a potassium transporter is with 10^2 to 10^4 ions per second several orders of magnitude lower than the transport rate of a potassium channel (10^7 to 10^8 ions per second).

Currently, we can only speculate about the function of the potassium transporter during the viral life cycle. Since it is expressed early/late we assume that it is used for host manipulation, e.g. by changing the ionic millieu within the cell.

4.5. Materials and Methods

Isolation of the HAKCV-1 gene and cloning

The genome of chlorella virus Fr483 consists of double-stranded DNA with coding regions that do not contain introns with the exception of a predicted intron in a tRNA gene (Fitzgerald et al. 2007a). This made the direct isolation by PCR possible, and isolation of viral RNA and reverse-transcription was not necessary. A PCR with Phusion DNA Polymerase was used to directly amplify the gene encoding hakcv-1 with primers containing specific restriction sites for cloning following a standard PCR protocol. A diluted virus suspension was directly added to the PCR mixture as Template. A single band appeared

at ~ 2000 bp (**Fig. 37**). For the expression in yeast, the hakcv-1 gene was cloned into a modified version of the expression vector pYES2/CT (Minor et al. 1999) at BamHI and XhoI sites using the primer sequences hakcv-1-BamHI-for: 5'- TAT GGA TCC ATG TCT GAA ACA GGA GTT -3' and hakcv-1-XhoI-rev: 5'- TAT CTC GAG TCA AAT TTC ATA GGA TGC -3'.

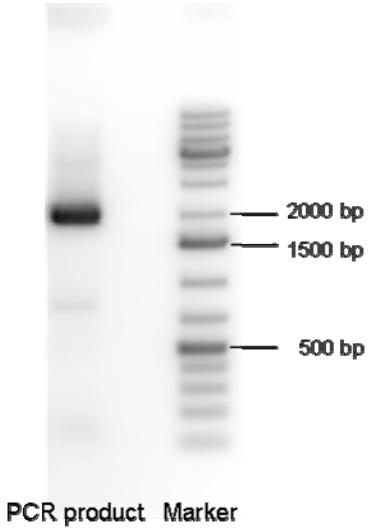

Fig. 37: Amplification of the hakcv-1 gene

Yeast Complementation Assay

Selection experiments were performed as reported previously (Minor et al., 1999, Balss et al. 2008). The hakcv-1 construct was transformed into the SGY1528 yeast strain (*Mat a ade*2–1 *can*1–100 *his*3–11,15 *leu*2–3,112 *trp*1–1 *ura*3–1 *trk*1::HIS3 *trk*2::TRP1; Tang et al. 1995), which is deficient in endogenous K^+ uptake systems. Yeasts from the same stock were grown in parallel under nonselective conditions on plates containing 100 mM KCl and under selective conditions on agar containing 1 mM KCl or 0.5 mM KCl. Growth experiments were done at 30°C for two to three days.

Rb^+ Uptake Experiments

Two different experiments were performed: (A) Yeasts transformed with either the *hakcv-1* gene or empty vector pYES2 were grown in 50 mM K^+ synthetic medium (1.75 g/l YNB without amino acids, ForMedium™ UK, CYN7505, pH was adjusted to 5.8 with ammonium hydroxide soltion before autoclaving) to an OD600 of ~ 0.3 at 28 °C, 50 mM RbCl was added to the medium at time zero and the course of Rb^+ uptake was followed. (B) Yeasts transformed with either the *hakcv-1* gene or empty vector pYES2 were grown in 50 mM K^+ synthetic medium and then starved for 2 hours in K^+ free

starvation medium (1.75 g/l YNB without amino acids, ForMedium^{TM} UK, CYN7505, pH was adjusted to 5.8 with ammonium hydroxide soltion before autoclaving) at 28 °C. After two hours, 0.5 mM RbCl was added to the medium and the course of Rb^+ uptake was followed. Rb^+ was quantified with atomic emission spectrophotometry (Rodriguez-Navarro and Ramos 1984). Both experiments were performed three times. Values are means ± S.D..

Northern-Blot hybridization

2 x 10^9 cells *Chlorella* Pbi or 3 x 10^9 cells *Chlorella* SAG 3.83 cells were collected at 0, 10, 20, 30, 45, 60, 90, 120, 180, 240, 360 and 480 minutes after infection with Fr483 (m.o.i. = 3) and ATCV-1 (m.o.i. = 5) respectively. Cells were frozen in liquid nitrogen and stored at -80 °C. RNA was extracted with TRIzol reagent (Invitrogen), denatured with formaldehyde, separated on a 1.5 % denaturing formaldehyde agarose gel, and then transferred to a nylon membrane. A full-length probe for the hakcv genes N110R (Fr483) and Z696R (ATCV-1) was amplified by PCR for the hybridization. The probe was labelled with ^{32}P-dATP by using the Random Primers DNA labelling kit (Invitrogen). The membrane was pre-hybridized in 10 mL Church buffer (1 % BSA, 1 mM EDTA, 0.5 M $NaPO_4$, 7 % SDS, pH 7.2) for 2 h at 65 °C, hybridized in the Church buffer and denatured probe for 16 h at 65 °C. After hybridization, the membrane was washed four times with 50 °C warm 0.1 x SSC, 0.1 % SDS. The signal detection was done with a Storm Phosphorimager and ImageQuant software (Molecular Dynamics, Inc., Sunnyvale, CA).

***Chlorella* Pbi cell culture and virus purification**

Chlorella Pbi was grown in FES medium (Reisser *et al*. 1986). Virus Fr483 was produced and purified as described for NC64A virus PBCV-1 in Van Etten *et al*. 1983.

Phylogeny

A BLASTP search with the HAKCV-1 (ORF N110R) (accession # YP_001425742) amino acid sequence was conducted using the NCBI non-redundant protein sequences database with default settings. The sequence was blasted against the genomes of “plants”, “bacteria”, “archaea”, “fungi”, “animals” and “viruses”. Similar proteins with significant E-values (<e-50) were used for phylogenetic analyses and can be found in **Tab. 2** (4.7 Appendix).

Phylogenetic trees were made using the server at www.phylogeny.fr with the default parameters. Rooting was done at mid-point (Dereeper and Guignon *et al.* 2008).

4.6. References

Bonza, M. C., Martin, H., Kang, M., Lewis, G., Greiner, T., Giacometti, S., Van Etten, J. L., De Michaelis, M. I., Thiel, G., Moroni, A. (2010): A functional calcium-transporting ATPase encoded by chlorella viruses. *Journal of General Virology*, **91**, 2620. doi:10.1099/vir.0.021873-0

Banuelos, M. A., Klein, R. D., Alexander-Bowman, S. J., Rodríguez-Navarro, A. (1995): A potassium transporter of the yeast *Schwanniomyces occidentalis* homologous to the Kup system of *Escherichia coli* has a high concentrative capacity. *EMBO Journal*, **14**, 3021.

Cao, Y., Jin, X., Huang, H., Derebe, M. H., Levin, E. J., Kabaleeswaran, V., Pan, Y., Punta, M., Love, J., Weng, J., Quick, M., Ye, S., Kloss, B., Bruni, R., Martinez-Hackert, E., Hendrickson, W. A., Rost, B., Javitch, J. A., Rajashankar, K. R., Jiang, Y. and Zhou, M. (2011): Crystal structure of a potassium ion transporter, TrkH. *Nature*, **471**, 336. doi:10.1038/nature09731

Chatelain, F. C., Gazzarrini, S., Fujiwara, Y., Arrigoni, C., Domigan, C., Ferrara, G., Pantoja, C., Thiel, G., Moroni, A., Minor, D. L. (2009): Selection of Inhibitor-Resistant Viral Potassium Channels Identifies a Selectivity Filter Site that Affects Barium and Amantadine Block. *PLoS ONE*, **4**, e7496. doi:10.1371/journal.pone.0007496

Chen, F., Suttle, C. A. (1995): Amplification of DNA polymerase gene fragments from viruses infecting microalgae. *Appl. Environ. Microbiol.*, **61**, 1274.

Chen, F., Suttle, C. A., Short, S. M. (1996): Genetic diversity in marine algal virus communities as revealed by sequence analysis of DNA polymerase genes. *Appl. Environ. Microbiol.*, **62**, 2869.

De Angelis, P. L., Jing, W., Graves, M. V., Burbank, D. E., Van Etten, J. L. (1997): Hyaluronan synthase of chlorella virus PBCV-1. *Science*, **278**, 1800.

Dereeper, A.*, Guignon, V.*, Blanc, G., Audic, S., Buffet, S., Chevenet, F., Dufayard, J. F., Guindon, S., Lefor,t V., Lescot, M., Claverie, J. M., Gascuel, O. (2008): Phylogeny.fr: robust phylogenetic analysis for the non-specialist. *Nucleic Acids Res.*, 2008 Jul 1;36(Web Server issue):W465-9. Epub 2008 Apr 19. (PubMed) *: joint first authors

Dollo, L. (1893): Les lois de l'évolution. *Bulletin de la Société Belge de Géologie de Paléontologie et d'Hydrologie*, **7**, 164.

Epstein, E., Rains, D. W., Elzam, O. E. (1963): Resolution of dual mechanisms of potassium absorption by barley roots. *PNAS*, **49**, 684.

Fitzgerald, L. A., Graves, M. V., Li, X., Feldblyum, T., Hartigan, J. Van Etten, J. L. (2007a): Sequence and annotation of the 314-kb MT325 and the 321-kb FR483 viruses that infect *Chlorella* Pbi. *Virology*, **358**, 459.

Gazzarrini, S., Severino, M., Lombardi, M., Morandi, M., DiFrancesco, D., Van Etten, J. L., Thiel, G., Moroni, A. (2003): The viral potassium channel Kcv: structural and functional features. *FEBS Letters*, **552**, 12

Gazzarrini, S., Kang, M., Epimashko, S., Van Etten, J. L., Dainty, J., Thiel, G., Moroni, A. (2006): *Chlorella* virus MT325 encodes water and potassium channels that interact synergistically. *PNAS*, **103**, 5355.

Gebhardt, M., Hoffgaard, F., Hamacher, K., Kast, S. M., Moroni, A., Thiel, G. (2011a): Membrane Anchoring and Interaction between Transmembrane Domains are Crucial for K^+ Channel Function. *JBC*, **286**, 11299. doi:10.1074/jbc.M110.211672

Gebhardt, M., Tayefeh, S., Baumeister, D., Hertel, B., Greiner, T., Van Etten, J. L., Moroni, A., Kast, S. M., Thiel, G. (2011b): The relevance of Lys snorkeling in the outer transmembrane domain of small viral K^+ channels. Submitted.

Grabov, A. (2007): Plant KT/KUP/HAK Potassium Transporters: Single Family – Multiple Functions. *Annals of Botany*, **99**, 1035.

Hanson, L. A., Rudis, M. R., Vasquez-Lee, M., Montgomery, R. D. (2006): A broadly applicable method to characterize large DNA viruses and adeno-viruses based on the DNA polymerase gene. *Virol. J.*, **3**, 28.

Hick, C. and Hick, A. (2009): Intensivkurs Physiologie. Third Edition. Elsevier GmbH, Urban & Fischer Verlag, München. ISBN 978-3-437-41893-8

Hille, B. (2001): Ion Channels of Excitable Membranes. Third Edition. Sinauer Associates, Inc., Sunderland, Massachusetts, USA.

Kang, M., Moroni, A., Gazzarrini, S., DiFrancesco, D., Thiel, G., Severino, M., Van Etten, J. L. (2004a): Small potassium ion channel proteins encoded by chlorella viruses. *PNAS*, **101**, 5318. doi:10.1073/pnas.0307824100

Kang, M., Graves, M., Mehmel, M., Moroni, A., Gazzarrini, S., Thiel, G., Gurnon, J. R., Van Etten, J. L. (2004b): Genetic diversity in chlorella viruses flanking *kcv*, a gene that encodes a potassium ion channel protein. *Virology*, **326**, 150. doi:10.1016/j.virol.2004.05.023

Kim, E., Myoung Kwak, J., Uozumi, N., Schroeder, J. (1998): *At*KUP1: An Arabidopsis Gene Encoding High-Affinity Potassium Transport Activity. *The Plant Cell*, **10**, 51. doi:10.1105/tpc.10.1.51

Ko, C. H. and Gaber, R. F. (1991): TRK1 and TRK2 Encode Structurally related K+ Transporters in Saccharomyces cerevisiae. *Molecular and Cellular Biology*, **11**, 4266.

Martínez, J. L., Sychrova, H., Ramos, J. (2011): Monovalent cations regulate expression and activity of the Hak1 potassium transporter in *Debaryomyces hansenii*. *Fungal Genetics and Biology*, **48**, 177. doi:10.1016/j.fgb.2010.06.013

Mehmel, M., Rothermel, M., Meckel, T., Van Etten, J. L., Moroni, A., Thiel, G. (2003): Possible function for virus encoded K^+ channel Kcv in the replication of chlorella virus PBCV-1. *FEBS Letters*, **552**, 7. doi:10.1016/S0014-5793(03)00776-2

Minor, D. L., Masseling, S. L., Jan, Y. N., Jan, L. Y. (1999): Transmembrane Structure of an Inwardly Rectifying Potassium Channel. *Cell*, **96**, 879. doi:10.1016/S0092-8674(00)80597-8

Plugge, B., Gazzarrini, S., Nelson, M., Cerana, R., Van Etten, J. L., Derst, C., DiFrancesco, D., Moroni, A., Thiel, G. (2000): A Potassium Channel Protein Encoded By Chlorella Virus PBCV-1. *Science*, **287**, 1641. doi:10.1126/science.287.5458.1641

Ramos, J., Contreras, P., Rodríguez-Navarro, A. (1985): A potassium transport mutant of *Saccharomyces cerevisiae*. *Arch Microbiol*, **143**, 88.

Reisser, W., Becker, B., Klein, T. (1986): Studies on ultrastructure and host range of a *Chlorella* attacking virus. *Protoplasma*, **135**, 162.

Rigas, S., Debrosses, G., Haralampidis, K., Vicente-Agullo, F., Feldmann, K. A., Grabov, A., Dolan, L., Hatzopoulos, P. (2001): *TRH1* encodes a Potassium Transporter Required for Tip Growth in Arabidopsis Root Hairs. *Plant Cell*, **13**, 139.

Rodriguez-Navarro, A. and Ramos, J. (1984): Dual system for potassium transport in Saccharomyces cerevisiae. *J Bacteriol*, **159**, 940.

Rodríguez-Navarro, A. and Rubio, F. (2006): High-affinity potassium and sodium transport systems in plants. *Journal of Experimental Botany*, **57**, 1149. doi:10.1093/jbx/erj068

Santa-Maria, G. E., Rubio, F., Dubcovsky, J., Rodríguez-Navarro, A. (2001): The HAK1 gene of barley is a member of a large gene family and encodes a high-affinity potassium transporter. *The Plant Cell*, **9**, 2281.

Schleyer, M. and Bakker, E. P. (1993): Nucleotide sequence and 3'-end deletion studies indicate that the K(+)-uptake protein from kup from *Escherichia coli* is composed of a hydrophobic core linked to a large and partially essential hydrophilic C terminus. *J Bacteriol*, **175**, 6925.

Szczerba, M. W., Britto, D. T., Kronzucker, H. J. (2009): K^+ transport in plants: Physiology and molecular biology. *Journal of Plant Physiology*, **166**, 447. doi:10.1016/j.jplph.2008.12.009

Tang, W., Ruknudin, A., Yang, W.-P., Shaw, S.-Y., Knickerbocker, A., Kurtz, S. (1995): Functional Expression of a Vertebrate Inwardly Rectifying K^+ Channel in Yeast. *Molecular Biology of the Cell*, **6**, 1231.

Thiel, G., Moroni, A., Dunigan, D., VanEtten, J. (2010a): Initial Events Associated with Virus PBCV-1 Infection of *Chlorella* NC64A. *Progress in Botany*, **71**, 169. doi:10.1007/978-3-642-02167-1_7

Thiel, G., Baumeister, D., Schroeder, I., Kast. S. M., Van Etten, J. L., Moroni, A. (2010b): Minimal art: Or why small viral K^+ channels are good tools for understanding structure function relations. *Biochimica et Biophysica Acta*, **1808**, 580. doi:10.1016/j.bbamem.2010.04.008

Van Etten, J. L., Burbank, D. E., Kuczmarski, D., Meints, R. H. (1983): Virus infection of culturable chlorella-like algae and development of a plaque assay. *Science*, **219**, 994.

Van Etten, J. L., Lane, L. C., Dunigan, D. D. (2010): DNA viruses – the really big ones (Giruses). *Ann. Rev. Microbiol.*, **64**, 83.

Yanai-Balser, G. M., Dunan, G. D., Eudy, J. D., Wang, D., Li, X., Agarkova, I. V., Dunigan, D. D., Van Etten, J. L. (2010): Microarray Analysis of *Paramecium bursaria* Chlorella Virus 1 Transcription. Journal of *Virology*, **84**, 532. doi:10.1128/JVI.01698-09

Zhu, Y.-G. and Smolders, E. (2000): Plant uptake of radiocaesium: a review of mechanism, regulation and application. *Journal of Experimental Botany*, **51**, 1635.

4.7. Apendix

Tab. 2: Homologs of N110R with respective similarities (%)

Organism	Domain	Accession #	% similarity to N110R
ATCV-1	Virus	YP_001427177	55
TN603	Virus	ORF Y68_050R	57
Arabidopsis lyrata subsp. *lyrata*	Plant	XP_002863130	36
Arabidopsis thaliana (HAK5)	Plant	NP_567404	36
Populus trichocarpa	Plant	XP_002303014	34
Arabidopsis thaliana (TRH1)	Plant	NP_194095.2	35
Zea mays	Plant	NP_001148930	37
Ricinus communis	Plant	XP_002521896	32
Thellungiella halophila	Plant	ABO76902	35
Phytolacca acinosa	Plant	AAX13997	36
Vitis vinifera	Plant	XP_002264560	34
Oryza sativa Japonica Group	Plant	NP_001045298	34
Phragmites australis	Plant	BAE93348	35
Mesembryanthemum crystallinum	Plant	AAK53758	35
Physcomitrella patens subsp. *patens*	Plant	XP_001773728	35
Chlamydomonas reinhardtii	green Alga	XP_001700451	35
Botryotinia fuckeliana B05.10	Fungus	XP_001554184	32
Talaromyces stipitatus ATCC 10500	Fungus	XP_002482094	32
Magnaporthe oryzae 70-15	Fungus	XP_365422	32
Arthroderma otae CBS 113480	Fungus	XP_002847150	30
Aspergillus oryzae RIB40	Fungus	XP_001821738	29
Aspergillus clavatus NRRL 1	Fungus	XP_001273808	29
Aspergillus niger	Fungus	XP_001399699	30
Aspergillus flavus NRRL3357	Fungus	XP_002379685	30
Neurospora crassa OR74A	Fungus	XP_964946	33
Methanosarcina acetivorans C2A	Archaea	NP_618072	30
Methanosarcina barkeri str. Fusaro	Archaea	YP_306942	31
Candidatus *Methanoregula boonei* 6A8	Archaea	YP_001404526	34
Candidatus *Methanosphaerula palustris* E1-9c	Archaea	YP_002466744	31
Methanospirillum hungatei JF-1	Archaea	YP_502350	30
Chlorobium phaeobacteroides DSM 266	Bacteria	YP_912218	34
Thiobacillus denitrificans ATCC 25259	Bacteria	YP_315823	32
Chlorobium limicola DSM 245	Bacteria	YP_001943875	33
Aromatoleum aromaticum EbN1	Bacteria	YP_159072	32
Burkholderia thailandensis E264	Bacteria	ZP_05587240	33
Chlorobaculum parvum NCIB 8327	Bacteria	YP_001999537	33
Bdellovibrio bacteriovorus HD100	Bacteria	NP_968854	32
Laribacter hongkongensis HLHK9	Bacteria	YP_002794126	32
Desulfovibrio magneticus RS-1	Bacteria	YP_002952960	33

5. Chapter 4 – Diverse but conserved phycodnavirus potassium ion channel proteins question the virus molecular piracy hypothesis

5.1. Abstract

Phycodnaviruses are large dsDNA, algal-infecting viruses, which encode many genes with homologs in prokaryotes and eukaryotes. Among the products of these genes are the smallest proteins known to form functional K^+ channels. To trace the origin of the viral K^+ channel we compared the sequences of the K^+ channel pore modules from seven phycodnaviruses to K^+ channels from the alga *Chlorella* NC64A, the host for two of the viruses. A comprehensive phylogenetic comparison indicates, that the viral K^+ channel proteins are not related to the host channel proteins; the viral proteins form a separate clade. A consensus sequence of the viral channel proteins resembles a protein of unknown function from a proteobacterium. However, there is no indication that the bacterial protein forms a functional K^+ channel; the bacterial protein also lacks the consensus sequence of all K^+ channels. These results suggest that the viral channel proteins did not come from a proteobacterium. The primitive architecture of the viral channels, the long evolutionary distance between some viruses, and the disjunct positions of the viral K^+ channels in phylogenetic trees supports an alternative hypothesis that predicts the viral proteins could be the origin of K^+ channels in algae and perhaps higher organisms.

5.2. Importance

Currently there is a debate about the role of viruses in evolution. The traditional view is that viruses evolved by stealing genes from their hosts. A more recent line of thinking proposes that viruses pre-date modern cells and that they are a source of cellular genes. On the background of this debate it is interesting to find that some viruses code for proteins that are similar to the potassium (K^+) channels in eukaryotes. The evolutionary history of the viral K^+ channels can be tested by comparing the genes for K^+ channels from a host with those from two viruses. The results of bioinformatic comparisons show, that the K^+ channels from viruses, that are only distantly related, share more similarities than the channels from a distinct virus/host pair. These results challenge the canonical pickpocket nature of viruses and underscore the uniqueness and ancient origin of viral genes.

5.3. Introduction

In recent years many virus-encoded proteins with ion channel activity have been described (Fischer and Sansom 2002; Ciampor 2003; Gonzales and Carrasco 2003; Thiel *et al.* 2010b). On a sequence basis these proteins have little in common with one another, except that all of them are approximately

100 amino acids in size and their membrane-spanning domains are α-helices (Fischer and Sansom 2002). Most viral encoded channel proteins have no similarity to bacterial or eukaryotic proteins suggesting that they are unique to the viruses. The one exception is the channel forming protein Vpu from *Human Immuno-deficiency Virus*-1 (HIV-1), which slightly resembles the first transmembrane domain of eukaryotic TASK channels; this suggests that HIV-1 acquired the gene via molecular piracy (Hsu *et al.* 2004).

A different situation occurs with ion channel proteins from the virus family *Phycodnaviridae*. These large dsDNA viruses, that infect algae (Wilson *et al.* 2009), have gene products with the structural and functional hallmarks of eukaryotic and prokaryotic K^+ channels (Thiel *et al.* 2010b). The best-studied viral K^+ channel is Kcv (K^+ channel chlorella virus) from virus PBCV-1 (*Paramecium bursaria* Chlorella Virus-1) (Plugge *et al.* 2000). Like complex eukaryotic channels, this channel functions as a tetramer (Shim *et al.* 2007; Pagliuca *et al.* 2007). Compared to other K^+ channel proteins, the monomer is small, consisting of only 94 amino acids (Thiel *et al.* 2010b; Plugge *et al*. 2000). The monomer forms a structure with two transmembrane domains, which are linked by a pore helix including a selectivity filter present in all K^+ channels (Tayefeh *et al.* 2009). Hence, Kcv is essentially the pore module present in all K^+ channels. In this context, it is not surprising that Kcv exhibits the basic properties of K^+ channels such as ion selectivity, gating and sensitivity to blockers (Plugge *et al.* 2000; Pagliuca *et al.* 2007; Gazzarrini *et al.* 2003). Circumstantial evidence suggests that an active Kcv channel is required for PBCV-1 infection (Thiel *et al.* 2010a; Greiner *et al.* 2009). The virus particle probably contains the channel in its internal membrane. During the early phase of infection, the viral internal membrane presumably fuses with the host plasma membrane. This fusion process initiates rapid depolarization of the host plasma membrane, which results in a rapid loss of K^+ from the host (Neupärtl *et al.* 2008). As a consequence, the internal turgor pressure of the host alga decreases, which makes it easier for the virus to eject its DNA into the host cell.

Subsequently, K^+ channels have been discovered in three other members of the *Phycodnaviridae*, which infect different hosts (Delaroque *et al.* 2001; Gazzarrini *et al.* 2006; Gazzarrini *et al.* 2009; Fitzgerald *et al*. 2007a-c). Like PBCV-1, some of these viruses (e.g. ATCV-1 and MT325) infect different *Chlorella* species in a strictly host specific manner (Fitzgerald *et al* 2007a-c). Although, the K^+ channels present in these viruses are similar, they have major structural differences. The most obvious difference is their size as well as the organization of their cytoplasmic domains (Thiel *et al.* 2010b). Differences also exist in their physiological properties when expressed in heterologous systems. For example, Kcv from PBCV-1 (Kcv_{PBCV-1}) has a lower open probability than the corresponding channel from virus ATCV-1

(*Acanthocystis turfacea* Chlorella Virus-1; Kcv_{ATCV-1}). Also, Kcv_{PBCV-1} conducts Rb^+ better than K^+, whereas the situation is reversed in Kcv_{ATCV-1} (Gazzarrini *et al.* 2009).

A K^+ channel protein is also encoded by *Ectocarpus siliculosus* Virus-1 (EsV-1), another member of the *Phycodnaviridae* (Delaroque *et al.* 2001). EsV-1 has a different life cycle compared to the *Chlorella* viruses; it infects the marine filamentous brown alga *Ectocarpus siliculosus*, and it has a lysogenic life cycle. The *Chlorella* viruses are lytic and infect fresh water algae (Van Etten *et al.* 2002; Delaroque *et al.* 1999). The hosts, namely the coccal green alga *Chlorella* and the filamentous brown alga *Ectocarpus*, are distantly related (Cock *et al.* 2010). Their last common ancestor probably dates back 500 million years (Yoon *et al.* 2004).

The *Chlorella* viruses and the *Ectocarpus* virus are not closely related, although they both have large genomes of 280 to 370 kbp (Delaroque *et al.* 2001; Fitzgerald *et al.* 2007a-c; Delaroque *et al.* 1999). The prototype *Chlorella* virus PBCV-1 has ~365 protein encoding sequences (CDS), but only ~35 % of them code for proteins of known function. A comparison of PBCV-1 encoded proteins with those from EsV-1 indicates that only about 10 % of the proteins exist in both viruses (Delaroque *et al.* 1999). Among their common gene products is a K^+ channel protein (Delaroque *et al.* 2001). The EsV-1 channel protein, KesV, is 124 amino acids in size, which is slightly larger than those from the *Chlorella* viruses (Chen *et al.* 2005; Balss *et al.* 2008). On a sequence basis, however, Kesv resembles the *Chlorella* virus channel proteins and under certain conditions is functional in heterologous expression systems (Balss *et al* 2008). The major difference between Kesv and the Kcv channels is in the sorting of the proteins within cells (Balss *et al* 2008). In heterologous expression systems, the Kcv channels sort into the secretory pathway and finally move to the plasma membrane. In contrast, the Kesv channel is targeted to the mitochondria (Balss *et al* 2008). This difference in sorting probably reflects different functional roles for the channels because of the different lifestyles of the viruses.
These findings prompted us to examine the origin and the evolution of the viral K^+ channel proteins and the hypothesis, that viruses acquire functional proteins from their hosts. The fact, that K^+ channels from all eukaryotes contain a common pore structure, which resembles the viral K^+ channels, conjures up the traditional assumption that viruses are mere “pick pockets” (Moreira and Lopez-Garcia 2009) and acquire their genes from the host via molecular piracy. If molecular piracy occurs, the viral channel proteins should be simplified versions of their respective host channel proteins. This traditional view on virus evolution has been challenged by recent comparative genomic studies of the phycodnaviruses and prokaryotic DNA viruses. These studies reveal that virus evolution can best be understood in terms of reticulated “trees” and mosaic evolution (Villareal 2008). This means that large DNA viruses fundamentally have a network-based history that does not trace back to a single gene or

set of genes. Hence, the ancestor should probably have exchanged vast pools of genetic elements horizontally and generated a reticulated network of genes. Clearly, this view is consistent with the genetics of phycodnavirus evolution as these viruses have protein-encoding genes with both prokaryotic and eukaryotic characteristics, which probably did not come from a single source.

To understand the evolution of the viral K^+ channels and test the "molecular piracy hypothesis" in the *Phycodnaviridae*, we set up the smallest test set of sequences possible. The set up is depicted in **Fig. 38** and consists of seven sequences of K^+ channels from different phycodnaviruses. The viruses can be distinguished according to their hosts. Six viruses replicate in different species of the unicellular green alga *Chlorella*. Two of these six viruses specifically infect *Chlorella* NC64A. The seventh phycodnavirus infects the brown alga *Ectocarpus siliculosus*, which is only distantly related to the green algae; its K^+ channel sequence can be considered as a negative control for this study. The viral channels are compared to the K^+ channels from a host and a non-host. The recent genomic sequencing of *Chlorella* NC64A provides the sequences of all seven K^+ channels for the host of two viruses. A K^+ channel sequence from the green alga *Chlamydomonas reinhardtii*, a non host of phycodnaviruses and a close relative of the *Chlorella* species, serves as a negative control. The results establish that the viral channels are not related to the host algal channels. This finding together with the similarity between the viral channels suggests a different scenario; derivation of these channels from an ancestral virus.

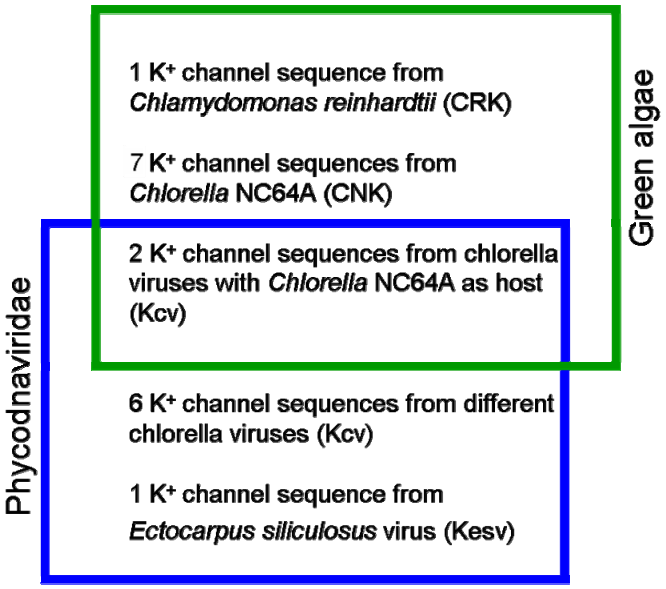

Fig. 38: **Minimal sequence set to test molecular piracy hypothesis.**
Seven sequences of K^+ channels are from different phycodnaviruses. Six of them replicate with a degree of host specificity in different species of the green alga *Chlorella*. *Chlorella* NC64A is a specific host for two of these viruses. The seventh phycodnavirus infects the alga *Ectocarpus*, a brown alga, which is only distantly related to the green algae. The K^+ channel sequence of the *Ectocarpus* virus is a negative control for the molecular piracy hypothesis. The viral channels are compared to the K^+ channels from hosts and non-hosts. The host channels consist of all seven K^+ channels from *Chlorella* NC64A. A K^+ channel sequence from the green alga *Chlamydomonas reinhardtii*, a non-host of phycodnaviruses and a close relative of the *Chlorellas*, serves as negative control.

5.4. Results

Virus sequence analysis

The sequences for seven virus-encoded channel proteins are reported in **Fig. 39**. Most of these channels have been shown to be functional (Plugge *et al.* 2000; Gazzarrini *et al.* 2006; Gazzarrini *et al.* 2009). The amino acid sequence of the viral K^+ channel proteins vary even within the same species. For example, screening of 40 virus isolates from a single species, all of which replicate in the alga *Chlorella* NC64A, revealed that the channel proteins differed by as many as 16 amino acids from Kcv_{PBCV-1} (Kang *et al.* 2004; Gazzarrini *et al.* 2004). The channel protein from the *Chlorella* NC64A virus NY-2A (Kcv_{NY-2A}) is also included in the alignment in **Fig. 39**. Ortholog channel proteins from viruses, which replicate in *Chlorella* Pbi or *Chlorella* SAG 3.83 are also each represented by two viruses.

Fig. 39. Multiple sequence alignment of K^+ channel proteins from different phycodnaviruses.
The genes, that code for these proteins, originate from viruses with different host specificities. Kcv_{PBCV-1} and Kcv_{NY-2A} are from NC64A viruses, Kcv_{MT325} and Kcv_{CVM-1} are from Pbi viruses, and Kcv_{ATCV-1} and Kcv_{TN603} are from SAG viruses. The channel Kesv originates from virus EsV-1, which replicates in *Ectocarpus siliculosus*. The selectivity filter sequence is in black; aromatic amino acids upstream of the filter are marked in grey, and the transmembrane domains are underlined.

The alignment indicates the seven viral channel proteins have about 23 % amino acid identity and 60 % amino acid similarity. Notably, all of the channel proteins have the canonical selectivity filter sequence, which is typical for all K^+ channel proteins from prokaryotes and eukaryotes. The six members of the subfamily of channels from the *Chlorella* viruses are more similar to each other than to

the K^+ channel protein from the *Ectocarpus* virus. Hence, the diversity between the viral channels is correlated with the differences between the hosts.

Chlorella NC64A K^+ channel proteins

The recent sequencing of the *Chlorella* NC64A genome (Blanc *et al.* 2010), the host for viruses PBCV-1 and NY-2A, allows us to address the question of whether the viral K^+ channels are more closely related to their host or to one another. Consequently, we searched the *Chlorella* NC64A sequence for putative K^+ channel proteins employing the following strategies:

1) All the gene products were screened for the highly conserved motifs in the filter region, GYG, GFG and GLG, which are present in all known K^+ channel proteins (Heginbotham *et al.* 1994; Lesage *et al.* 1996).

2) The sequences of all K^+ channels and cyclic nucleotide gated channel (CNG) from *Arabidopsis thaliana* plus additional members of other K^+ channel families (Kir, Kv, TPA, Tandem) from animals and bacteria were compared to the *Chlorella* NC64A genome using BLAST.

All genes with a positive hit were then subjected to a BLAST search of the NCBI protein database to identify proteins with similarities to K^+ channels. This search identified seven CDSs in the *Chlorella* NC64A genome with the hallmarks of K^+ channels. The seven CDSs for putative K^+ channel proteins are designated CNK1-7 for *Chlorella* NC64A K^+ channel proteins 1-7. In the present study we restricted the analysis to the pore module of these proteins, namely the pore helix, the selectivity filter and the two transmembrane domains, that are flanking these. To identify the pore modules of the *Chlorella* NC64A channel proteins, all seven amino acid sequences were subjected to several predictive algorithms for transmembrane domains (see material and methods). Consensus predictions of the pore modules are reported in **Fig. 40**. The alignment indicates, that the pore modules of the *Chlorella* NC64A channels are heterogenous. However, it is important to note, that all the proteins have the typical features of K^+ channels, namely: i) the K^+ channel consensus sequence, ii) two transmembrane domains, iii) a pore helix and iv) aromatic amino acids upstream of the consensus sequence.

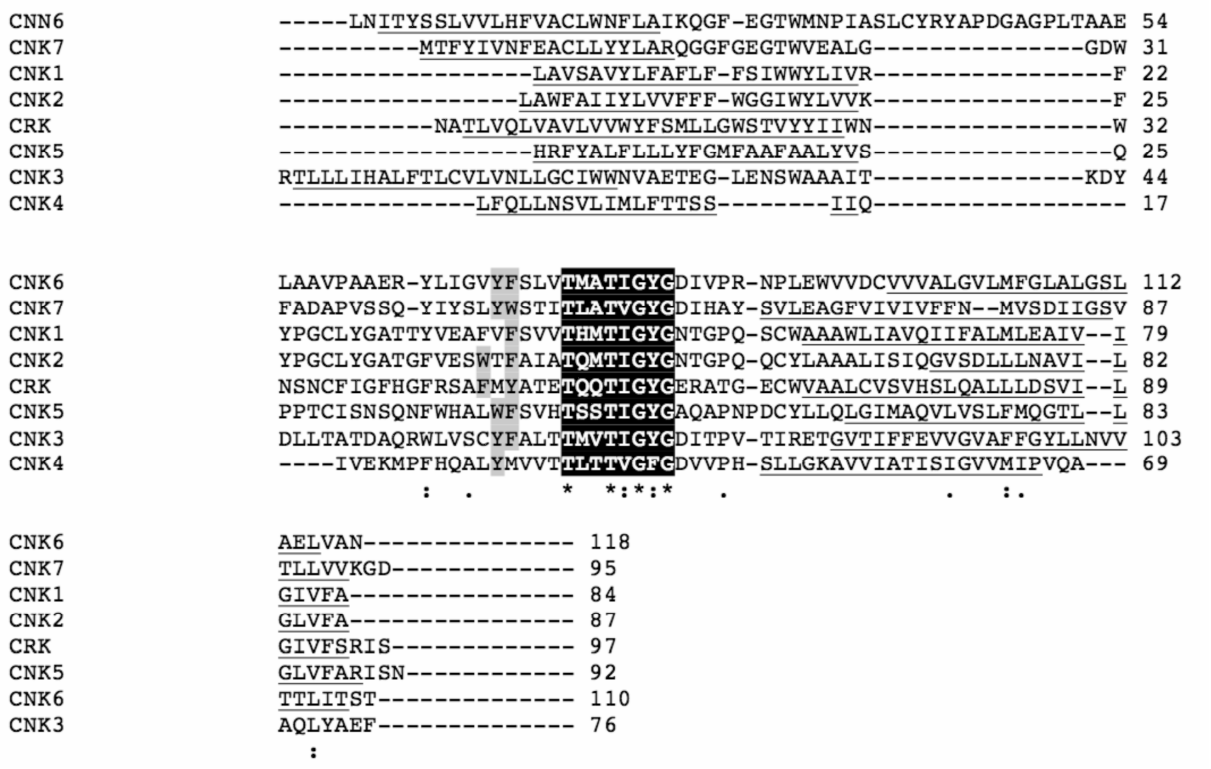

Fig. 40: Multiple sequence alignment of pore modules of K^+ channel proteins from *Chlorella* NC64A.

For comparison a K^+ channel protein, CRK from the green alga *Chlamydomonas reinhardtii*, is also included. The pore-forming unit begins with the transmembrane domain prior to the selectivity filter, and it finishes at the end of the transmembrane domain after the filter. The locations of the respective transmembrane domains were predicted from secondary structure predictions. The selectivity filter sequence is in black; aromatic amino acids upstream of the filter are marked in grey; the transmembrane domains are underlined. Worth noting is the K^+ channels conserved selectivity filter sequence and an otherwise overall low degree of similarity between the channels.

Phylogenetic analysis of K^+ channel proteins

For a phylogenetic comparison of the viral and algal channels we only included the pore modules in the analyses. **Fig. 41** shows the consensus tree of phylogenies for the viral and *Chlorella* NC64A channel proteins obtained by Bayesian estimation from nucleotide and amino acid sequences, as well as by maximum parsimony with amino acid sequences. The results of different analytic strategies consistently identified the same channel sequence (CNK1), which was included twice as an internal control, as identical. The same analyses indicated that the viral channels form one clade, which is clearly separated from the second clade containing the algal channels. Not surprisingly a K^+ channel (CRK) from another unicellular green alga, *Chlamydomonas reinhardtii*, grouped with those from *Chlorella* NC64A. The clear separation between the viral K^+ channels and the algal channels occurs when either amino acids or nucleotides are used in the analyses. Furthermore, the same results are obtained by different statistical-phylogenetic models (see Materials and Methods). The distance between the viral channels and the host channels is further supported by some interesting details in the phylogenies. *Chlorella* NC64A is only a host for two viruses, PBCV-1 and NY-2A. The close relationship of the channels from these two viruses is consistent with the fact that both viruses are isolates from the same species. It is interesting to note, however, that among the viral channel proteins the proteins from these two viruses are the most distant from *Chlorella* NC64A proteins. The channel that is most closely related to the *Chlorella* NC64A channels is Kesv from virus EsV-1. The EsV-1 host, however, is very distantly related to the green algae *Chlorella* and *Chlamydomonas* (Cock *et al.* 2010).

We then estimated the phylogenetic distance between the channels on the basis of an evolutionary clock, provided by the phylip-programs protml/protmlk. Notably this procedure must be used with caution because the use of an evolutionary clock is only valid when crude estimates of the relative mutation rates in the viruses and the algae are available. Collectively, the data indicate that the viral channels have a long evolutionary history. Even the two channels Kcv_{PBCV-1} and Kcv_{NY-2A}, both from viruses that infect the same alga species, reveal a large distance. This finding, however, is not so surprising if we consider the overall differences between the two virus genomes and the differences in their genome structure (Fitzgerald *et al.* 2007a-c). Notably, the function of the two channels with respect to their pharmacology and voltage-dependency is also quite different (Kang *et al.* 2004; Gazzarrini *et al.* 2004). Taken together, the tree presented in **Fig. 41** indicates that the K^+ channel proteins encoded by viruses PBCV-1 and NY-2A are not the result of molecular piracy from their host *Chlorella* NC64A.

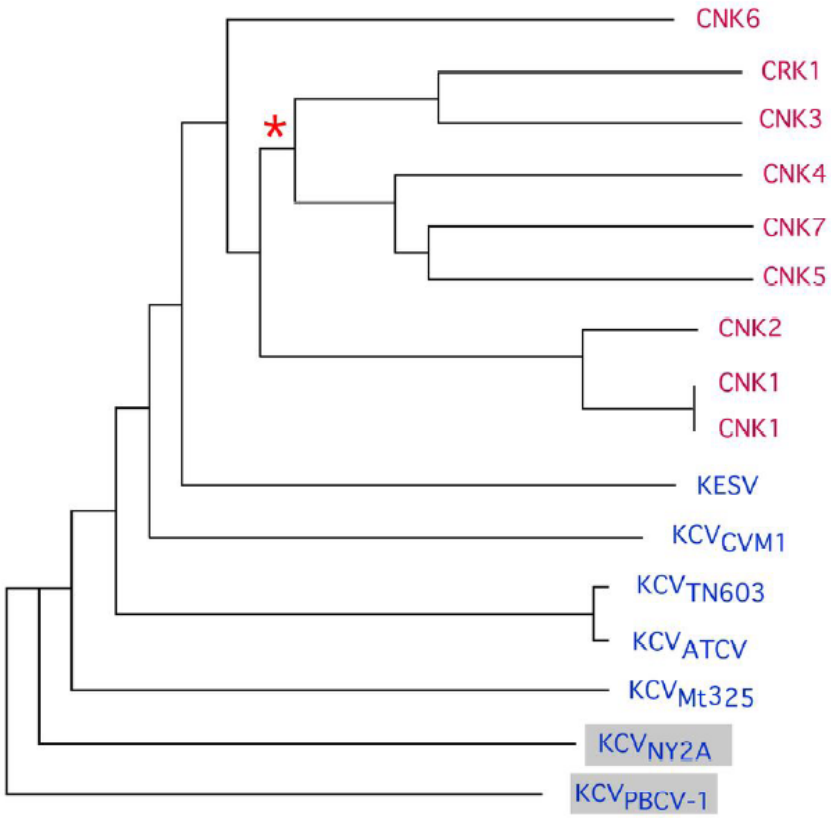

Fig. 41:

Consensus, unrooted tree obtained by Bayesian estimates of phylogenies for the amino acid and nucleotide sequences, as well as for a protein parsimony approach. All clades had a statistical support of 100 percent with reference to the six independent trees computed (Bayesian estimate) or the statistical support with reference to the 1,000 replicas fed into the protpars program (protein parsimony). The only difference between these is a weaker support in one of clades (50% support, as indicated by the red star). Note that all phylogenetic approaches resulted in the same tree. This rather surprising observation is made possible by our minimal sequence setup. In larger data sets with more unrelated or weakly linked organisms one would obtain diverging results on with various methods. Red entries indicate algae channels, while blue entries are viral channels.

Search for the ancestor of the viral K^+ channels

The fact that all viral K^+ channel proteins group together in a common clade (**Fig. 41**) motivated us to identify a consensus sequence from the viral channels using the standard procedure in the Biopython software. The consensus sequence shown in **Fig. 42** was then used in a Blast search to hunt for similar channel proteins. The search resulted in one hit, albeit with only moderate significance, a protein (labeled LPA) from the marine proteobacterium *Labrenzia alexandrii* DFL-11 (Gene bank number NZ_EQ973121).

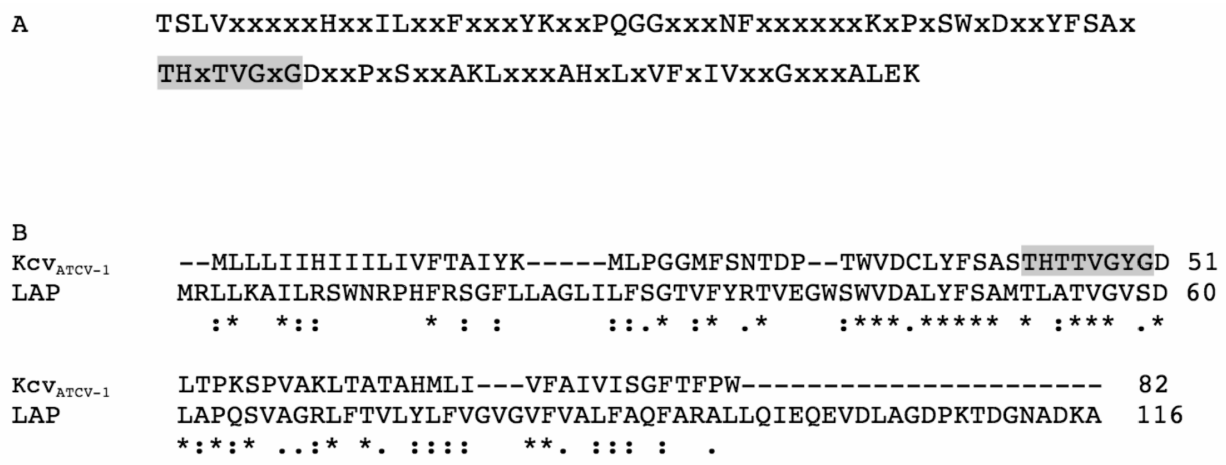

Fig. 42:

The consensus sequence of viral K^+ channel pore is similar to protein LAP from proteobacterium *Labrenzia alexandrii* DFL-11. (A) Consensus sequence of viral K^+ channels. (B) Alignment of K^+ channel Kcv_{ATCV-1} with protein LAP from Labrenzia alexandrii DFL-11 (data bank ZP_05113853). Identical amino acids are indicated by (*), conserved or semi-conserved amino acids are indicated by (:) and (.) respectively. Note that the consensus sequence of K^+ channels (grey box) is only partially conserved in the bacterial protein.

Fig. 42 shows an alignment of LPA of *Labrenzia alexandrii* DFL-11 and Kcv_{ATCV-1}, the viral channel that is most similar to LPA. The alignment reveals many identical or similar amino acids in the transmembrane domains. However, LPA from *Labrenzia alexandrii* DFL-11 lacks the canonical sequence of a K^+ channel (Heginbotham *et al.* 1994; Lesage *et al.* 1996) and probably does not function as a K^+ channel. The conservation of this domain in all K^+ channel proteins including those from the viruses makes it unlikely that the viral channels came from this proteobacterium.

We tested the functionality of LPA as a K^+ channel by cloning and expressing its gene in mutants of yeast that are devoid of K^+ uptake systems. These mutants only grow in a medium with high K^+ (100 mM). Growth on a medium with low K^+ only can occur by expressing a heterologous K^+ channel (Minor *et al.* 1999). The data in **Fig. 43** show that all yeast mutants grow on medium with high K^+ indicating their general fitness. Growth on medium with low K^+ only occurs when cells are transformed with the functional viral K^+ channel Kcv_{PBCV-1}. These results are similar to those obtained previously indicating that functional viral K^+ channels can rescue the yeast mutants under selective conditions (Balss *et al.* 2008). Expression of LPA from *Labrenzia alexandrii* DFL-11 does not rescue the mutant defect. This result does not provide definitive proof that LPA is not a K^+ channel protein, but indicates that it probably does not form a functional channel in yeast.

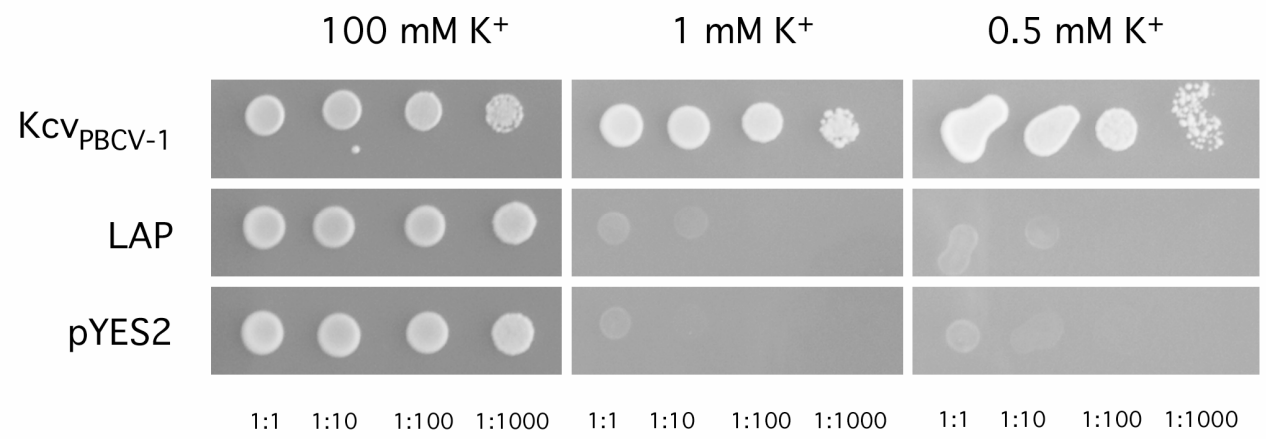

Fig. 43:

Growth phenotype of yeast ΔtrkΔtrk2 mutants transformed with different genes. Yeast cells were transformed with either an empty vector pYES2, with the viral K^+ channel Kcv_{PBCV-1}, or the protein LAP from *Labrenzia alexandrii* DFL-11. All yeasts were grown on non-selective medium containing either 100 mM K^+ or lesser amounts. Only yeast transformed with Kcv_{PBCV-1} grew on selective medium with low 0.5 mM and 1 mM K^+ concentrations.

Finally, we tested the unlikely possibility that *Labrenzia alexandrii* DFL-11 is an alternate host for the chlorella viruses (Yamada *et al.* 2006). The bacteria were incubated with a high titer of chlorella viruses. No lysis of the bacteria occurred after four days suggesting that the marine proteobacterium is not a host for the chlorella viruses.

5.5. Discussion

The data presented in this study indicate that there is not a close relationship between viral-encoded and host-encoded K^+ channel proteins in the algal virus system. Negative controls placed between viruses and their respective hosts. Therefore, it is doubtful that the viruses acquired their channel-encoding genes from their algal hosts via molecular piracy. The analysis also indicates that the viral K^+ channels are closely related to each other in spite of the large evolutionary distance between some of the viruses (Van Etten *et al.* 2002). The statistical support is strong, as different methods applied to both nucleotide and amino acid sequences result in the same phylogenies.

Using sequences with probable different evolutionary rates avoids the pitfall of the long-branch attraction artifact (Bergsten 2005). Collectively, the results contradict the molecular piracy hypothesis, and suggest an alternative hypothesis that the small and diverse K^+ channel genes might originate from viruses. This hypothesis of a viral origin for channel proteins is not that surprising when one considers that many other viruses code for very simple proteins with ion channel function (Fischer and Sansom 2002; Ciampor 2003; Gonzales and Carrasco 2003; Thiel *et al.* 2010b; Wang *et al.* 2010).

Since viruses have high mutation and recombination rates as well as very high reproduction rates relative to their hosts, a relaxed selection due to complementation indicates that a genetic basis of potassium channel origin from viruses might be well grounded. This is consistent with the occurrence of many small genes of unknown function in viral genomes (ORFans) (Yin and Fischer 2008; Kwan *et al.* 2005). The forces, which determine species specificity among channel proteins, could be assigned to virus-virus competition. The activity of the channels from the chlorella viruses is probably essential for infection and in a later step also important in preventing hyper-infection (Greiner *et al.* 2009; Neupärtl *et al.* 2008). Since the viral channels contribute to depolarization of the host plasma membrane and since some virus species seem to out-compete others in an experimental setting by the speed with which they depolarize their host (Greiner *et al.* 2009), it is reasonable to assume that this competition is a driving force for channel diversification. The fact, that the channel from virus EsV-1 is associated with the mitochondria, suggests that this channel acquired protein domains from the host that sort the protein to this organelle. The competition for the right molecular sorting machinery must have affected the evolution of this protein. Since the EsV-1 protein is in the mitochondria, this channel might be part of an early anti-apoptotic system important for viral persistence.

Phylogenetic comparison of other genes from phycodnaviruses including PBCV-1 and EsV-1 with orthologs from bacteria, Archaea and Eukarya suggests that some of these viral genes are either at or near the base of the phylogenetic trees (Villareal and DeFilippis 2000; Takemura 2001; Filée *et al.* 2003; Bell 2001). The basal position of viral genes in the tree of life implies that not only K^+ channels but also other prokaryotic and eukaryotic genes could be of viral origin (Villareal and DeFilippis 2000; Takemura 2001; Filée *et al.* 2003; Bell 2001). In this context, our current results support the hypothesis that the viral channels might be ancestors of all K^+ channels. Comparative analysis of diverse K^+ channels suggests that eukarya and prokarya obtained their K^+ channels from a common precursor that provided the common pore-forming segment (Milkman 1994). The small size of the viral channels, which is basically the pore-forming segment, their functional simplicity, their self assembly into tetramers and their robustness (Thiel *et al.* 2010b) suggests that they are indeed primitive and could predate more complex K^+ channel proteins. Also the fact that some large DNA viruses might predate the separation of the three main branches of cellular life namely bacteria, archea and eukarya (Benson *et al.* 2004) is consistent with the idea that viral channels could be the common ancestor of complex K^+ channels. Some viruses like EsV-1, which incorporates its genome into the host genome by lysogeny (Cock *et al.* 2010), could link virus driven gene emergence to host survival and evolution. Our results suggest that the molecular piracy hypothesis does not explain the host-virus-systems under investigation. To develop a complete picture that viruses evolved channels and inserted them into hosts will require a comprehensive phylogenetic tree including the recently sequenced

genome of *Ectocarpus siliculosus*. Advanced information theory methods (Hamacher 2008; Weil *et al.* 2009) might provide additional insight into the ancestry and origin of these functional proteins.

5.6. Materials and Methods

Sequences

Six Kcv type K^+ channel proteins from chlorella viruses PBCV-1, NY-2A, MT325, CVM-1, ATCV-1, TN603, and one Kesv channel from virus EsV-1 were analyzed. We also identified seven K^+ channel protein sequences in *Chlorella* NC64A (see below), the host for viruses PBCV-1 and NY-2A. The sequence of a putative K^+ channel from the non-host green alga *Chlamydomonas reinhardtii* was also included in the analyses. These sequences were aligned with CLUSTALW2 standard parameters that produced a seed file for all further phylogenetic computations.

Channel sequences were obtained from NCBI for *Chlamydomonas reinhardtii* channel CRK and for virus channels Kcv_{PBCV-1}, Kcv_{NY-2A}, Kcv_{Mt325}, Kcv_{ATCV-1} and Kesv. Additional sequences for Kcv_{CVM-1} and KcvTN603 were obtained from the Chlorella virus database:
http://greengene.uml.edu/database/database.html.
Chlorella NC64A channels were obtained from DOE joint genome institute (JGI) at http://genome.jgi-psf.org/cgi-bin/ToGo?species=ChlNC64A_1 (**Tab. 3**).

Tab. 3: Channel sequences

Sequence	gene bank number	cds/ORF
Chlamydomonas reinhardtii channel CRK	XP_001691185.1	-
Kcv_{PBCV-1}	AAQ16129	A250L
KcvNY-2A	YP_001497532	B336R
KcvMt325	ABT13737	M183R
KcvATCV-1	YP_001427066	Z585R
KcvCVM-1	-	P59_023
KcvTN603	-	Y02_007R
Kesv	NP_077708 08	EsV-223
CNK1	-	IGS.gm_1_00193
CNK2	-	estExt.fgenesh3.pg.C_40067
CNK3	-	IGS.gm_20_00009
CNK4	-	fgenesh3_pg.C_scaffold_9000225
CNK5	-	IGS.gm_7_00033
CNK6	-	IGS.gm_18_00217

Sequence analysis

Three independent approaches were used in the phylogenetic experiment. This reduces a potential sensitivity of our results to the phylogenetic methods employed:

1) Bayesian estimation of phylogeny from the nucleotide sequences.
2) Bayesian estimation of phylogeny from the translated amino acid sequences.
3) Protein Sequence Parsimony Methods as implemented in protpars of the phylip package (Felsenstein 1989) were applied to the translated amino acid sequences.

For the derivation of amino acid phylogenies by Bayesian estimation we used the MrBayes package (Huelsenbeck and Ronquist 2001; Ronquist and Huelsenbeck 2003). We made six independent trees; we used standard parameters, but increased the number of iterations to 70.000.000 to reach convergence. Here the standard deviation of split frequencies reached 10^{-3}. For the final trees we obtained a consensus tree by the consensus program of the phylip package Version 3.67 (Felsenstein 1989).

For the Bayesian estimation of phylogeny of the nucleotide sequences we again used MrBayes, and reached good convergence after 3.600.000 iterations. We performed five independent runs and computed a consensus tree as above. The protein parsiomony was performed on 1.000 randomized replicas by the protpars program of Phylip. From the resulting 1.000 trees we computed a consensus tree as above. Finally, we used protein sequence phylogenies and molecular clock estimates with the Promlk program of the Phylip suite, using 1.000 randomly shuffled seed sequence sets. The consensus sequence of the viral K^+ channels was obtained from an alignment of the pore modules of these channels and calculated with a tool in the Biophyton software (http://biopython.org/wiki/Main_Page). The pore module comprises the amino acid sequences from the beginning of the outer transmembrane domain to the end of the inner transmembrane domain. The pore model of all channels was identified from the primary amino acid sequences using the following prediction algorithms: DAS, HMMTOP, SOSUI, TMpred, TMHMM, TopPred, MPEx. We used a consensus result for the prediction of the TMDs.

Saccharomyces cerevisiae complementation assays

Selection experiments were performed as reported previously (Balss *et al.* 2008). *Labrenzia alexandrii* DFL-11 was kindly provided by Irene Wagner-Döbler (GBF Braunschweig). The LAP protein from *Labrenzia alexandrii* DFL-11 was cloned into the vector pYES2 at BamHI- and XhoI-sites. Either Kcv_{PBCV-1}, LAP or empty cevtor pYES2 was transformed into the SGY1528 yeast strain (Mat a ade2–1 can1–100 his3–11,15 leu2–3,112 trp1–1 ura3–1 trk1::HIS3 trk2::TRP1; Tang et al. 1995), which is deficient in endogenous K^+ uptake systems. Yeasts from the same stock were grown in parallel under nonselective conditions on plates containing 100 mM KCl and on selective conditions on agar containing 1 mM KCl or 0.5 mM KCl. Growth experiments were conducted at 30 °C.

5.7. References

Balss, J., Mehmel, M., Baumeister, D., Hertel, B., Delaroque, N., Chatelain, F. C., Minor, D. J., Van Etten, J. L., Moroni, A., and Thiel, G. (2008): Transmembrane domain length of viral K^+ channels is a signal for mitochondria targeting. *PNAS*, **105,** 12313. doi:10.1073/pnas.0805709105

Blanc, G., Duncan, G., Agarkova, I., Borodovsky, M., Gurnon, J., Kuo, A., Lindquist, E., Lucas, S., Panilinan, J., Polle, J., Salamov, A., Terry, A., Yamada, T., Dunigan, D. D., Grigoriev, I. V., Claverie, J.-M., VanEtten, J. L. (2010): The *Chlorella variabilis* NC64A genome reveals adaptation to photosynthesis, coevolution with viruses, and cryptic sex. *Plant Cell*, **22**, 2943. doi:10.1105/tpc.110.076406

Bell, P. J. L. (2001): Viral eukaryogenesis: was the ancestor of the nucleus a complex DNA virus? *J. Mol. Evolution*, **53**, 251. doi:10.1007/s002390010215

Benson, S.D., Bamford, J. K., Bamford, D. K., Burnett, R. M. (2004): Does common architecture reveal a viral linage spanning all three domains of life? *Mol. Cell.*, **16**, 673

Bergsten, J. 2005. A review of long-branch attraction. *Cladistics*, **21**, 163.

Chen, J., Cassar, S. C., Zhang, D., Gopalakrishnan, **M. (2005):** A novel potassium channel by Ectocarpus siliculosus virus. *Biochem Biophys. Res. Commun*, **326**, 887.

Ciampor, F. (2003): The ion channels coded by viruses. *Acta Microbiol. Immunol. Hung.*, **50,** 433. doi:10.1556/AMicr.50.2003.4.9

Cock, J. M., Sterck, L., Rouzé, P., Scornet, D., Allen, A. E., Amoutzias, G., Anthouard, V., Artiguenave, F., Aury, J., Badger, J. H., Beszteri, B., Billiau, K., Bonnet, E., Bothwell, J. H., Bowler, C., Boyen, C., Brownlee, C., Carrano, C. J., Charrier, B., Cho, G. Y., Coelho, S. M., Collén, J., Corre, E., Da Silva, C., Delage, L., Delaroque, N., Dittami, S. M., Doulbeau, S., Elias, M., Farnham, G., Gachon, C. M. M., Gschloessl, B., Heesch, S., Jabbari, K., Jubin, C., Kawai, H., Kimura, K., Kloareg, B., Küpper, F. C., Lang, D., Le Bail, A., Leblanc, C., Lerouge, P., Lohr, M., Lopez, P. J., Martens, C., Maumus, F., Michel, G., Miranda-Saavedra, D., Morales, J., Moreau, H., Motomura, T., Nagasato, C., Napoli, C. A., Nelson, D. R., Nyvall-Collén, P., Peters, A. F., Pommier, C., Potin, P., Poulain, J., Quesneville, H., Read, B., Rensing, S. A., Ritter, A., Rousvoal, S., Samanta, M., Samson, G., Schroeder, D. C., Ségurens, B., Strittmacher, M., Tonon, T., Tregear, J. W., Valentin, K., von Dassow, P., Yamagishi, T., Van de Peer, Y. & Wincker, P. (2010): The Ectocarpus genome and the independent evolution of multicellularity in brown algae. *Nature*, **465**, 617. doi:10.1038/nature09016

Delaroque, N., Maier, I., Knippers, R., Müller, D. G. (1999): Persistent virus integration into the genome of its algal host, *Ectocarpus siliculosus* (Phaeophyceae). *J. Gen. Virol.*, **80**, 1367.

Delaroque, N., Müller, D. G., Bothe, G., Pohl, T., Knippers, R., and Boland, W. (2001): The complete DNA sequence of the *Ectocarpus siliculosus* virus EsV-1 genome. *Virology*, **15**, 112. doi:10.1006/viro.2001.1028

Felsenstein, J. (1989): PHYLIP - Phylogeny Inference Package (Version 3.2). *Cladistics*, **5**, 164.

Filée, J., Forterre, P., Laurent, J. (2003): The role played by viruses in the evolution of their hosts: a view based on informational protein phylogenies. *Res. Microbiol.*, **154**, 237.

Fischer, W.B., and Sansom, M.S. (2002): Viral ion channels: structure and function. *Biochim. Biophys. Acta.*, **1561**, 27. doi:10.1016/S0304-4157(01)00009-0

Fitzgerald, L.A., Graves, M. V., Li, X., Feldblyum, T., Hartigan, J., and Van Etten, J. L. (2007a): Sequence and annotation of the 314-kb MT325 and the 321-kb FR483 viruses. *Virology*, **358,** 459. doi:10.1016/j.virol.2006.08.034

Fitzgerald, L.A., Graves, M.V., Li, X., Feldblyum, T., Nierman, T. and Van Etten, J. L. (2007b): Sequence and annotation of the 369-kb NY-2A and 345-kb AR158 viruses that infect Chlorella NC64A. *Virology*, **358,** 472. doi:10.1016/j.virol.2006.08.033

Fitzgerald, L.A., Graves, M. V., Li, X., Hartigan, J., Pfitzner, A. J., Hoffart, E., and Van Etten, J. L. (2007c): Sequence and annotation of the 288-kb ATCV-1 virus that infects an endosymbiontic chlorella strain of the heliozoon Acanthocystis turfacea. *Virology*, **362**, 350. doi:10.1016/j.virol.2006.12.028

Gazzarrini, S., Severino, M., Lombardi, M., Moranti, M., DiFrancesco, D., Van Etten, J. L., Thiel, G., Moroni, A (2003): The viral potassium channel Kcv: structural and functional features. *FEBS Lett.*, **552**, 12. doi:10.1016/S0014-5793(03)00777-4

Gazzarrini, S., Kang, M., Van Etten, J. L., Tayefeh, S., Kast, S. M., DiFrancesco, D., Thiel, G., Moroni, **A. (2004):** Long-distance interactions within the potassium channel pore are revealed by molecular diversity of viral proteins. *J. Biol. Chem.*, **279**, 28443. doi:10.1074/jbc.M401184200

Gazzarrini, S., Kang, M., Epimashko, S., Van Etten, J. L., Dainty, J., Thiel, G., Moroni, A. (2006): Chlorella virus MT325 encodes water and potassium channels that interact synergistically. *PNAS*, **103,** 5355. doi:10.1073/pnas.0600848103

Gazzarrini, S., Kang, M., Abenavoli, A., Romani, R., Olivari, C., Gaslini, D., Ferrara, G., Van Etten, J. L., Kreim, M., Kast, S. M., Thiel, G., Moroni, A. **(2009):** Eighty-two amino acids are sufficient for making a potassium selective channel. *Biochemical J.*, **420**, 295. doi:10.1042/BJ20090095

Gonzalez, M.E., and Carrasco, L. (2003): Viroporins. *FEBS Lett.*, **552**, 28. doi:10.1016/S0014-5793(03)00780-4

Greiner, T., Frohns, F., Kang, M., Van Etten, J. L., Käsmann, A., Moroni, A., Hertel, B., Thiel, G. (2009): Chlorella viruses prevent multiple infections by membrane depolarization of the host. *J. Gen Virol.*, **90**, 2033. doi:10.1099/vir.0.010629-0

Hamacher, K. (2008): Relating sequence evolution of HIV1-protease to its underlying molecular mechanics. *Gene*, **422**, 30.

Heginbotham, L., Lu, Z. Abramson, T., MacKinnon, R. (1994): Mutations in the K^+ channel signature sequence. *Biophys. J.*, **66**, 1061.

Hsu, K., Seharaseyon, J., Dong, P., Bour, S., and Marbán, E. (2004): Mutual functional destruction of HIV-1 Vpu and host TASK-1 channel. *Molecular Cell*, **14**, 259. doi:10.1016/S1097-2765(4)00183-2

Huelsenbeck, J. P., Ronquist, F. (2001): MRBAYES: Bayesian inference of phylogenetic trees. *Bioinformatics*, **17**, 754.

Kang, M., Moroni, A., Gazzarrini, S., DiFrancesco, D., Thiel, G., Severino, M., Van Etten, J. L.. (2004): Small potassium ion channel protein encoded by chlorella viruses. *PNAS,* **101**, 5318. doi:10.1073/pnas. 0307824100

Kwan, T., Liu, J., DuBow, M., Gros, P., Pelletier, J. (2005): The complete genomes and proteomes of 27 Staphylococcus aureus bacteriophages. *PNAS*, **102,** 5174. doi:10.1073/pnas.0501140102

Lesage, F., Guillemare, E., Fink, M., Duprat, F. Lazdunski, M., Romey, G., Barhanin, J. (1996): TWIK-1, a ubiquitous human weakly inward rectifying K^+ channel with a novel structure. *EMBO Journal*, **15**, 1004.

Milkman, R. (1994): An Escherichia coli homologue of eukaryotic potassium channel proteins. *PNAS*, **91**, 3510.

Minor, D. L., Masseling, S. J., Jan, Y. N., Jan, L. Y. (1999): Transmembrane Structure of an Inwardly Rectifying Potassium Channel. *Cell*, **96**, 879. doi:10.1016/S0092-8674(00)80597-8

Moreira, D., Lopez-Garcia, P. (2009): Ten reasons to exclude viruses from the tree of life. *Nat. Rev. Microbiol.*, **7**, 306. doi:10.1038/nrmicro2108

Neupärtl, M., Meyer, C., Woll, I., Frohns, F., Kang, M., Van Etten, J. L., Kramer, D., Hertel, B., Moroni, A. and Thiel, G. (2008): Chlorella viruses evoke a rapid release of K^+ from host cells during the early phase of infection. *Virology*, **372**, 340. doi:10.1016/j.virol.2007.10.024

Pagliuca, C., Goetze, T. A., Wagner, R., Thiel, G., Moroni, A. and Parcej, D. (2007): Molecular properties of Kcv, a viral-encoded K^+ channel. *Biochemistry*, **46**, 1079. doi:10.1021/bi061530w

Plugge, B., Gazzarrini, S., Nelson, M., Cerana, R., Van Etten, J. L., Derst, C., DiFrancesco, D., Moroni, A., and Thiel, G. (2000): A potassium ion channel protein encoded by chlorella virus PBCV-1. *Science*, **287**, 1641. doi:10.1126/science.287.5458.1641

Ronquist, F., and Huelsenbeck, J. P. (2003): MRBAYES 3: Bayesian phylogenetic inference under mixed models. *Bioinformatics*,**19**, 1572.

Shim, J.W., Yang, M. and Gu, L. Q. (2007): In vitro synthesis, tetramerization and single channel characterization of virus-encoded potassium channel Kcv. *FEBS Letters*, **581**, 1027. doi:10.1016/j.febslet.2007.02.005

Takemura, M. (2001): Poxviruses and the origin of the eukaryotic nucleus. *J. Mol. Evolution*., **52**, 419. doi:10.1007/s002390010171

Tang, W., Ruknudin, A., Yang, W.-P., Shaw, S.-Y., Knickerbocker, A., Kurtz, S. (1995): Functional Expression of a Vertebrate Inwardly Rectifying K^+ Channel in Yeast. *Molecular Biology of the Cell*, **6**, 1231.

Tayefeh, S., Kloss, T., Kreim, M., Gebhardt, M., Baumeister, D., Hertel, B, Richter, C., Schwalbe, H., Moroni, A., Thiel, G., Kast, S. M. (2009): Model development for the viral Kcv potassium channel. *Biophys. J.*, **96**, 485. doi:10.1016/j.bpj.2008.09.050

Thiel, G., Moroni, A., Dunigan, D., Van Etten, J. L. (2010a): Initial Events Associated with Virus PBCV-1 Infection of *Chlorella* NC64A. *Progress in Botany*, **71**, 169. doi:10.1007/978-3-642-02167-1_7

Thiel, G., Baumeister, D., Schroeder, I., Kast, S. M., Van Etten, J. L., and Moroni, A. (2010b): Minimal art: or why small viral K^+ channels are good tools for understanding basic structure and function relations. *Biochim. Biophys. Acta*, **1808**, 580. doi:10.1016/j.bbamem.2010.04.008

Wilson, W. H., Van Etten, J. L., Allen, M. J. (2009): The Phycodnaviridae: the story of how tiny giants rule the world. *Curr. Top. Microbiol. Immunol.*, **328**, 1. doi: 10.1007/978-3-540-68618-7_1

Van Etten, J.L, Graves, M.V., Müller, D.G., Boland, W., Delaroque, N. (2002): Phycodnaviridae-large DNA algal viruses. *Arch. Virol.*, **147**, 1479. doi:0.1007/s00705-002-0822-6

Villarreal, L.P., DeFilippis, V. R. (2000): A hypothesis for DNA viruses as the origin of eukaryotic replication proteins. *J. Virol.*, **74**, 7079.

Villarreal, L. P. (2008): The widespread evolutionary significance of viruses. *Origin and Evolution of Viruses* (eds: E. Domingo, C.R. Parrish and J.J. Holland), 477. New York: Academic Press.

Wang, K., Xie, S., Sun, B. (2010): Viral proteins function as ion channels. *Biochim Biophys. Acta,* **1808**, 510. doi:10.1016/j.bbamem.2010.05006

Weil, P., Hoffgaard, F., Hamacher, K. **(2009):** Estimating sufficient statistics in co-evolutionary analysis by mutual information. *Comp. Biol. Chem.*, **33**, 440.

Yamada, T., Onimatsu, H., Van Etten, J. L. (2006): Chlorella viruses. *Adv. Virus Res.*. **66**, 293.

Yin, Y., Fischer, D. (2008): Identification and investigation of ORFans in the viral world. *BMC Genomics*, **9**, 24. doi:10.1186/1471-2164-9-24

Yoon, H.S., D.J. Hackett, C. Ciniglia, G. Pinto, and D. Bhattacharya (2004): A molecular timeline for the origin of photosynthetic eukaryotes. *Mol. Biol. Evol.*, **21**, 809. doi:10.1093/molbev/msh075

6. Summary

Large DNA viruses are a source of transport proteins with minimal structure and robust function. In the first part I characterized two new variants of the K^+ channel Kcv. The two Kcvs, namely Kcv_{Smith} and $Kcv_{Next\text{-}to\text{-}Smith}$, have a monomer size of only 82 amino acids, but exhibit most of the hallmarks of K^+ channel pores, i.e. two transmembrane domains (TMs), a pore region and a selectivity filter, with the conserved sequence TxxTxGYGD. The two channels differ in 11 amino acids with most of the differences in the outer and the inner TM. Both channels are fully functional with selectivity for K^+; they also conduct Rb^+ and NH_4^+, but no Na^+ and Li^+. The selectivity of the two channels differs, even though they have an identical filter region. Mutational studies revealed that an exchange of a single amino acid in the outer TM already changed in $Kcv_{Next\text{-}to\text{-}Smith}$ the selectivity for K^+ and Rb^+ towards the selectivity of Kcv_{Smith}, implying a relevance of the outer TM for selectivity. The two channels are sensitive to Ba^{2+} and Cs^+, but not to TEA or amantadine. Both channels are fully blocked by Ba^{2+} and the responsible binding site for Ba^{2+} in the filter region could be identified by site-directed mutagenesis. Most notable is the difference in the mode of Cs^+ block. While Kcv_{Smith} was blocked is a moderate voltage-dependent manner, $Kcv_{Next\text{-}to\text{-}Smith}$ showed an extremely steep block with complex kinetics. Again, mutational studies revealed the relevance and sensitivity of the amino acid composition in the outer TM for the block.

The second protein of interest is a putative K^+ transporter encoded by virus Fr483. Analysis of the sequence revealed high similarity to plant potassium transporters including a conserved putative signature sequence; topology prediction algorithms revealed structural similarity with known K^+ transporters. Yeast complementation assays and Rb^+ uptake experiments have shown that the transporter protein is functional. Northern blot hybridization confirmed that the transporter gene is expressed during the infection cycle. The function of the protein is yet unclear. Overall, this is the first functional potassium transporter encoded by a virus.

In the third part, we made phylogenetic analyses together with the group of Prof. Hamacher (TU Darmstadt). The generated trees show that K^+ channels from the alga *Chlorella* NC64A are most distantly related to channels of viruses, which infect it, thus, they were most likely not acquired from the hosts. By generating a consensus sequence of the viral channels we also found a bacterial protein, which has high sequence similarity to $Kcv_{ATCV\text{-}1}$, but is probably not a K^+ channel. Overall, it is not clear from were the chlorella viruses acquired their channel proteins, and it is possible that they are even the architects of these.

7. Zusammenfassung

Große DNA-Viren sind eine Quelle für Transport-Proteine mit minimaler Struktur und robuster Funktion. Im ersten Teil habe ich zwei neue Varianten des Kaliumkanals Kcv charakterisiert. Die beiden Kcvs, Kcv_{Smith} und $Kcv_{Next\text{-}to\text{-}Smith}$, habe eine Länge von nur 82 Aminosäuren pro Monomer, weisen aber alle Merkmale einer Kaliumkanal-Pore auf, dies sind zwei Transmembran-Domänen (TMs), eine Poren-Region und ein Selektivitäts-Filter mit der konservierten Sequenz TxxTxGYGD. Die beiden Kanäle unterscheiden sich in 11 Aminosäuren vor allem in der äußeren und der inneren TM. Beide Kanäle sind voll funktionell mit Selektivität für K^+; sie leiten zudem Rb^+ und NH_4^+, aber kein Na^+ und kein Li^+. Die Selektivität der beiden Kanäle unterscheidet sich, obwohl sie identische Filter-Regionen haben. Mutations-Studien zeigten, dass der Austausch einer einzelnen Aminosäure in der äußeren TM von $Kcv_{Next\text{-}to\text{-}Smith}$ bereits die Selektivität für K^+ und Rb^+ in Richtung der Selektivität von Kcv_{Smith} verschiebt, was die Relevanz der äußeren TM für die Selektivität andeutet. Die zwei Kanäle sind sensitiv gegenüber Ba^{2+} und Cs^+, aber nicht gegenüber TEA oder Amantadin. Beide Kanäle werden komplett durch Ba^{2+} blockiert und die verantwortliche Bindestelle für Ba^{2+} in der Filter-Region konnte durch site-directed Mutagenese identifiziert werden. Vor allem bemerkenswert ist der Unterschied im Caesium-Block. Während Kcv_{Smith} in moderat spannungsabhängiger Weise blockiert wurde, zeigte $Kcv_{Next\text{-}to\text{-}Smith}$ einen extrem steilen Block mit komplexer Kinetik. Wieder zeigten Mutations-Studien die Relevanz und Sensitivität der Aminosäure-Zusammensetzung der äußeren TM für den Block.

Das zweite Protein von Interesse ist ein putativer Kaliumtransporter der vom Chlorella-Virus Fr483 kodiert wird. Die Analyse der Sequenze zeigte hohe Ähnlichkeit zu pflanzlichen Kaliumtransportern, inklusive einer konservierten putativen Signatur-Sequenz; Topologie-Vorhersage-Algorithmen zeigten eine strukturelle Ähnlichkeit zu bekannten Kaliumtransportern. Hefe-Komplementations-Tests und Rb^+-Aufname-Experimente haben gezeigt, dass das Transporter-Protein funktionell ist. Northern Blot-Hybridisierung bestätigte, dass das Transporter-Protein während des Infektionszyklus exprimiert wird. Die Funktion des Proteins ist noch unklar. Alles in allem ist dies der erste funtkionelle Kalium-Transporter, der von einem Virus kodiert wird.

Im dritten Teil haben wir zusammen mit der Gruppe von Prof. Hamacher (TU Darmstadt) phylogenetische Analysen durchgeführt. Die erzeugten Bäume zeigen, dass Kaliumkanäle von der Alge *Chlorella* NC64A am weitesten von Kanälen entfernt sind, die von Viren stammen, die sie infizieren, was bedeutet, dass letztere wahrscheinlich nicht vom Wirt übernommen wurden. Durch Erzeugung einer Konsensus-Sequenz der viralen Kanäle haben wir zudem ein bakterielles Protein gefunden, das eine hohe Sequenz-Ähnlichkeit zu $Kcv_{ATCV\text{-}1}$ hat, aber wahrscheinlich kein Kaliumkanal ist. Insgesamt

ist nicht klar woher die Chlorella-Viren ihre Kanäle haben, und es ist möglich, dass sie sogar die Architekten dieser sind.

8. Danksagung

Ich möchte zum Abschluss Allen danken, die zum Gelingen dieser Doktorarbeit beigetragen haben. Mein Dank gilt:

Herrn Prof. Dr. Gerhard Thiel, für die Betreuung dieser Arbeit über spannende und spannungsabhängige kleine Virus-Proteine. Sowie für hilfreiche Tipps und Ideen, Auslandseinsätze und leckere Freitagsbrötchen.

Herrn Prof. Dr. Adam Bertl, für hilfreiche Ratschläge und die Übernahme des Koreferats.

Herrn Prof. Dr. James Van Etten, für die Möglichkeit in seinem Labor in Nebraska arbeiten zu können. Außerdem möchte Ich den Mitgliedern des Van Etten-Labs für die nette Aufnahme und die schöne Arbeitsatmosphäre dort danken. Besonderer Dank geht hier an **Giane Yanai-Balser**, sowie an **James Gurnon**, **David Dunigan** und **Irina Agarkova**, die auch außerhalb des Labors für mich da waren.

Meinen Mitbewohnern in Kinderzimmer 1: Vor allem **Manuela Gebhardt**, die mir viele Jahre lang mit Rat und Tat zur Seite stand, sowie **Bastian Roth**, **Alice Kress**, **Christian Braun**, **Charlotte von Chappuis** und **Timo (2) Wulfmeyer**. Danke für die tolle Arbeitsatmosphäre!

Fenja Siotto, für die angenehme Zusammenarbeit während ihrer Diplomarbeit (und die tollen Daten).

Brigitte Hertel, für die Erklärung der x-ten Methode, die ich unbedingt mal ausprobieren wollte.

Den übrigen Mitgliedern der **AG Thiel** und der gesamten **AG Homann**, insbesondere **Vera Bandmann,** für eine schöne Zeit, inklusive Mittagessen, Freitags-Frühstück, Pizza-Essen, Grillen, Tischkickern, Klettern, Weihnachtsfeiern usw.

Den TAs für die Unterstützung im Labor: **Silvia Haase**, für schöne Western-Blots; **Sylvia Lenz**, für besonders grüne Algen; **Mirja Skrablin** und **Christine Gibhardt**, für (meist) gut patch-bare Zellen; **Brigitte Hehl**, für immer blitz-blankes Labor-Geschirr.

Virus Smith, **Virus Next-to-Smith** und **Virus Fr483** für ihre schicken Proteine.

Besonderer Dank gilt zudem meiner Familie und meinen Freunden für die Zeit “neben” der Doktorarbeit.

9. Curriculum vitae

Name Timo Greiner

Date of birth 04.02.1980

Place of Birth Erbach/Odenwald

Education

1986 to 1990 Primary school, Michelstadt/Hessen

1990 to 1992 “Förderstufe” Michelstadt/Hessen

1992 to 1999 Gymnasium Michelstadt/Hessen

Academic Experience

10/2000 to 9/2003 study of chemistry at the TU Darmstadt

10/2003 to 7/2007 study of biology at the TU Darmstadt

2007/2008 diploma thesis at the TU Darmstadt (Institute of Botany) in the Membrane Biophysics Group of Prof. Gerhard Thiel with the title “Konkurrenz unter *Chlorella* NC64A Viren” (“Competition between *Chlorella* NC64A viruses”)

4/2008 to now Ph.D. thesis at the TU Darmstadt (Institute of Botany) in the Membrane Biophysics Group of Prof. Gerhard Thiel

9/2009 to 4/2010 visit at the University of Lincoln, Nebraska (USA) in the lab of Prof. James L. Van Etten (Nebraska Center of Virology)

10. Publications

Agarkova, I., Dunigan, D. D., Gurnon, J., Greiner, T, Barres, J., Thiel, G., VanEtten, J. L. (2008): Chlorovirus-Mediated Membrane Depolarization of *Chlorella* alters Secondary Active Transport of Solutes. *Journal of Virology*, **82**, 12181. doi:10.1128/JVI.01687-08

Bolduan, S., Votteler, J., Lodermeyer, V., Greiner, T., Koppensteiner, H., Schindler, M., Thiel, G., Schubert, U. (2011): Ion channel activity of HIV-1 Vpu is dispensable for counteraction of CD317. submitted

Bonza, M. C., Martin, H., Kang, M., Lewis, G., Greiner, T., Giacometti, S., Van Etten, J. L., De Michaelis, M. I., Thiel, G., Moroni, A. (2010): A functional calcium-transporting ATPase encoded by chlorella viruses. *Journal of General Virology*, **91**, 2620. doi:10.1099/vir.0.021873-0

Gebhardt, M., Tayefeh, S., Baumeister, D., Hertel, B., Greiner, T., Van Etten, J. L., Moroni, A., Kast, S. M., Thiel, G. (2011b): The relevance of Lys snorkeling in the outer transmembrane domain of small viral K^+ channels. Submitted.

Greiner, T., Frohns, F., Kang, M., Van Etten, J. L., Käsmann, A., Moroni, A., Hertel, B. and Thiel, G. (2009): Chlorella viruses prevent multiple infections by membrane depolarization of the host. *J. Gen Virol.*, **90**, 2033-2039. doi 10.1099/vir.0.010629-0

Hamacher, K., Greiner, T., Van Etten, J. L., Gebhardt, M., Villareal, L. P., Moroni, A., Thiel. G. (2011): Diverse but Conserved Phycodnavirus Potassium Ion Channel Proteins Question the Viral Molecular Piracy Hypothesis. Submitted.

11. Affidavit

Herewith, I declare, that I prepared the present Doctoral thesis

“Characterization of novel potassium transport proteins from Chlorella viruses”

on my own and with no other sources and aids than quoted. This thesis has not been submitted to any other examination authority in its current or an altered form, and it has not been published.

Darmstadt, 05.05.2011

_____
Dipl.-Biol. Timo Greiner

12. Eidesstattliche Erklärung

Ich erkläre hiermit an Eides statt, dass ich die vorliegende Dissertation selbstständig und nur mit den angegebenen Hilfsmitteln angefertigt habe.
Ich habe bisher noch keinen Promotionsversuch unternommen.

Darmstadt, 05.05.2011

_____
Dipl.-Biol. Timo Greiner

13. Own Work

Experiments, data analysis and writing of the present thesis were done by myself with the following exceptions:

Chapter 2:
Sequences of Kcv_{604}, $Kcv_{607.3}$ and Kcv_{608} in **Fig. 6 A** were provided by Dr. Ming Kang (UNL Nebraska/USA).

Site-directed mutagenesis and electrophysiological characterization of the $Kcv_{Next\text{-}to\text{-}Smith}$ mutants were done by Ms. Fenja Siotto (Diploma student, TU Darmstadt/Germany) under my supervision.

Chapter 3:

Rubidium flux experiments were done by Mari Carmen Alvarez and José Ramos (Cordoba/Spain).

Chapter 4:
Phylogenetic analyses were done by Prof. Kay Hamacher (TU Darmstadt/Germany).

14. List of Abbreviations

ATCV-1	*Acanthocystis turfacea* Chlorella virus -1
bp	base pairs
dsDNA	double stranded Desoxyribonucleic acid
EGFP	Enhanced Green Fluorescent Protein
EsV-1	*Ectocarpus siliculosus* virus-1
HEK293	Human Embryonic Kidney 293 cell
HIV-1	Human immunodeficiency virus-1
I/V relation	current-voltage relation
KcsA	K^+ channel from *Streptomyces lividans*
Kcv	K^+ Channel Chlorella Virus
Kesv	K^+ channel from *Ectocarpus siliculosus* virus-1
OD 600	optical density at 600 nm
PBCV-1	*Paramecium bursaria* Chlorella virus -1
p.i.	post infection
rpm	revolutions per minute
S.D.	standard deviation
TEA	tetraethyl-amonium ion
TMD	Transmembrane domain
wt	wildtype